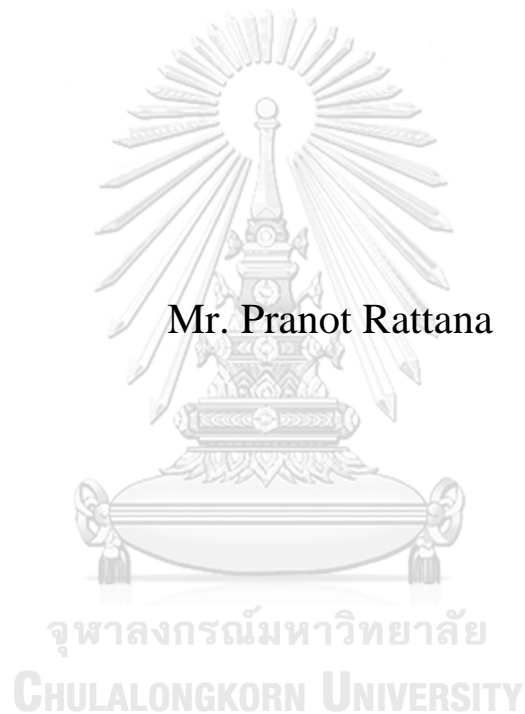


**STRATIGRAPHY AND GEOCHEMISTRY OF ROCK SALT  
FROM MAHA SARAKHAM FORMATION  
IN CHANGWAT CHAIYAPHUM, NORTHEASTERN  
THAILAND**



**A Thesis Submitted in Partial Fulfillment of the Requirements  
for the Degree of Master of Science in Geology  
Department of Geology  
FACULTY OF SCIENCE  
Chulalongkorn University  
Academic Year 2020  
Copyright of Chulalongkorn University**

ลำดับชั้นหินและธรณีเคมีของเกลือหินจากหมวดหินมหาสารคามจังหวัดชัยภูมิ ภาค  
ตะวันออกเฉียงเหนือ ประเทศไทย



วิทยานิพนธ์นี้เป็นส่วนหนึ่งของการศึกษาตามหลักสูตรปริญญาวิทยาศาสตรมหาบัณฑิต  
สาขาวิชาธรณีวิทยา ภาควิชาธรณีวิทยา  
คณะวิทยาศาสตร์ จุฬาลงกรณ์มหาวิทยาลัย  
ปีการศึกษา 2563  
ลิขสิทธิ์ของจุฬาลงกรณ์มหาวิทยาลัย



ประณต รัตนา : ลำดับชั้นหินและธรณีเคมีของเกลือหินจากหมวดหินมหาสารคามจังหวัด  
ชัยภูมิ ภาคตะวันออกเฉียงเหนือ ประเทศไทย. ( STRATIGRAPHY AND  
GEOCHEMISTRY OF ROCK SALT FROM  
MAHA SARAKHAM FORMATION IN CHANGWAT  
CHAIYAPHUM, NORTHEASTERN THAILAND) อ.ที่  
ปรึกษาหลัก : ศ. ดร.มนตรี ชูวงศ์, อ.ที่ปรึกษาร่วม : ผศ. ดร.สกลวรรณ ชาวไชย

หมวดหินมหาสารคาม เป็นพื้นที่ที่มีการตกสะสมของแร่โพแทชขนาดใหญ่ ในที่ราบสูงโคราช ของภาคตะวันออกเฉียงเหนือของประเทศไทย และภาคกลางของประเทศลาว หมวดหินมหาสารคาม ประกอบด้วยเกลือหินสามชั้น (ชั้นล่าง ชั้นกลาง และชั้นบน) สลับชั้นกับหินโคลน ซึ่งแร่โพแทชเกิดสะสมตัวร่วมกับตอนบนของเกลือหินชั้นล่าง จากการศึกษาที่ผ่านมายังคงเป็นที่โต้เถียงถึงต้นกำเนิดการสะสมตัวของเกลือหินมาจากน้ำทะเล หรือน้ำจืด (น้ำร้อนและ/ หรือการผสมกันของน้ำ) วัตถุประสงค์ของการศึกษานี้เพื่อวิเคราะห์ต้นกำเนิดของเกลือหินโดยใช้องค์ประกอบธาตุและไอโซโทป นอกจากนี้มีการเทียบสัมพันธ์ลำดับชั้นหินของห้ำหลุมเจาะ (K-201– 205) ที่ตั้งอยู่ในอำเภอบำเหน็จณรงค์และจัตุรัส จังหวัดชัยภูมิ ประเทศไทย ได้แสดงถึงโครงสร้างโดมของเกลือหินบริเวณส่วนข้างของชั้นหินคดโค้งถูกแปลความจากการเทียบสัมพันธ์ลำดับชั้นหินตามลักษณะหินของหลุมเจาะ K-201 K-202 K-203 และ K-205 ซึ่งพบชั้นเกลือหินสองชั้นและมีแร่โพแทชในเกลือหินชั้นล่าง การวิเคราะห์ธรณีเคมีของเกลือหินชั้นกลาง/บน และเกลือหินชั้นล่าง ในหลุมเจาะ K-203 และธาตุหายากของดินโคลนในห้ำหลุมเจาะบ่งบอกถึงธาตุหลักและธาตุส่วนน้อยมีความสอดคล้องตามสูตรเคมีของเกลือหินและค่าไอโซโทปของ โบรอนของแร่เฮไลต์ส่วนใหญ่ (12.26‰ -32.62‰) มาจากน้ำทะเล อย่างไรก็ตามพบค่าความผิดปกติของแร่คาร์บอเนตโดยค่าไอโซโทปของโบรอน (12.26‰) อนุমানถึงความเป็นไปได้ที่อาจมีการไหลของน้ำร้อนเข้ามาในแอ่งโคราช ธาตุหายากของของดินโคลนถูกเปรียบเทียบกับธาตุหายากของหินทรายจากแอ่งซีเหมา ประเทศจีน พบว่ารูปแบบธาตุหายากมีความคล้ายกัน ซึ่งอนุমানถึงแหล่งต้นกำเนิดที่เหมือนกันของทั้งสองหินตะกอนเศษหินนี้

สาขาวิชา ธรณีวิทยา

ลายมือชื่อนิสิต

ปีการศึกษา 2563

ลายมือชื่อ อ.ที่ปรึกษาหลัก

ลายมือชื่อ อ.ที่ปรึกษาร่วม

# # 6172001223 : MAJOR GEOLOGY

KEYWOR Borehole K-203 Rock salt Salt dome Boron isotope Geochemistry  
D:

Pranot Rattana : STRATIGRAPHY AND GEOCHEMISTRY OF ROCK SALT FROM MAHA SAKHAM FORMATION IN CHANGWAT CHAIYAPHUM, NORTHEASTERN THAILAND. Advisor: Prof. MONTRI CHOOWONG, Ph.D. Co-advisor: Asst. Prof. SAKONVAN CHAWCHAI, Ph.D.

Maha Sarakham Formation is one of massive potash deposits in the Khorat Plateau extending from northeastern of Thailand to central of Lao PDR. Maha Sarakham Formation consists of three rock salt members (the lower, middle and upper members) interbedded with claystone. Potash minerals are associated with the thick bed of rock salt in the upper part of lower salt member. Previous studies are still under discussion on whether the origin of rock salt from marine or non-marine (hydrothermal origin and mixed fluids) deposit. The purpose of this study is to analyze the origin of rock salt based on elemental compositions and isotope analysis. In addition, stratigraphic correlations were done in five boreholes (K-201-205) located in Amphoe Bamnetnarong and Chaturat, Changwat Chaiyaphum, Thailand. As stratigraphical correlation results, the rock salt shows a dome structure. The limbs of salt dome are interpreted from lithostratigraphy correlations of K-201, K-202, K-203 and K-205 based on two beds of rock salt and potash zone in the lower salt member. The geochemical analysis of the lower and middle/upper rock salts in borehole K-203, and rare earth elements (REE) of claystone in five boreholes suggests that major and trace elements showing contents according to the formula of minerals and  $\delta^{11}\text{B}$  value (12.26‰ -32.62‰) indicates almost halite influenced seawater. However, the anomaly of carnallite by  $\delta^{11}\text{B}$  value (12.26‰) preferred possible influx of hydrothermal into the Khorat basin. REE of claystone are comparable with the REE in sandstone from the Simao Basin of China, the similar of REE pattern inferred the identical provenances both of clastic sedimentary rocks.

CHULALONGKORN UNIVERSITY

Field of Study: Geology

Student's Signature

Academic 2020

.....  
Advisor's Signature

Year:

.....  
Co-advisor's Signature

.....

## ACKNOWLEDGEMENTS

The author would like to express the thankful to Department of Mineral Resources for support the information of boreholes and scholarship for studying in major geology, degree of Master of Science at Chulalongkorn University.

First of all, I would like to express my sincere thanks to my advisor, professor Montr Choowong for his inestimable support, guidance, knowledge and dedication during the preparation of this research that enable my research to finish completely. And I would like to express the appreciation to my co-advisor, assistant professor Sakonvan Chawchai for her invaluable advice, guidance and constant encouragement throughout the course of this research. I am most grateful for her support and advice not only the research but also many problems in my life. This research would not have been completed without all a moral support and encouragement that I have always received from her.

Secondly, I would like to express my grateful thank to Professor Maoyong He, Professor Liangcheng Tan and Professor Jianghu Lan from State Key Laboratory of Loess and Quaternary Geology, Institute of Earth Environment, Chinese Academy of Sciences, Xi'an, China to their support when I live in China for two months and advice about boron concentration and boron isotopic composition.

Then, I would like to thank you Mister Thanaz Watcharamai, Miss Amporn Chaikham, Miss Maythira Sriwichai Miss Waraphorn Phromsuwan and Mister Natthawut Suppaiboon for their support to borehole analysis and sampling collection in field work.

Finally, I also thank to all friends for their friendship and my family for their encouragement throughout the study. Without their kindness this research would not have reached a final stage.

Pranot Rattana

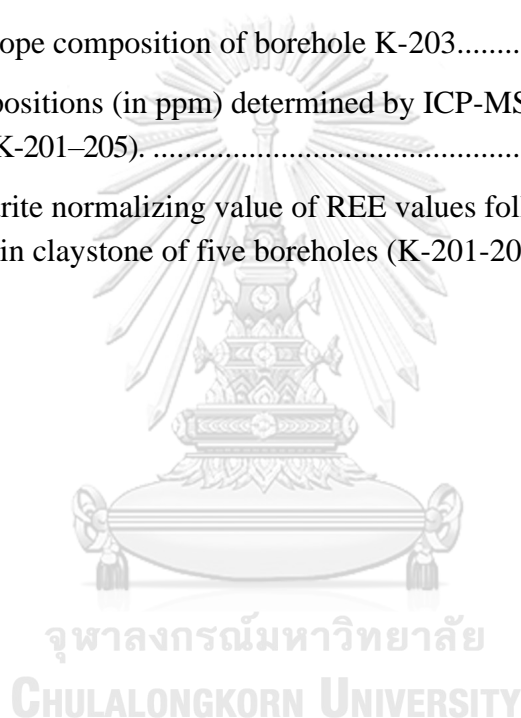
## TABLE OF CONTENTS

|  | <b>Page</b> |
|--|-------------|
| ABSTRACT (THAI) .....  | iii         |
| ABSTRACT (ENGLISH).....  | iv          |
| ACKNOWLEDGEMENTS .....   | v           |
| TABLE OF CONTENTS .....  | vi          |
| LIST OF TABLES .....   | viii        |
| LIST OF FIGURES .....  | ix          |
| Chapter 1 Introduction .....   | 15          |
| 1.1 Background.....  | 15          |
| 1.2 Objectives .....   | 16          |
| 1.3 Study area .....   | 16          |
| 1.4 Methodology.....   | 18          |
| 1.5 Benefits .....   | 18          |
| Chapter 2 Literature Review .....  | 19          |
| 2.1 Tectonic setting.....  | 19          |
| 2.2 Geological setting.....  | 21          |
| 2.2.1 Triassic rocks.....  | 23          |
| 2.2.2 Jurassic – Cretaceous rocks .....  | 23          |
| 2.2.3 Cretaceous rocks.....  | 24          |
| 2.2.4 Cretaceous-Paleogene rocks .....   | 24          |
| Chapter 3 Methodology .....  | 36          |
| 3.1 Study area .....   | 36          |
| 3.2 Sampling and Sample Preparation.....   | 37          |
| 3.3 Geochemical analysis .....   | 39          |
| 3.3.1 Atomic Absorption Spectroscopy (AAS), Titration and UV-Visible<br>Spectroscopy analysis..... | 39          |
| 3.3.2 Inductively coupled plasma mass spectrometry (ICP-MS).....                                   | 42          |

|  |     |
|--|-----|
| 3.3.3 Boron concentrations and Boron Isotope ( $\delta^{11}\text{B}$ ) .....                     | 44  |
| Chapter 4 Results .....  | 46  |
| 4.1 Stratigraphy of boreholes K-201 K-202 K-203 K-204 and K-205 .....                            | 46  |
| 4.1.1 Borehole K-201 .....   | 46  |
| 4.1.2 Borehole K-202 .....   | 53  |
| 4.1.3 Borehole K-203 .....   | 59  |
| 4.1.4 Borehole K-204 .....   | 65  |
| 4.1.5 Borehole K-205 .....   | 69  |
| 4.2 Geochemistry of rock salt in borehole K-203.....   | 74  |
| 4.2.1 Elemental compositions of evaporitic rocks .....   | 74  |
| 4.2.2 Boron isotope of evaporitic rocks .....  | 79  |
| 4.3 Rare earth elements (REE) compositions of clastic rocks.....                                 | 80  |
| Chapter 5 Discussion .....   | 90  |
| 5.1 Stratigraphic correlation .....  | 90  |
| 5.2 The origins of evaporitic rock base on geochemical characteristics in borehole<br>K-203..... | 97  |
| 5.3 The provenance of clastic unit in five boreholes (Borehole K-201-205) .....                  | 102 |
| Chapter 6 Conclusion.....  | 107 |
| 6.1 Conclusion .....   | 107 |
| 6.2 Recommendation .....   | 107 |
| REFERENCES .....   | 2   |
| VITA.....  | 8   |

## LIST OF TABLES

|  | <b>Page</b> |
|--|-------------|
| Table 1 Sequence of precipitation of evaporitic rocks (Suwanich, 1986) .....   | 32          |
| Table 2 The Summary of the different issues of the Maha Sarakham Formation from many researchers.....                                      | 35          |
| Table 3 Elemental compositions of anhydrite, halite and carnallite of borehole K-203. ....   | 75          |
| Table 4 Boron isotope composition of borehole K-203.....   | 79          |
| Table 5 REE compositions (in ppm) determined by ICP-MS analysis of clay and sand in five boreholes (K-201–205). ....                       | 82          |
| Table 6 The chondrite normalizing value of REE values following Taylor and McLennan (1985) in claystone of five boreholes (K-201-205)..... | 86          |



## LIST OF FIGURES

|   | <b>Page</b> |
|---|-------------|
| Figure 1 Flow chart illustration of the methodology of this study. ....   | 18          |
| Figure 2 Major tectonic units in the mainland Southeast Asia showing the location of the Khorat Plateau basin (Minezaki et al., 2019). ....   | 20          |
| Figure 3 Stratigraphy of the Khorat Plateau (El Tabakh et al., 1999). ....  | 21          |
| Figure 4 Idealized map showing marine water inflow into the Khorat Plateau near Bamnet Narong area at the southwestern corner of the Khorat Plateau (El Tabakh et al., 1999). ....  | 21          |
| Figure 5 Geologic map showing the distribution of the Khorat Group located in northeastern of Thailand (modified from DMR, 2010). (A) Index map of Thailand (B) locations of Khorat and Sakon Nakhon basins in northeastern Thailand (C) the study area located in Amphoe Bamnetnarong and Amphoe Chaturat, Changwat Chaiyaphum, Thailand. .... | 22          |
| Figure 6 Model of salt anticline in Maha Sarakham Formation of Khorat Group (modified from Suwanich, 1986). ....  | 25          |
| Figure 7 Lithostratigraphy “A” (see figure 7) showing complete lithostratigraphic sequence discovered three salt beds (Suwanich, 1986). ....  | 26          |
| Figure 8 Model showing the progressive dissolution of the lithostratigraphy of Maha Sarakham Formation (Utha-Aroon, 1993). ....   | 27          |
| Figure 9 Model showing the deformation of salt anticline structure (Yumuang et al., 1986). ....   | 27          |
| Figure 10 Lithostratigraphy “B” (see figure 7) showing incomplete lithostratigraphic sequence discovered two salt beds (Suwanich, 1986). ....   | 28          |
| Figure 11 Lithostratigraphy “C” (see figure 7) showing incomplete lithostratigraphic sequence discovered one salt bed (Suwanich, 1986). ....  | 29          |
| Figure 12 Lithostratigraphy “D” (see figure 7) showing incomplete lithostratigraphic sequence discovered one salt bed without potash zone (Suwanich, 1986). ....  | 30          |
| Figure 13 Models of the bar-basin (A) the transgressive phase (B) the regressive phase (Yumuang et al., 1986) ....  | 31          |

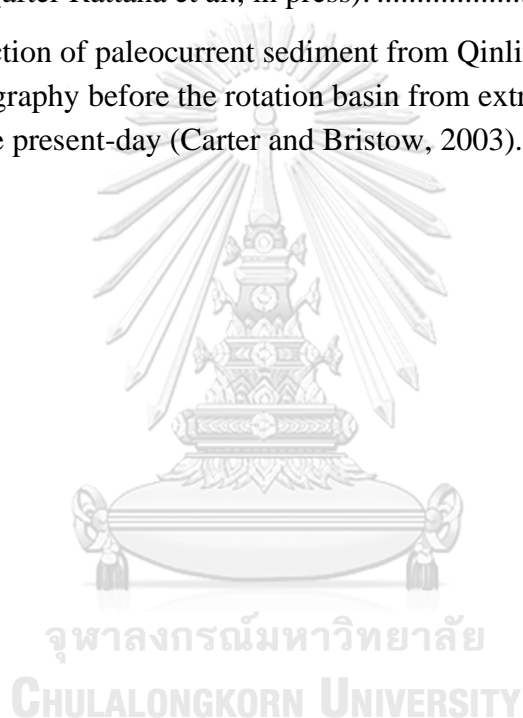
|  |    |
|--|----|
| Figure 14 Chondrite-normalized REE patterns of sandstone in the Mengyejing Formation from the Simao Basin, China plotted using chondrite normalizing values of Taylor and McLennan (1985) (modified from Wang et al., 2014).....                                 | 33 |
| Figure 15 The late Cretaceous paleogeography showing direction of sediment paleocurrent and direction of marine inlet of the Simao basin and the Khorat Plateau (Wang et al., 2014). .....   | 34 |
| Figure 16 The direction of paleoseawater from Shan Boundary ocean inflow into the Lanping-Simao basin and the Sakon Nakhon and Khorat basins respectively (Qin et al., 2020). .....  | 34 |
| Figure 17 Enhanced ALOS DEM map of the study area. (A) Index map of Thailand (B) locations of Khorat and Sakon Nakhon basins in northeastern Thailand (C) the study area located in Amphoe Bamnetnarong and Amphoe Chaturat, Changwat Chaiyaphum, Thailand. .... | 37 |
| Figure 18 Borehole's analysis of rock salt at Mineral and Rock Research Center Changwat Rayong, Department of Mineral Resources.....   | 38 |
| Figure 19 The sampling sites for geochemical analyses in five boreholes (K-201-205). .....   | 39 |
| Figure 20 Flame Furnace Atomic Absorption Spectroscopy at the Department of Mineral Resources. ....  | 40 |
| Figure 21 Titration analysis at the Department of Mineral Resources. ....  | 41 |
| Figure 22 A HITACHI U-2900 spectrophotometer at the Department of Mineral Resources. ....  | 42 |
| Figure 23 Diluted solution for analyzed boron concentrations in laboratory of boron at IEECAS.....   | 43 |
| Figure 24 A Perkin Elmer Nexion 300D ICP-MS at IEECAS. ....  | 43 |
| Figure 25 Diluted solution for analyzed boron isotope in laboratory of boron at IEECAS.....  | 44 |
| Figure 26 A NEPTUNE Plus MC-ICP-MS (Thermo Fisher Scientific, Germany) at IEECAS.....  | 45 |
| Figure 27 The range boron isotopic composition for form of evaporitic rocks to relate the provenance distinguished between marine and non-marine (modified from Palmer and Swihart, 1996).....   | 45 |

|  |    |
|--|----|
| Figure 28 a section of lower portion of unit S1 of K-201. Clear, transparent, white, and smoky dark bands halite close to the contact of orange and honey halite associate with reddish brown clay at 152.2 meters T = top; B = bottom. .... | 46 |
| Figure 29 Core photographer showing piece of halite of unit S1 from K-201. T = top; B = bottom. ....   | 47 |
| Figure 30 Core photographers showing several color bands salt interbedded with carnallite of unit S1 from K-201. T = top; B = bottom. ....   | 47 |
| Figure 31 Close up of carnallite showing granular and medium to coarse grained at 117.8 meters from K-201. ....  | 48 |
| Figure 32 Core photographer showing mudstone of unit C1 from K-201. T = top; B = bottom. ....  | 48 |
| Figure 33 Core photographer showing honey halite associated with inclined smoky dark bands halite of unit S2 from K-201. T = top; B = bottom. ....   | 49 |
| Figure 34 Core photographer showing halite associated with anhydrite stringers that gray, white and dark smoky anhydrite bands overlying inclined halite beds of unit S2 from K-201. ....  | 49 |
| Figure 35 Core photographer showing siltstone of unit C2 from K-201. T = top; B = bottom. ....   | 50 |
| Figure 36 Core photographer showing clayey sand at 13.4-15 meters and sand at 10-13.4 meters of unit C2 from K-201. T = top; B = bottom. ....  | 51 |
| Figure 37 Lithological description of borehole K-201 of Maha Sarakham Formation in Changwat Chaiyaphum, northeastern Thailand. ....  | 52 |
| Figure 38 Core photographer showing halite of unit S1 from K-202. T = top; B = bottom. ....  | 54 |
| Figure 39 Core photographer showing sylvinite and halite of unit S1 from K-202. T = top; B = bottom. ....  | 54 |
| Figure 40 Core photographer showing bluish sylvite and halite of unit S1 from K-202. T = top; B = bottom. ....   | 54 |
| Figure 41 A) Transparent sylvite crystals showing cube of unit S1 from K-202. B) Close up of blue halite of unit S1 from K-202. ....   | 55 |
| Figure 42 Core photographer showing mudstone of unit C1 from K-202. T = top; B = bottom. ....  | 55 |
| Figure 43 Close up of Anhydrite showing micro folded, drag fold and faulting of middle anhydrite unit from K-202. ....   | 56 |

|   |    |
|---|----|
| Figure 44 Core photograph showing reddish brown mudstone until then very dark greenish gray claystone at 52.9 meters of unit C2 from K-202. T = top; B = bottom. ....                                       | 56 |
| Figure 45 Lithological description of borehole K-202 of Maha Sarakham Formation in Changwat Chaiyaphum, northeastern Thailand. ....   | 58 |
| Figure 46 Core photograph showing halite associated with anhydrite stringers at lower part of unit S1 from K-203. T = top; B = bottom. ....   | 60 |
| Figure 47 Core photograph showing carnallite mixing halite of medium unit S1 from K-203. T = top; B = bottom. ....  | 60 |
| Figure 48 Core photograph showing several color bands salt of upper unit S1 from K-203. T = top; B = bottom. ....   | 60 |
| Figure 49 Core photograph showing claystone of unit C1 from K-203. White circle = fragments of carnallite; T = top; B = bottom. ....  | 61 |
| Figure 50 Core photograph showing halite of lower unit S2 from K-203. T = top; B = bottom. ....   | 62 |
| Figure 51 Core photograph showing anhydrite marker at 130.0-131.4 meters of middle unit S2 from K-203. T = top; B = bottom. ....  | 62 |
| Figure 52 Core photograph showing halite associated with anhydrite stringers of upper unit S2 from K-203. T = top; B = bottom. ....   | 62 |
| Figure 53 Core photographs showing claystone of unit C2 from K-203. T = top; B = bottom. ....   | 63 |
| Figure 54 Lithological description of borehole K-203 of Maha Sarakham Formation in Changwat Chaiyaphum, northeastern Thailand. ....   | 64 |
| Figure 55 Core photograph showing halite associated with anhydrite stringers of unit S1 from K-204. T = top; B = bottom. ....   | 65 |
| Figure 56 Core photograph showing anhydrite at 62.0-62.4 meters of unit S1 from K-204. T = top; B = bottom. ....  | 66 |
| Figure 57 Core photograph showing reddish brown claystone and dark reddish gray claystone mixing with breccias of anhydrite and gypsum at 31.0-33.5 meters of unit C1 from K-204. T = top; B = bottom. .... | 66 |
| Figure 58 Lithological description of borehole K-204 of Maha Sarakham Formation in Chaiyaphum province, northeastern Thailand. ....   | 68 |
| Figure 59 Core photograph showing sylvite intergrown with halite and carnallite at 135.0-137.0 meters of unit S1 from K-205. T = top; B = bottom. ....  | 69 |

|  |     |
|--|-----|
| Figure 60 Core photograph showing halite associated with inclined anhydrite stringers of unit S1 from K-205. T = top; B = bottom. ....   | 70  |
| Figure 61 Core photograph showing reddish brown claystone of unit C1 from K-205. T = top; B = bottom. ....   | 70  |
| Figure 62 Core photograph showing anhydrite 66.6-70.0 meters of middle anhydrite unit from K-205. T = top; B = bottom. ....  | 71  |
| Figure 63 Core photograph showing reddish brown claystone of unit C2 from K-205. T = top; B = bottom. ....   | 71  |
| Figure 64 Lithological description of borehole K-205 of Maha Sarakham Formation in Changwat Chaiyaphum, northeastern Thailand.....   | 73  |
| Figure 65 Range of $\delta^{11}\text{B}$ within borehole K-203 (modified from Palmer & Swihart, 1996; Swihart et al., 1986; Vengosh et al., 1992).....   | 80  |
| Figure 66 Chondrite-normalized REE patterns representative the average of unit C1 and C2 plotted using chondrite normalizing values of Taylor and McLennan (1985). ....  | 81  |
| Figure 67 A direction of cross-section A-A' (SW and NE) references from Map L7018 (1997) by Royal Thai Survey Department.....  | 92  |
| Figure 68 A cross-section A-A' (boreholes; K-201–205) show lithostratigraphic correlation. Black dash line = the correlation of rock members; Red dash line = a forecast of correlation of rock members (after Rattana et al., in press). ....   | 93  |
| Figure 69 The Bouguer anomaly map of this study area in five boreholes; K-201-205 (blue circle) (after Shen & Siritongkham, 2020) .....  | 94  |
| Figure 70 Model of the Maha Sarakham Formation compared lithostratigraphic columns in this study (modified from Suwanich, 1983). Solid line showing the locations and depth of five boreholes. ....  | 95  |
| Figure 71 A cross-section A-A' show a dome structure and lithostratigraphic correlation with located of five boreholes (K-201–205).....  | 96  |
| Figure 72 Profile of elemental compositions and boron isotopic composition compared sampling depths in borehole K-203. (after Rattana et al., in press).....   | 98  |
| Figure 73 model stage of origins of Maha Sarakham Formation (after Rattana et al., in press).....  | 101 |
| Figure 74 $\delta^{11}\text{B}$ values of halite and carnallite of Borehole K-203 in this study using $\delta^{11}\text{B}$ values to distinguish non-marine and marine origins based on Palmer and Swihart (1996); Swihart et al. (1986); Vengosh et al. (1992). the $\delta^{11}\text{B}$ ranges of marine evaporitic rocks compares with previous studies from the Sakon Nakhon |     |

|  |     |
|--|-----|
| Basin (Ren et al., 2018; Tan et al., 2010; Zhang et al., 2013) and the Khorat Basin (Qin et al., 2020) (after Rattana et al., in press).....   | 102 |
| Figure 75 Major tectonic units in the mainland Southeast Asia showing the location of the study area of REE in Simao basin (blue star) and location of this study area (modified from Minezaki et al., 2019).....  | 104 |
| Figure 76 Chondrite normalized REE patterns representative each clastic unit in five boreholes plotted. The gray shade showing previous work of chondrite normalized REE patterns in Simao basin consist of Zhenyuan, Jingu, Simao, Mengia and Jiangcheng area (Wang et ai., 2014). Normalizing values of chondrite are Taylor and McLennan (1985) (after Rattana et al., in press). ..... | 105 |
| Figure 77 the direction of paleocurrent sediment from Qinling foreland into Khorat Basin of paleogeography before the rotation basin from extrusion and the located of Khorat basin in the present-day (Carter and Bristow, 2003). .....   | 106 |



## Chapter 1

### Introduction

#### 1.1 Background

The Khorat plateau of northeastern Thailand, as a part of the Indochina microplate, has been formed by continuous uplift for a long period of time probably throughout the Late Cenozoic (Bunopas et al., 2001; Metcalfe, 2017; Sone & Metcalfe, 2008; Sone et al., 2012). The uplift has formed the Khorat plateau with two sub-basins, Sakon Nakhon basin in the north and Khorat basin in the south, separated by Phu Phan ranges which lie in the NW-SE direction (El Tabakh et al., 1999; Songtham et al., 2011). Cretaceous Maha Sarakham Formation is overlain unconformably by salt-bearing deposits consisting of clastic sedimentary rocks and evaporite deposits (rock salts and potash). These rock salts and potash are made into fertilizer for agricultural industry, which is potentially economic in Thailand. Thus, an understanding of stratigraphic and depositional environment of these evaporite sediments is necessary and can be useful for exploration criteria and potash mining.

The stratigraphy of Maha Sarakham Formation has been extensively studied based on several exploration projects. Since 1973, Department of Mineral Resources (DMR) has conducted over 190 investigated drilling boreholes and described lithostratigraphic column in both basins. (Hite, 1971; Suwanich, 1986). Bamnet Narong, the study area in Changwat Chaiyaphum has been previously studied; lithostratigraphy and sedimentary facies have been defined (Yumuang et al., 1986) and sulphur isotope analysis of anhydrite and bromine concentration in halite have been used to indicate the depositional environment and post-depositional changes of Maha Sarakham Formation (El Tabakh et al., 1999). The results suggested a marine depositional environment.

Boron isotope analysis can be used to distinguish between marine and non-marine evaporate settings (Fan et al., 2015; Liu et al., 2000; Palmer & Swihart, 1996; Swihart et al., 1986; Vengosh et al., 1992). For Suvannakhet basin in Laos, extending part of the Sakon Nakhon basin from NE Thailand, Tan et al. (2010) and Ren et al. (2018) analyzed boron isotope in halite. These results indicated that evaporite deposits formed primarily due to evaporation of seawater. In addition, boron isotope analysis has been investigated in the Khorat basin. Qin et al. (2020) reported the values of boron isotope of anhydrite and halite are indicated marine origin. Recently, Ren et al. (2018) studied on boron and bromine concentrations in carnallite and sylvite and Li et al. (2020) analyzed  $\delta^{37}\text{Cl}$  and  $\text{Br} \times 10^3/\text{Cl}$  of halite and potash layers that these

results are mentioned hydrothermal/freshwater deposits in the late stage of evaporation in the Khorat Plateau.

In this study, we purpose to make stratigraphic correlation and to analyze elemental compositions and boron isotope in the rock salt of borehole K-203 and REE in claystone of five boreholes (K-201 K-202 K-203 K-204 and K-205) that drilled by DMR in 2018 (Figure 1). Borehole K-203 has drilled longest depth from another boreholes so it is offered most geochemical data to examine the depositional environments of evaporite deposit in the Khorat basin.

## 1.2 Objectives

1.2.1 To correlate stratigraphy of boreholes K-201 K-202 K-203 K-204 and K-205 of Maha Sarakham Formation in Changwat Chaiyaphum, northeast Thailand.

1.2.2 To analyze geochemical compositions of rock salts of boreholes K-203.

## 1.3 Study area

This study area focuses on the best way to interpret the depositional processes and environments of rock salt deposited with many methods that are stratigraphic correlation and geochemical analysis. These methods are studied from five boreholes which are located at Amphoe Bamnetnarong and Chaturat, Changwat Chaiyaphum. Five boreholes including K-201 K-202 K-203 K-204 and K-205 were selected for this study with the permission from the Department of Mineral Resources (DMR). In this study, five boreholes have been identified (Figure 1).

The borehole K-201 is located within Nong I – Lo temple, Tambon Ban Tan, Amphoe Bamnet Narong, Changwat Chaiyaphum. This borehole is in topographic map in scale 1:50,000, series L7018 sheet no. 5340 III sheet name “KING AMPHOE SAP YAI” (Thai Royal Survey Department, 1997) between latitude 15°30'48.8" N and longitude 101°44'1.1" E.

The borehole K-202 is located on Ban Mai Na Di, Tambon Ban Kham, Amphoe Chatturat, Changwat Chaiyaphum. This borehole is in topographic map in scale 1:50,000, series L7018 sheet no. 5340 III sheet name “KING AMPHOE SAP YAI” (Thai Royal Survey Department, 1997) between latitude 15°31'32.1" N and longitude 101°44'43.8" E.

The borehole K-203 is located on Ban Non Khro Tai, Tambon Ban Kham, Amphoe Chatturat, Changwat Chaiyaphum. This borehole is in topographic map in scale 1:50,000, series

L7018 sheet no. 5340 II sheet name “AMPHOE CHATURAT” (Thai Royal Survey Department, 1997) between latitude  $15^{\circ}31'36.5''$  N and longitude  $101^{\circ}45'26.7''$  E.

The borehole K-204 is located on Ban Mai Na Di, Tambon Ban Kham, Amphoe Chaturat, Changwat Chaiyaphum. This borehole is in topographic map in scale 1:50,000, series L7018 sheet no. 5340 III sheet name “KING AMPHOE SAP YAI” (Thai Royal Survey Department, 1997) between latitude  $15^{\circ}31'11.8''$  N and longitude  $101^{\circ}44'50.3''$  E.

The borehole K-205 is located within Ban Kut Khaen Samakkhi School, Tambon Ban Tan, Amphoe Bamnet Narong, Changwat Chaiyaphum. This borehole is in topographic map in scale 1:50,000, series L7018 sheet no. 5340 III sheet name “KING AMPHOE SAP YAI” (Thai Royal Survey Department, 1997) between latitude  $15^{\circ}32'08.0''$  N and longitude  $101^{\circ}43'35.3''$  E.

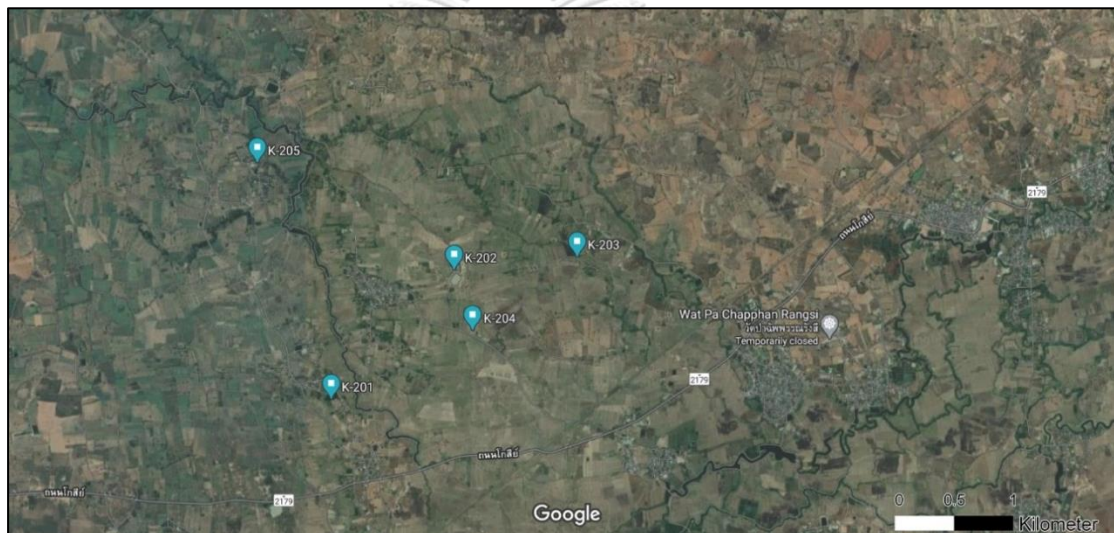


**Figure 1** Satellite image of the study area, which is located at Amphoe Bamnetnarong and Chaturat, Changwat Chaiyaphum.

## 1.4 Methodology

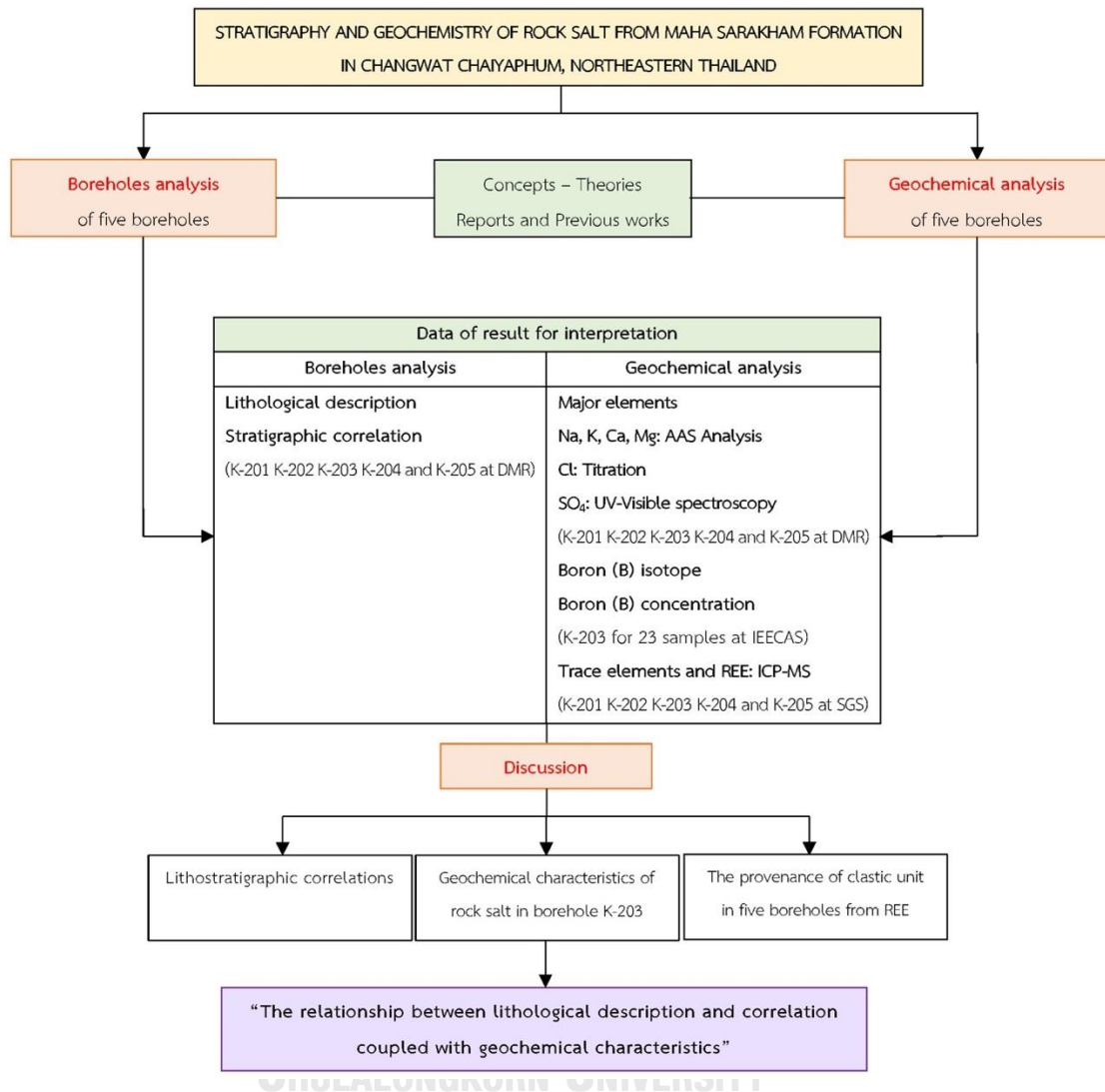


**Figure 1** Flow chart illustration of the methodology of this study.

## 1.5 Benefits

It is expected that lithological description and correlation coupled with geochemical analysis of rock salt will provide the better understanding on the depositional environment and post-depositional environment of Maha Sarakham Formation in Khorat basin.

## **Chapter 2**

### **Literature Review**

#### **2.1 Tectonic setting**

The several continental blocks of Thailand comprise the Sibumasu block, Inthanon zone, SuKhothai zone and Indochina block are assembled by the collision and opening and closure of paleo-ocean. During middle Permian to late Triassic, a collision of two blocks between the Sibumasu block (west) and the Indochina block (east) as Pale-Tethys Ocean close that produced is created the Khorat Plateau (Bunopas et al., 2001). The Indochina block has the enormous basin in the Khorat Plateau that basin is located on the northeastern Thailand and central Laos PDR. Tectonically, the margin of Indochina block is Songma suture and the South China block to the north, and Nan – Uttaradi suture, SuKhothai zone, Inthanon zone and Sibumasu block to the west (Figure 3; Minezaki et al., 2019; Sone & Metcalfe, 2008). The subsequently, the half-graben basins and were created by the tectonic activity (relaxation or extension) and during late Triassic to early Cretaceous period the continental sedimentary rocks namely Khorat Group that input to these basin (Figure 4; El Tabakh et al., 1999; Racey et al., 1996). During middle Cretaceous (Albian - Cenomanian) (Hansen et al., 2016; 2002; Sattayarak et al., 1991), from west edge of a half-graben basin was inundated by seawater (Figure 5; El Tabakh et al., 1999) that seawater precipitated the Cretaceous evaporitic rocks namely the Maha Sarakham Formation. These formation overly thick beds of continental sedimentary rock (Huai Hin Lat - Khok Kuat Formation). The deformation of the Khorat Plateau (clockwise rotational motion and southward displacement)

Sato et al. (2007) was rotated by the collision of continental between India and Eurasia (Himalaya orogeny) during early Paleocene. After these collision, the Khorat Plateau was separated into two basins, Sakon Nakhon basin in the north and Khorat basin in the south by the Phu Phan ranges lies in the NW-SE direction (El Tabakh et al., 1999; Meesook, 2000; Songtham et al., 2011; Veeravinantanakul et al., 2018).

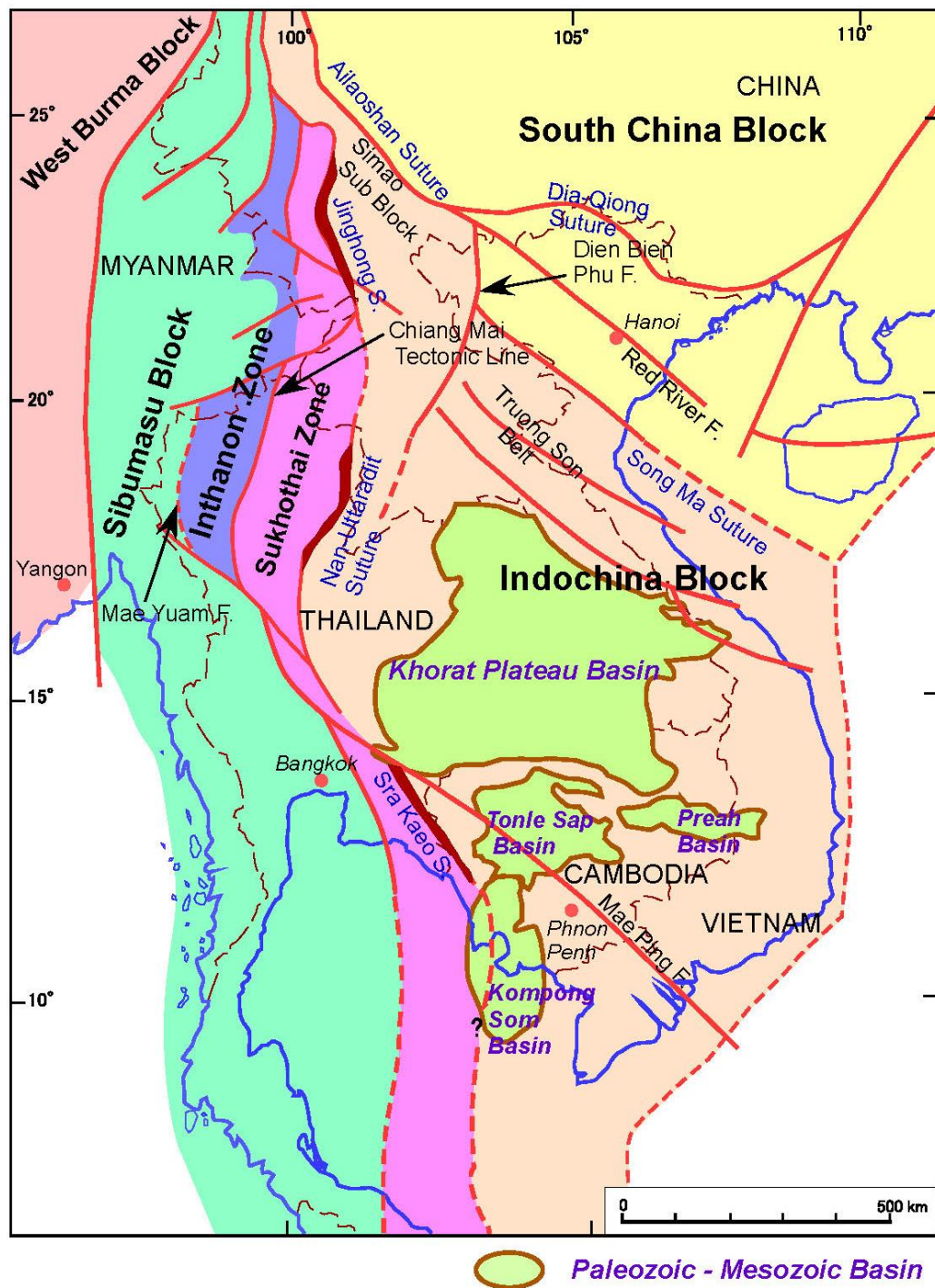


**Figure 2** Major tectonic units in the mainland Southeast Asia showing the location of the Khorat Plateau basin (Minezaki et al., 2019).

## 2.2 Geological setting

Geological data of the Khorat Plateau is modified based on geologic map of Thailand with scale 1 : 1,000,000 (DMR, 2010) and it consists mainly of several sedimentary rock formations namely Khorat Group with age ranging during Triassic to Quaternary period (Figure 4 and Figure 6).

| ERA              | TIME SCALE | SYSTEM PERIOD | SERIES EPOCHS    | LITHOLOGY             | FORMATION          | GROUP                                     | DEPOSITIONAL ENVIRONMENTS            | TECTONIC EPISODES                                  |            |
|------------------|------------|---------------|------------------|-----------------------|--------------------|---|--------------------------------------|--|------------|
| CENOZOIC         | 2.0        | Quaternary    |                  | Gravel                | Unnamed            | K H O R A T<br>G R O U P                  | Alluvial                             | India collides with Asia-Folding of Khorat Plateau |            |
|                  |            | Tertiary      |                  | Siltstone<br>Mudstone | Phu Tok            |   | Fluviatile                           |  |            |
| MESOZOIC         | 144        | Cretaceous    |                  | Rock salt<br>Mudstone | Maha Sarakham      | K H O R A T<br>G R O U P                  | Evaporitic                           | Interior Sag                                       |            |
|                  |            |               |                  | Sandstone<br>Shale    | Khok Kruat         |   | Fluviatile                           |  |            |
|                  |            |               |                  | Sandstone             | Phu Phan           |   | Fluviatile                           |  |            |
|                  |            | Upper         | Sandstone        | Sao Khua              | Fluviatile         |   |                                      |  |            |
|                  | 190        | Jurassic      | Middle           | Sandstone             | Phra Wihan         |   | Fluviatile                           |  |            |
|                  |            |               | Lower            | Sandstone             | Phu Khradung       |   | Fluviatile                           |  |            |
|                  | 200        | Triassic      | Upper            | Rhaetian              | Shale<br>Sandstone |   | Nam Phong                            |  | Fluviatile |
|                  |            |               |                  | Norian-Carnian        | Shale<br>Sandstone |   | Lower<br>Nam Phong<br>(Huai Hin Lat) |  | Fluviatile |
| Middle<br>Lower- |            |               | L.S Conglomerate | Triassic Fill         | Fluvio-Lacustrine  | Khorat Unconformity<br>Indosinian Orogeny |                                      |  |            |

**Figure 3** Stratigraphy of the Khorat Plateau (El Tabakh et al., 1999)

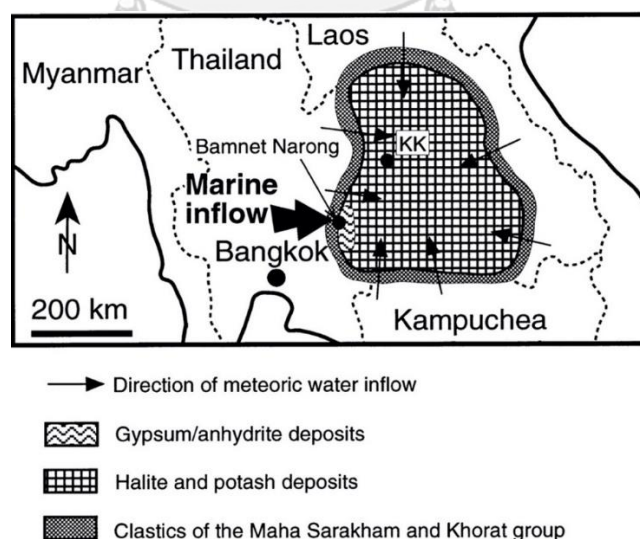


**Figure 4** Idealized map showing marine water inflow into the Khorat Plateau near Bamnet Narong area at the southwestern corner of the Khorat Plateau (El Tabakh et al., 1999).

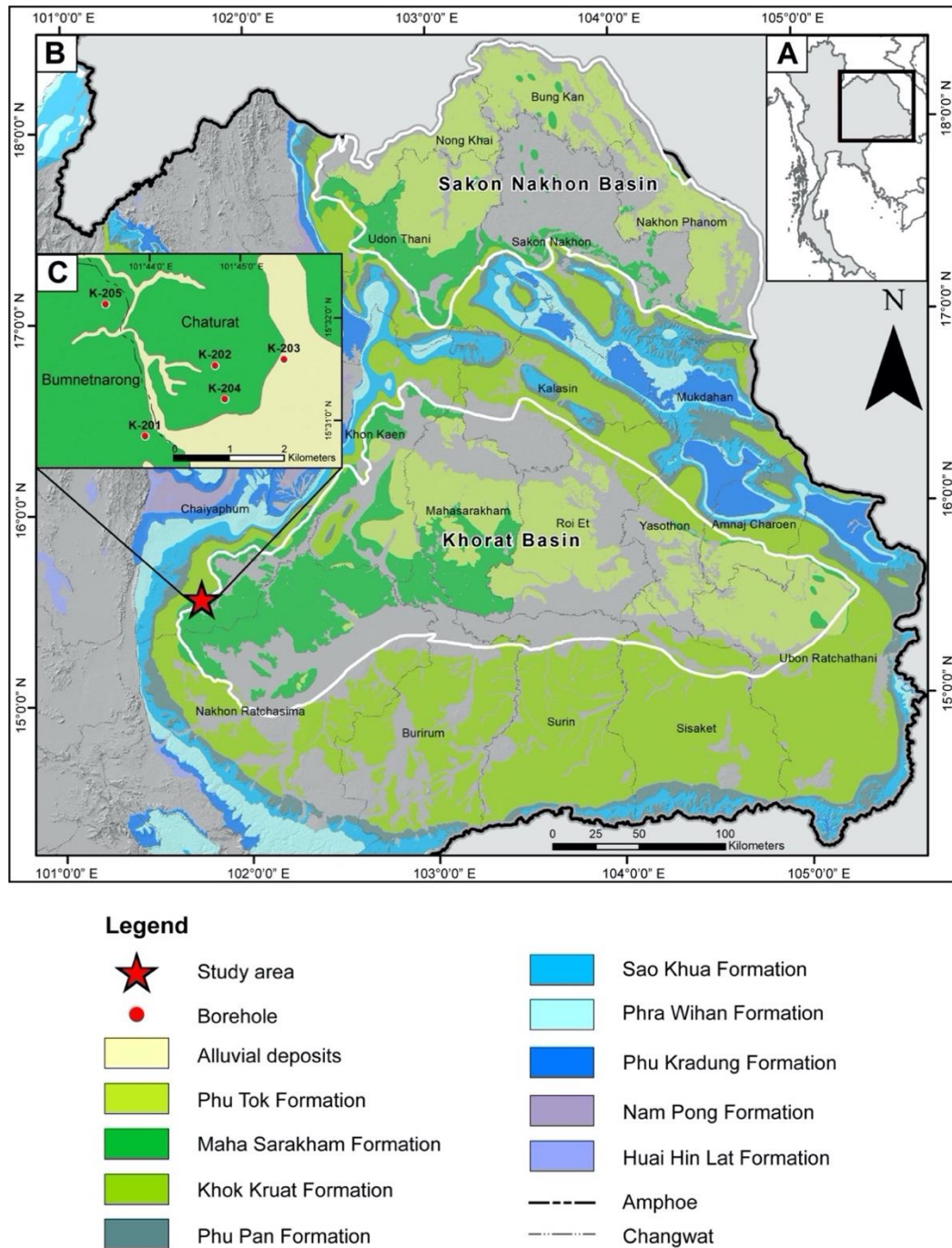


**Figure 5** Geologic map showing the distribution of the Khorat Group located in northeastern of Thailand (modified from DMR, 2010). (A) Index map of Thailand (B) locations of Khorat and Sakon Nakhon basins in northeastern Thailand (C) the study area located in Amphoe Bamnetnarong and Amphoe Chaturat, Changwat Chaiyaphum, Thailand.

The Khorat Group, Mesozoic sedimentary rocks, is composed of nine formations from bottom to top namely Huai Hin Lat, Nam Phong, Phu Kradung, Phra Wihan, Sao Khua, Phu Phan, Khok Kruat, Maha Sarakham and Phu Thok Formations. Details of each rock formation are as follow;

### **2.2.1 Triassic rocks**

Huai Hin Lat formation is unconformably overlaid the Triassic rocks, the oldest of Khorat Group, and underlined Nam Phong Formation (Sattayarak, 1983). They are mainly consisted of conglomerate, limestone conglomerate, grey to dark grey sandstone, siltstone, black shale and marl (DMR, 2014). It was deposited in fluvio-lacustrine environment under semi-arid during middle - late Triassic (DMR, 2014; El Tabakh et al., 1999). This formation is distributed along the western rim of the Khorat plateau.

Nam Phong Formation is contact with overlaid Huai Hin Lat formation and underlined Phu Kradung Formation (Sattayarak, 1983). They are mainly consisted of reddish-brown sandstone, siltstone and conglomerate (Sattayarak, 1983). It was deposited in fluvial deposits under semi-arid paleoclimate (DMR, 2014; El Tabakh et al., 1999; Sattayarak, 1983). This formation is distributed along the western rim of the Khorat plateau.

### **2.2.2 Jurassic – Cretaceous rocks**

Phu Kradung Formation is contact with overlaid Nam Phong Formation and underlined Phra Wihan Formation (Sattayarak, 1983). They are mainly three unit consisted of claystone, massive sandstone and massive sandstone interbedded with claystone from lower unit to upper unit (Sattayarak, 1983). It was deposited in meandering rivers environment under semi-arid during middle to lower Jurassic (DMR, 2014). This formation is distributed along the western rim of the Khorat plateau.

Phra Wihan Formation is contact with overlaid Phu Kradung Formation and underlined Sao Khua Formation (Sattayarak, 1983). They are mainly consisted of massive sandstone interbedded with siltstone and conglomerate (Sattayarak, 1983). It was deposited in braided streams environment under slightly humid paleoclimate during Middle Jurassic (DMR, 2014; El Tabakh et al., 1999; Sattayarak, 1983). This formation is distributed in central, throughout the Phu Phan Range, and along the western rim of the Khorat plateau.

Sao Khua Formation is contact with overlaid Phra Wihan Formation and underlined Phu Phan Formation (Sattayarak, 1983). They are mainly consisted of sandy mudstone interbedded with sandstone (DMR, 2014; El Tabakh et al., 1999). It was deposited in meandering

rivers under semi-arid condition (Meesook, 2000). This formation is distributed in central, throughout the Phu Phan Range, and along the western and southern rim of the Khorat plateau.

### **2.2.3 Cretaceous rocks**

Phu Phan Formation is contact with overlaid Sao Khua Formation and underlined Khok Kruat Formation (Sattayarak, 1983). They are mainly consisted of massive pebbly sandstone and conglomerate (Sattayarak, 1983). It was deposited in braided streams and meandering rivers environments under arid climate during upper Cretaceous (DMR, 2014; El Tabakh et al., 1999; Meesook, 2000; Sattayarak, 1983). This formation is distributed in central, throughout the Phu Phan Range, and along the western and southern rim of the Khorat plateau.

Khok Kruat Formation is contact with overlaid Phu Phan Formation and underlined unconformably of Maha Sarakham Formation (Sattayarak, 1983). They are mainly consisted of sandstone with some siltstone and claystone (Racey & Goodall, 2009; Sattayarak, 1983). It was deposited in meandering river system under semi-arid to arid during early Cretaceous (DMR, 2014; El Tabakh et al., 1999; Meesook, 2000; Sattayarak, 1983). This formation is widespread in southern of the Sakon Nakhon basin and rim of the Khorat basin.

### **2.2.4 Cretaceous-Paleogene rocks**

Maha Sarakham Formation is unconformably overlaid Khok Kruat Formation and underlined Phu Thok Formation (Sattayarak, 1983). This formation is distributed in central both the Sakon Nakhon and the Khorat basins. They are mainly three evaporite cycles divided into six units (Meesook, 2000; Racey et al., 1996) from bottom to top namely lower salt, lower clastic, middle salt, middle clastic, upper salt and upper clastic units (Figure 7).

Firstly, the lower salt is classified into three sections consist of the unconformably overlined the Khok Kruat Formation know as basal anhydrite, thick beds of halite interbedded with some anhydrite namely anhydrite stringers (El Tabakh et al., 1999) and potash minerals, respectively from lower to upper section. The potash minerals that deposited in Maha Sarakham Formation are consisted of sylvite, carnallite, tachyhydrite and accumulated with halite (El Tabakh et al., 1999; Suwanich, 1986). Secondly, the lower clastic is mostly comprised of reddish brown of claystone and overlined above the lower salt unit.

Thirdly, the middle salt is mainly contained dark honey color halite interbedded with dark smoky color halite or minor anhydrite and gypsum (El Tabakh et al., 1999) and overlined above the lower clastic unit. Next, the middle clastic was similarly to claystone in lower clastic unit and overlined above the middle salt unit. Meanwhile, the upper salt is mostly consisted of smoky gray to orange halite interbedded with minor anhydrite without potash minerals (El Tabakh et al.,

1999) and this unit overlies above the middle clastic unit. Finally, the upper clastic was similarly to claystone in lower and middle clastic units and overlies above the upper salt unit.

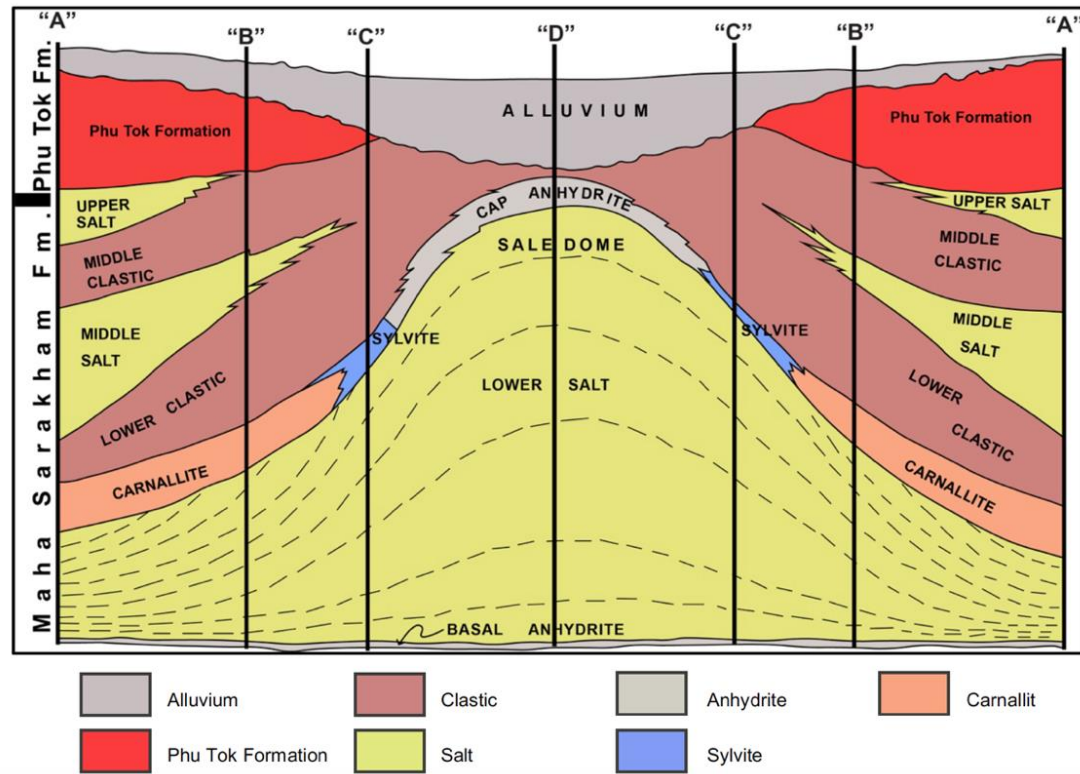


**Figure 6** Model of salt anticline in Maha Sarakham Formation of Khorat Group (modified from Suwanich, 1986)

The lithostratigraphic sequences of Maha Sarakham formation are identified two sequences including complete and incomplete sequences (Suwanich, 1986; Yumuang et al., 1986). The complete lithostratigraphic sequence (Figure 8) is almost contained all units, six units, of Maha Sarakham Formation. In contrast, the incomplete lithostratigraphic sequence is disappeared some unit from six units of Maha Sarakham Formation because of dissolution in anhydrite and halite by undersaturated groundwaters (Figure 10; Utha-Aroon, 1993). Yumuang et al. (1986) defined the deformation of salt anticline structure, post-depositional of rock salt, originated from different weight of overburdens and the high quality of plasticity of rock salt (Figure 11). Then, some unit of rock salt is disappeared from the original of evaporite stratigraphy or showing the residual of anhydrite interbedded with claystone.

| GROUP      | FORMATION               | MEMBER               | UNIT            | SYMBOL | RANGE OF THICKNESS (m.) | AVERAGE THICK. (m.) |       |
|------------|-------------------------|----------------------|-----------------|--------|-------------------------|---------------------|-------|
| KHORAT     | PHUTOK                  | Top Soil or Alluvium |                 |        | 1.00-15.24              | 6.38                |       |
|            |                         | Upper Clastic        |                 |        | 25.18-352.81            | 165.26              |       |
|            | MAHA SARAKHAM           | Upper Salt           | Up. Anhy.       |        |                         | 0-5.94              | 1.32  |
|            |                         |                      |                 |        |                         | 2.74-64.76          | 20.98 |
|            |                         | Middle Clastic       |                 |        |                         | 8.97-83.72          | 38.39 |
|            |                         |                      | Mid. Anhy.      |        |                         | 0-0.07              | 0.005 |
|            |                         | Middle Salt          |                 |        |                         | 21.55-114.91        | 85.76 |
|            |                         |                      | Lower Clastic   |        |                         | 0-61.35             | 21.90 |
|            |                         |                      | Low. Anhy.      |        |                         | 0-1.10              | 0.06  |
|            |                         |                      | Col. Salt       |        |                         | 0-8.75              | 2.33  |
|            |                         | Potash Zone          | Up. Sylvite     |        |                         | 0-3.04              | -     |
|            |                         |                      | Up. Carnallite  |        |                         | 0-5.28              | 1.24  |
|            |                         |                      | Tachyhydrite    |        |                         | 0-17.73             | 6.44  |
|            |                         |                      | Low. Carnallite |        |                         | 0-72.16             | 14.20 |
|            | Low. Sylvite            |                      |                 |        | 0-3.20                  | -                   |       |
|            | Lower Salt              |                      |                 |        | 17.47-148.47            | 61.88               |       |
|            |                         | Basal Anhydrite      |                 |        | 1.02-1.40               | 1.21                |       |
| KHOK KRUAT | Conglomerate, Sandstone |                      |                 | -      | -                       |                     |       |

Figure 7 Lithostratigraphy "A" (see figure 7) showing complete lithostratigraphic sequence discovered three salt beds (Suwanich, 1986).

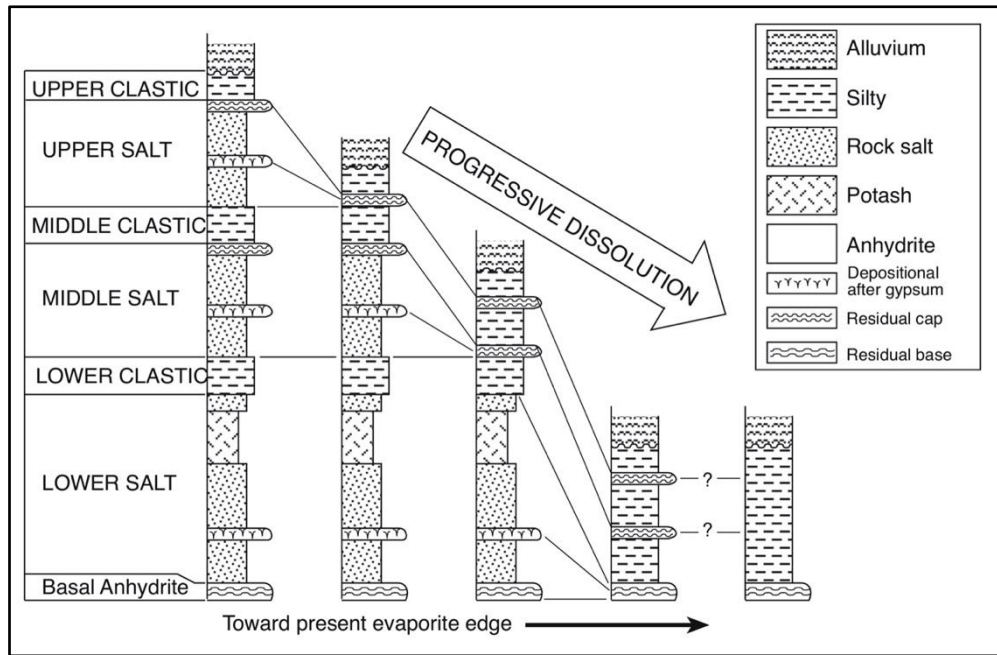


**Figure 8** Model showing the progressive dissolution of the lithostratigraphy of Maha Sarakham Formation (Utha-Aaron, 1993).

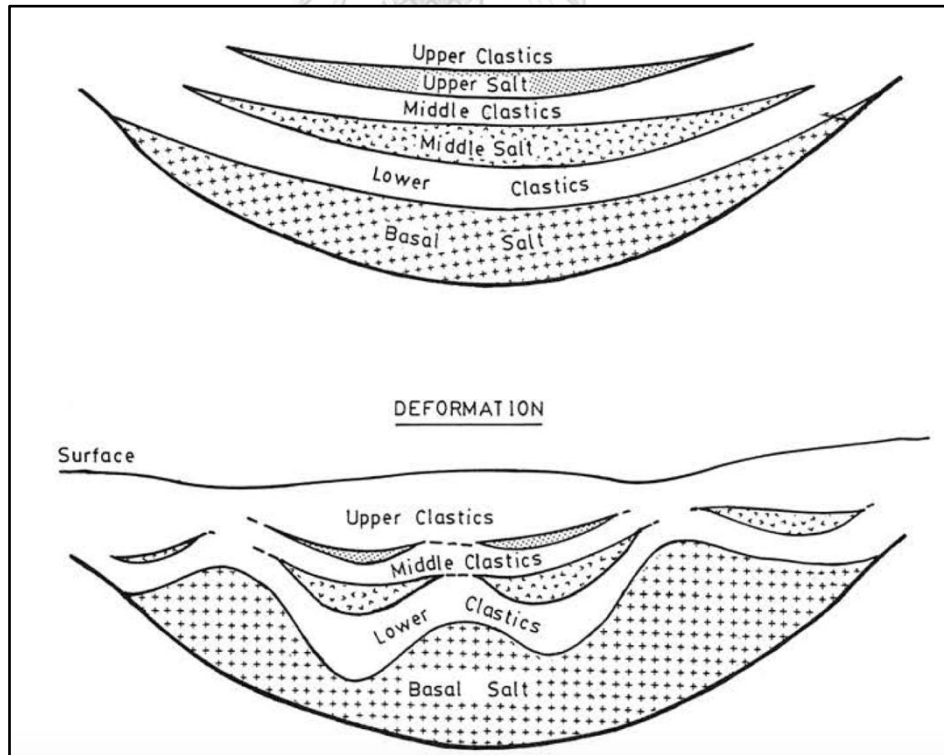


**Figure 9** Model showing the deformation of salt anticline structure (Yumuang et al., 1986).

Suwanich (1983) categorized the lithostratigraphic sequences, from many boreholes in the Khorat Plateau, into four sections consisted of section “A” (Figure 8) as the completed lithostratigraphic sequence with section “B”, “C” and “D” as the incomplete lithostratigraphic sequences. The lithostratigraphic sequences of section “B”, “C” and “D” are mainly consisted of two salt beds (Figure 11), one salt bed (Figure 12) and one salt bed without potash minerals (Figure 13), respectively.

| Group      | Formation       | Member                  | Unit           | Symbol       | Range of Thickness (m.) | Average Thick (m.) |       |
|------------|-----------------|-------------------------|----------------|--------------|-------------------------|--------------------|-------|
| KHORAT     | PHUTOK          | Top Soil or Alluvium    |                |              | 0-140.21                | 18.19              |       |
|            |                 | Upper Clastic           |                |              | 0-451.72                | 45.59              |       |
|            | MAHA SARAKHAM   |                         | Up. Anhy.      |              |                         | 0-9.72             | 1.81  |
|            |                 |                         | Middle Clastic |              |                         | 0-115.83           | 37.64 |
|            |                 |                         | Mid. Anhy.     |              |                         | 0-6.15             | 0.86  |
|            |                 |                         | Middle Salt    |              |                         | 0.17-171.95        | 64.89 |
|            |                 |                         | Lower Clastic  |              |                         | 0-67.27            | 24.47 |
|            |                 |                         | Low. Anhy.     |              |                         | 0-1.52             | 0.04  |
|            |                 |                         | Col. Salt      |              |                         | 0-45.52            | 3.49  |
|            |                 |                         | Potash Zone    | Up. Sylvite  |                         | 0-16.82            | 1.05  |
|            |                 |                         |                | Up. Carn.    |                         | 0-21.34            | 2.80  |
|            |                 |                         |                | Tachyhydrite |                         | 0-43.54            | 8.77  |
|            |                 | Low. Carn.              |                |              | 0-163.82                | 20.23              |       |
|            |                 | Low. Sylvite            |                |              | 0-19.56                 | 0.43               |       |
|            |                 | Lower Salt              |                |              | 21.66-347.93            | 120.88             |       |
|            | Basal Anhydrite |                         |                | 0.76-4.84    | 1.40                    |                    |       |
| KHOK KRUAT |                 | Sandstone, Conglomerate |                |              | -                       | -                  |       |

**Figure 10** Lithostratigraphy “B” (see figure 7) showing incomplete lithostratigraphic sequence discovered two salt beds (Suwanich, 1986).

| Group  | Formation     | Member               | Unit           | Symbol | Range of Thickness (m.) | Average Thick. (m.) |        |
|--------|---------------|----------------------|----------------|--------|-------------------------|---------------------|--------|
| KHORAT |               | Top Soil or Alluvium |                |        | 3.00-167.64             | 38.37               |        |
|        | PHUTOK        | Upper Clastic        |                |        | 0-94.54                 | 19.39               |        |
|        | MAHA SARAKHAM |                      | Up. Anhy.      |        |                         | 0-5.30              | 0.45   |
|        |               |                      | Middle Clastic |        |                         | 0-51.60             | 23.65  |
|        |               |                      | Mid. Anhy.     |        |                         | 0-10.77             | 0.91   |
|        |               |                      | Lower Clastic  |        |                         | 0-55.02             | 17.85  |
|        |               |                      | Cap Anhy.      |        |                         | 0-28.75             | 5.72   |
|        |               |                      | Lower Salt     |        |                         | 0-392.47            | 157.12 |
|        |               | Basal Anhydrite      |                |        | 0.76-6.20               | 1.41                |        |
|        | KHOK KRUAAT   | Conglo., Sandstone   |                |        | -                       | -                   |        |

**Figure 11** Lithostratigraphy “C” (see figure 7) showing incomplete lithostratigraphic sequence discovered one salt bed (Suwanich, 1986)

| Group       | Formation           | Member               | Unit           | Symbol      | Rang of Thickness (m.) | Average Thick. (m.) |       |
|-------------|---------------------|----------------------|----------------|-------------|------------------------|---------------------|-------|
| KHORAT      |                     | Top Soil or Alluvium |                |             | 3.00-94.49             | 25.97               |       |
|             | PHUTOK              | Upper Clastic        |                |             | 0-96.86                | 37.03               |       |
|             | MAHA SARA KHAM      |                      |                | Up. Anhy.   |                        | 0-2.00              | 0.35  |
|             |                     |                      | Middle Clastic |             |                        | 0-48.18             | 24.40 |
|             |                     |                      |                | Mid. Anhy.  |                        | 0.30-12.31          | 3.69  |
|             |                     |                      | Lower Clastic  |             |                        | 2.62-70.83          | 27.00 |
|             |                     |                      |                | Cap Anhy.   |                        | 0-0.30              | 0.05  |
|             |                     |                      |                | Col. Salt   |                        | 0-24.49             | 5.11  |
|             |                     | Potash Zone          |                | Up. Sylvite |                        | 0-12.65             | 5.30  |
|             |                     |                      |                | Up. Carn.   |                        | 0-10.51             | 3.16  |
|             |                     |                      |                | Tachy.      |                        | 0-9.29              | 1.10  |
|             |                     |                      |                | Low. Carn.  |                        | 0-150.91            | 25.46 |
|             |                     |                      | Low. Syl.      |             | 0-2.74                 | 0.25                |       |
|             |                     | Lower Salt           |                |             | 39.09-274.78           | 182.32              |       |
|             |                     | Basal Anhydrite      |                | 0.97-3.29   | 1.50                   |                     |       |
| KHOK KRUA T | Sandstone, Conglom. |                      |                | -           | -                      |                     |       |

**Figure 12** Lithostratigraphy “D” (see figure 7) showing incomplete lithostratigraphic sequence discovered one salt bed without potash zone (Suwanich, 1986)

In addition, the topic of the origins of depositional environment of Maha Sarakham Formation in Khorat Plateau is still debated in the present day. Hence, many studies were reported to identify characteristic and the evolution of Cretaceous evaporitic rocks. The origin of parent fluids for evaporite deposits in the Khorat Plateau are mostly classified to four viewpoints consisted of marine, non-marine, hydrothermal and the mixing fluids. Firstly, almost studies were making mention of the origin from seawater. They divided source rocks into two evidences by stratigraphy cooperated with sedimentology and geochemistry data. From stratigraphy and sedimentology are identified from characteristics of minerals, sediment facies and lithostratigraphy Japakasetr and Workman (1981); Suwanich (1986); and Yumuang et al. (1986) described the stratigraphy from 65 drillholes and inferred the bar-basin models (Figure 14) to explain the origin of Maha Sarakham Formation from seawater that model indicated deposited in a shallow epeiric sea with gentle slope when transgressive and regressive of seawater into the basin. However, the hypothesis of bar-basin is suggested the sequence of precipitation of evaporitic rocks this sequence showing the first stage to final stage of salt deposited (Table 1) consisted of Calcium Carbonate, Calcium Sulfate, Sodium Chloride, Potassium Chloride and Potassium and Magnesium, respectively (Suwanich, 1986). Geochemistry data was interpreted by bromine concentration and isotopic compositions of boron, strontium and sulphur these data are identified the marine origin (El Tabakh et al., 1999; Hite & Japakasetr, 1979; Qin et al., 2020; Ren et al., 2018; Tan et al., 2010; Zhang et al., 2013).

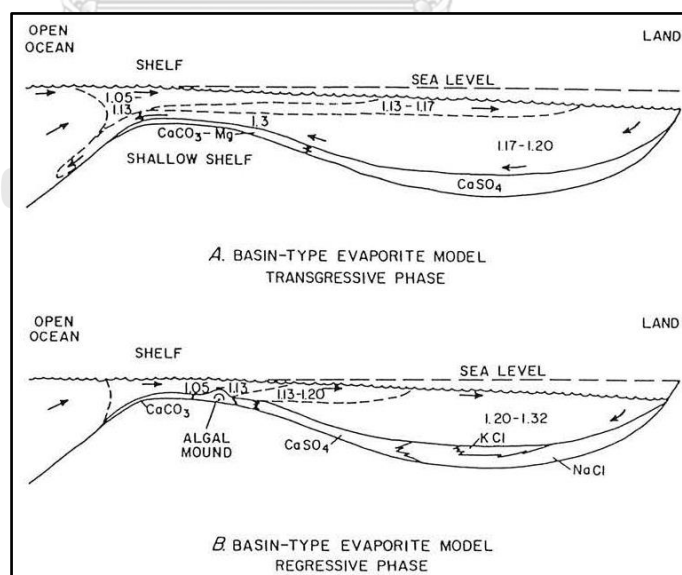


**Figure 13** Models of the bar-basin (A) the transgressive phase (B) the regressive phase (Yumuang et al., 1986)

**Table 1** Sequence of precipitation of evaporitic rocks (Suwanich, 1986)

|   | <b>Minerals</b>         | <b>Example</b>      | <b>The Chemical Formulas</b>                               | <b>Degree of Evaporation</b>  |
|---|-------------------------|---------------------|--|---|
| 1 | Calcium Carbonate       | Limestone           | CaCO <sub>3</sub>  | Prior Stage   |
| 2 | Calcium Sulfate         | Anhydrite<br>Gypsum | CaSO <sub>4</sub><br>CaSO <sub>4</sub> • 2H <sub>2</sub> O |  |
| 3 | Sodium Chloride         | Halite              | NaCl   |   |
| 4 | Potassium Chloride      | Sylvite             | KCl  |   |
| 5 | Potassium and Magnesium | Carnallite          | KCl • MgCl <sub>2</sub> •6H <sub>2</sub> O                 |   |
|   |                         |                     |  |   |

Secondly, the non-marine origin is identified by characteristic of continental clastic unit (Utha-Aroon, 1993) and the result of Bromine concentration in halite samples (Sun et al., 2019). Next, the parent rocks from hydrothermal identified by borate minerals (El Tabakh et al., 1999) and the geochemistry data of rock salt (Li et al., 2018; Ren et al., 2018). Finally, the other studies were represented the influence of mixing fluids as the consisted of different provenances fluids to forms the evaporitic rocks such as mainly marine with hydrothermal (El Tabakh et al., 1999; Timofeeff et al., 2006), mainly marine with hydrothermal and fresh water respectively (Ren et al., 2018) and hydrothermal or meteoric fluids in potash minerals of the lower salt unit (Li et al., 2020). The Maha Sarakham Formation was deposited under arid desert paleoclimate (Utha-Aroon, 1993) during middle Cretaceous (Albian - Cenomanian) (2016; Hansen et al., 2002; Sattayarak et al., 1991).

Even though, the origin of evaporite rocks are almost interested in many researchers, but the provenances of clastic units, continental sediments of the Khorat Plateau, are attentive topics not less than source of evaporite rocks. Mengyejing Formation is related to Maha Sarakham Formation because theses formations are inferred the similar of age and characteristic of sediment facies as sediment clastic rocks occurred with evaporitic rocks (Wang et al., 2014). Carter and Bristow (2003) interpreted the sources of sedimentary rocks from Qinling Orogenic Belt of zircons of Phu Kradung Formation with Fission track and U-Pb isotope.

Wang et al. (2014) analyzed using the geochemistry (REE patterns), zircon U–Pb chronology, and Hf isotope of sandstone in the Mengyejing Formation from the Simao Basin, China. REE patterns is showed the enriched of light rare earth element (LREE) relative to slightly flatted heavy rare earth element (HREE) and anomaly of Eu between 0.55-0.84 which is characterized of felsic rocks (Figure 15). These results of sandstone are suggested the temporally linked of Simao basin and the Khorat Plateau when high sea level of the Cretaceous ocean and this hypothesis supported with model of recharged the paleo-seawater (Figure 16 and 17; Qin et al., 2020). The model of recharged the paleo-seawater is identified the Meso-Tethys Ocean namely the Shan Boundary Ocean passed through Lanping-Simao basin and the Khorat Plateau during Triassic – Cretaceous. This model is interpreted based on the similarity of sedimentology, mineralogy and the provenance of evaporitic rocks between the Simao basin and the Khorat Plateau by the several lithostratigraphic columns from many countries in southeast Asia consisted of China, Myanmar, Laos, Cambodia and Thailand.

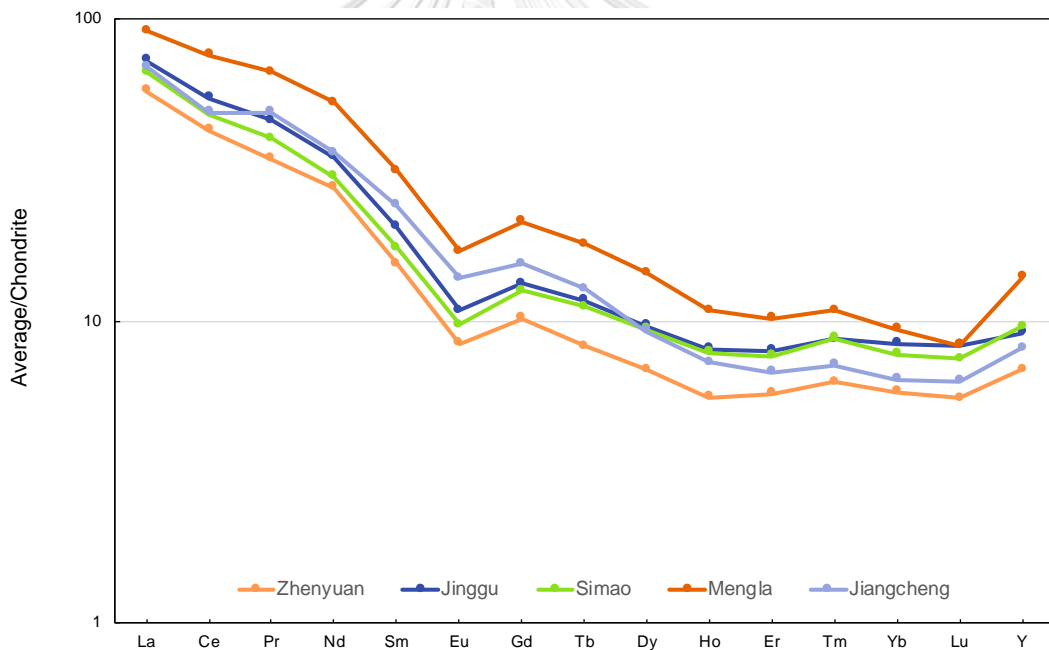


**Figure 14** Chondrite-normalized REE patterns of sandstone in the Mengyejing Formation from the Simao Basin, China plotted using chondrite normalizing values of Taylor and McLennan (1985) (modified from Wang et al., 2014)

Phu Thok Formation is on the top and youngest of the Khorat Group and overlies Maha Sarakham Formation (Sattayarak, 1983). They are mainly consisted of two types structure of reddish brown of sandstone. First type, sandstone is very large cross bedded and medium to coarse grained. Second type, sandstone is small wavy structures, very fine to silt grained and

Ripple marks. It was deposited in fluvial and eolian environments under semi-arid to arid climates during late Cretaceous – early Paleogene (El Tabakh et al., 1999). This formation is widespread in central and northern of the Khorat plateau.

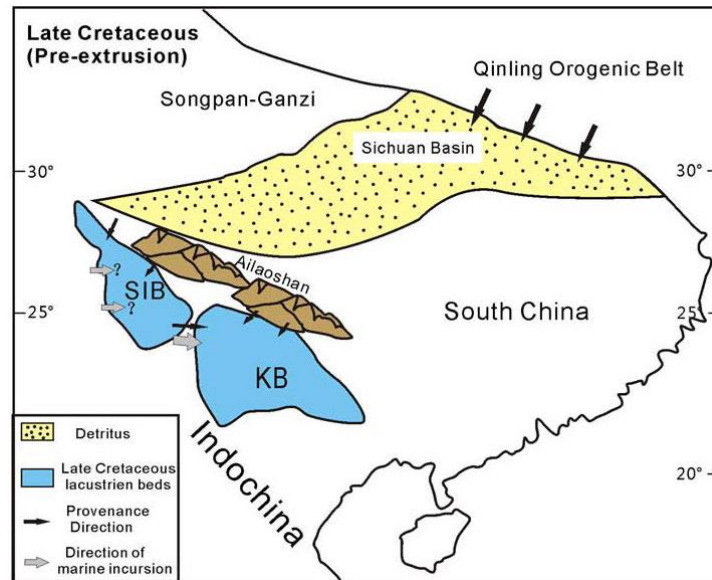


**Figure 15** The late Cretaceous paleogeography showing direction of sediment paleocurrent and direction of marine inlet of the Simao basin and the Khorat Plateau (Wang et al., 2014).

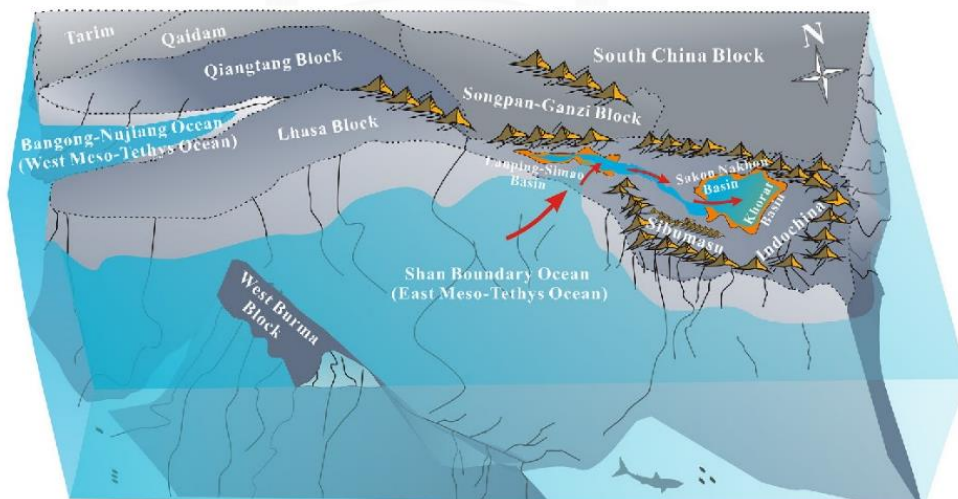


**Figure 16** The direction of paleoseawater from Shan Boundary ocean inflow into the Lanping-Simao basin and the Sakon Nakhon and Khorat basins respectively (Qin et al., 2020).

**Table 2** The Summary of the different issues of the Maha Sarakham Formation from many researchers.

| List of Reviews               | Sample                               | Methodology  | Study area         | Conclusion   |
|-------------------------------|--------------------------------------|--|--------------------|--|
| Japakasetr (1979)             | Drillholes                           | Lithology and Stratigraphy                               | Khorat Plateau     | Stratigraphic sequences                            |
| Japakasetr and Workman (1981) | Drillhole                            | Lithology and Stratigraphy                               | Khorat Plateau     |  |
| Suwanich (1983)               | Drillholes                           | Lithology and Stratigraphy                               | Khorat Plateau     |  |
| El Tabakh et al. (1999)       | Drillholes                           | Lithology and Stratigraphy                               | Khorat Plateau     |  |
| Sattayarak (1991)             | Kerogen of pollen                    | -  | Khorat Plateau     | Middle Cretaceous<br>(Albian - Cenomanian)         |
| Hansen et al. (2002)          | Claystone of the Middle Clastic Unit | Multiple isotopes  | Khorat basin       |  |
| Hansen et al. (2016)          | Anhydrites of the Middle Salt Unit   | Strontium isotope  | Khorat basin       |  |
| Hite and Japakasetr (1979)    | Drillholes                           | Bromine concentration                                    | Khorat Plateau     | Marine origin                                      |
| Yumuang et al. (1986)         | Drillholes                           | Lithology and Stratigraphy                               | Khorat Plateau     |  |
| El Tabakh et al. (1999)       | Anhydrite                            | Sulphur isotope  | Khorat Plateau     |  |
| Timofeeff et al. (2006)       | Halite                               | Bromine concentration                                    | Khorat Plateau     |  |
| Tan et al. (2010)             | Halite and Potash                    | Geochemical analysis                                     | Sakon Nakhon basin |  |
| Zhang et al. (2013)           | Borate minerals                      | Boron and Strontium isotopes                             | Sakon Nakhon basin |  |
| Ren et al. (2018)             | Halite                               | Boron isotope  | Sakon Nakhon basin |  |
| Qin et al. (2020)             | Gypsum, Anhydrite and Halite         | Boron isotope  | Sakon Nakhon basin |  |
|                               |                                      | Boron, Strontium and Sulphur isotopes                    | Sakon Nakhon basin |  |
|                               |                                      | Sedimentology and Mineralogy                             | Khorat Plateau     |  |
| Utha-aroon (1993)             | Drillholes                           | Boron and Bromine concentrations                         | Sakon Nakhon basin | Non-marine origin                                  |
| Ren et al. (2018)             | Carnallite and Sylvite               | Chlorine and Bromine concentrations                      | Sakon Nakhon basin |  |
| Sun et al (2019)              | Halite                               | Chlorine and Bromine concentrations                      | Sakon Nakhon basin |  |
| Li et al. (2020)              | Halite and Potash minerals           | Chlorine and Bromine concentrations and Chlorine isotope | Khorat basin       |  |
| El Tabakh et al. (1999)       | Tachyhydrite and Borate minerals     | Mineralogy   | Khorat Plateau     | Hydrothermal origin                                |
| Li et al. (2018)              | Halite                               | Strontium isotope  | Sakon Nakhon basin |  |
| Ren et al. (2018)             | Carnallite                           | Boron concentration                                      | Sakon Nakhon basin |  |
| Li et al. (2020)              | Halite and Potash minerals           | Chlorine and Bromine concentrations and Chlorine isotope | Khorat basin       |  |
| Carter and Bristow (2003)     | Zircons of Phu Kradung Formation     | Fission track and U-Pb isotope                           | Khorat Plateau     | Provenance of<br>claystone from the<br>Simao basin |
| Wang et al. (2014)            | Sandstone                            | U-Pb and Hf isotope and ICP-MS                           | Simao basin        |  |
| Qin et al. (2020)             | Drillholes                           | Lithology and Stratigraphy                               | Southeast Asia     |  |

## Chapter 3

### Methodology

#### 3.1 Study area

The Khorat Plateau is an area about 150,000 km<sup>2</sup> (Babel & Schreiber, 2014; Utharoon, 1993) in northeastern Thailand and central Laos PDR (Figure 18 A). The Khorat Plateau is covered the area between latitudes 14° – 19° and longitudes 101° – 106° and area's elevation about 100-200 meters above mean sea level. This plateau is forms by tectonic uplift and divides it by Phu Phan ranges in NW-SE direction into two basins inside, the Sakon Nakhon basin in the north and the Khorat basin in the south (Figure 18 B).

The sedimentary rocks of the plateau consist of conglomerate, sandstone, shale and evaporite known as the Khorat group. The evaporite in Khorat group is Maha Sarakham Formation that formation overlain unconformably by salt bearing deposits and is consisted of clastic sedimentary rocks and evaporite deposits including rock salt and potash. Maha Sarakham Formation is extended over in the Sakon Nakhon basin of about 21,000 km<sup>2</sup> and in the Khorat basin of about 36,000 km<sup>2</sup> (Hite & Japakasetr, 1979).

Study area is a part of Amphoe Bamnetnarong and Chaturat, Changwat Chaiyaphum in the Khorat basin. This area is cover from latitudes 15°32'08.0" N - 15°31'36.5" and longitudes 101°43'35.3" E - 101°44'1.1" E. They are altogether 5 drill-holes consist of K - 201, K - 202, K - 203, K - 204 and K - 205 in the study area (Figure 18 C and Figure 19) from the ground surface down to the depth range of 137 – 314 meters and the drillhole spacing range of 0.15 – 1.25 kilometers. This study area is only K - 203 and Maha Sarakham Formation (Figure 19). The geological data references by DMR (2010).

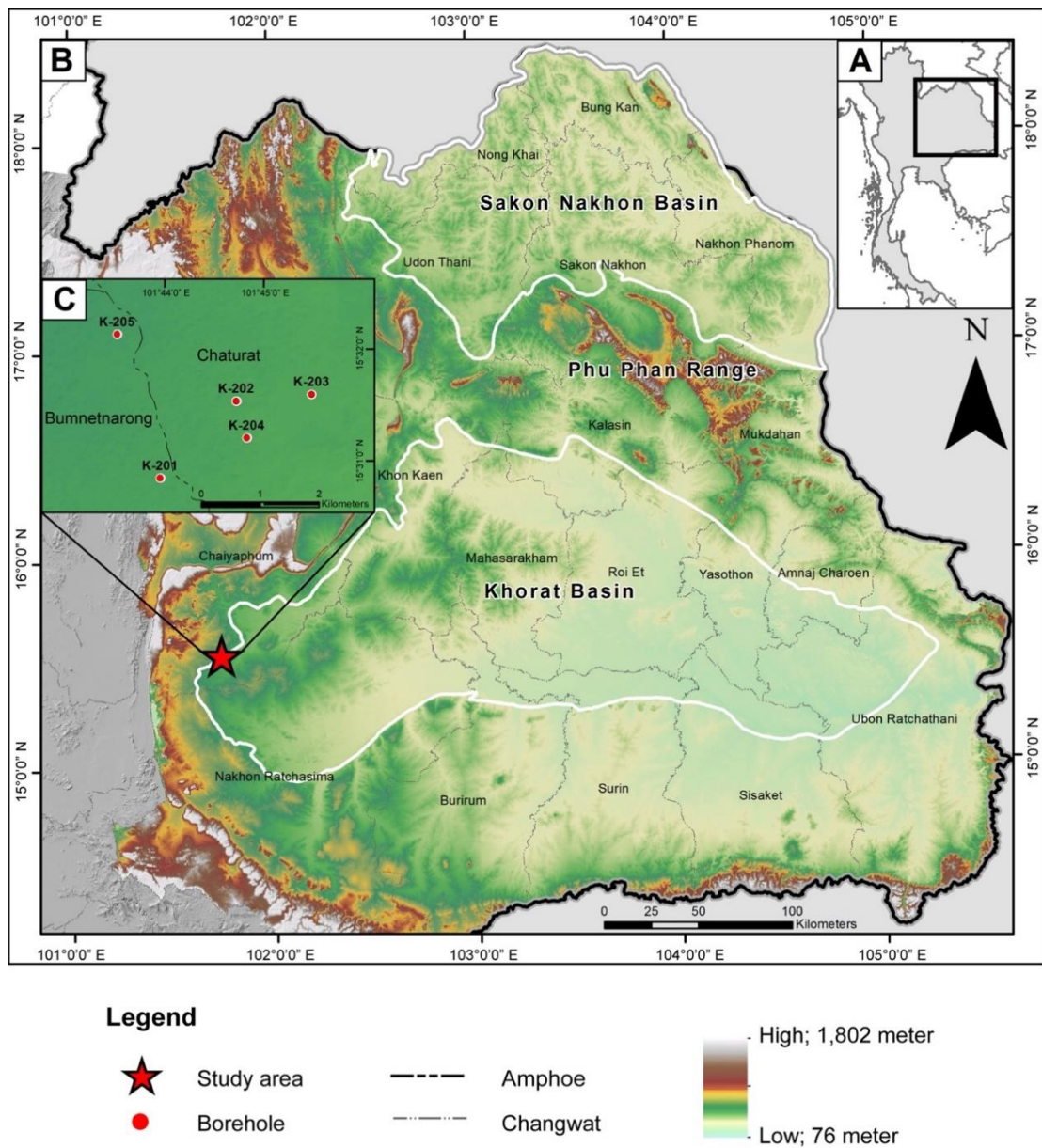


**Figure 17** Enhanced ALOS DEM map of the study area. (A) Index map of Thailand (B) locations of Khorat and Sakon Nakhon basins in northeastern Thailand (C) the study area located in Amphoe Bamnetnarong and Amphoe Chaturat, Changwat Chaiyaphum, Thailand.

### 3.2 Sampling and Sample Preparation

The samples in borehole were selected for whole rock geochemical analysis consisted of two mainly objectives. The firstly objective was suggested the origins of rock salt in borehole K-203. The secondly objective was represented the provenance of clastic rocks, that

interbedded with rock salts, from both basins between the Simao basin and the Khorat basin base on rare earth elements (REE) of clastic rock by the samples in five boreholes (K-201, K-202, K-203, K-204 and K-205). The sampling in borehole K-203 is using all of sequences (rock salt and claystone without Quaternary deposits) at the interval of 10 meter in ranges of depth from each unit until 314 meters in depth. The detailed steps of the sampling are as follows:

A) 54 samples for elemental composition in wt% and ppm.

B) 19 samples of halite and 4 samples of carnallite for boron concentrations (in ppb) and boron isotope.

C) 45 sample for REE of claystone in five boreholes; K-201-K-205 including 3 samples in K-201, 11 samples in K-202, 12 samples in K-203, 7 samples in K-204 and 12 samples in K-205 (Figure 20).

For sample preparation at the Department of Geology, Chulalongkorn University, Thailand, the chosen samples were crushed into small chips by geological hammer that covered with high quality plastic material. After that samples were divided by quartering method into 20 g into each geochemistry analysis.



**Figure 18** Borehole's analysis of rock salt at Mineral and Rock Research Center Changwat Rayong, Department of Mineral Resources.

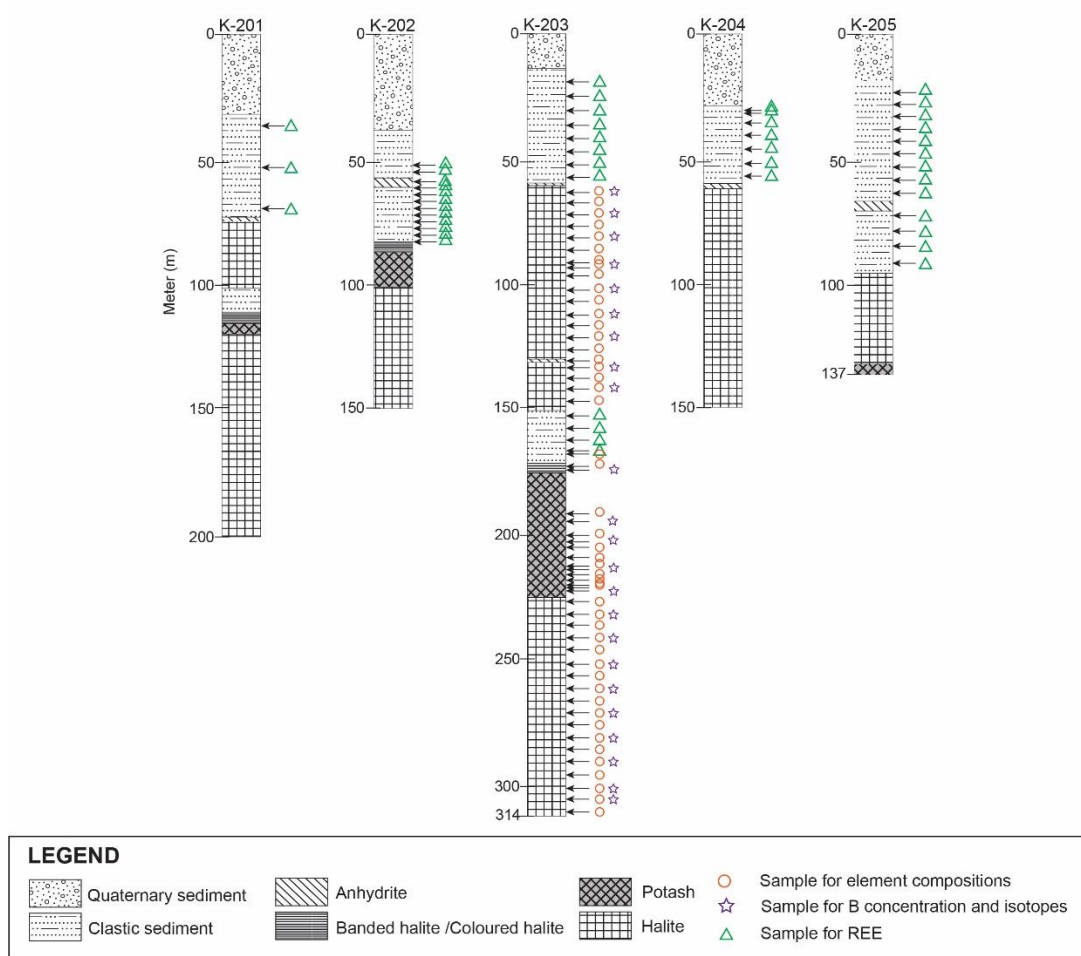


**Figure 19** The sampling sites for geochemical analyses in five boreholes (K-201-205).

### 3.3 Geochemical analysis

In this study, the geochemistry of evaporitic rocks was described the origin of rock salt and better understand how to be affected by chemistry components base on the results of geochemistry. Therefore, the geochemical analysis is divided into three sections including AAS, Titration and UV-Visible Spectroscopy analyses for major elements, inductively coupled plasma mass spectrometry (ICP-MS) for trace elements and REE and boron isotopic composition ( $\delta^{11}\text{B}$ ). The detailed of the several analyses are as follows:

#### 3.3.1 Atomic Absorption Spectroscopy (AAS), Titration and UV-Visible Spectroscopy analysis

**AAS Analysis** for cations: Na, K, Ca, and Mg

For AAS analysis, the samples were analysed at the Department of Mineral resources. The powdered samples of evaporitic rocks about  $1.000 \pm 0.001$  g were dissolved deionized water with 1 mL of HNO<sub>3</sub> 65 wt% and 1 mL of HF 48 wt% for organic matters, respectively. For elimination of SiO<sub>2</sub> put them on hotplates (250°C) until these solutions were dried. Next, all samples were added 5 mL of HNO<sub>3</sub> 65 wt% and dried its again add 5 mL of HNO<sub>3</sub> 65 wt% with deionized water after that set up all samples on hotplate (90°C) for 30 minutes.

All samples diluted into 250 mL of volumetric flasks namely solution B that were divided into two sections for dilution including 25-time and 625-time with 2.5 mL of CsCl and determined by Flame Furnace AAS (Figure 21). Last, the cations were calculated by this equation:

$$\text{Concentration (ppm)} = \frac{(\text{Absorbance}_{\text{sample}} - \text{Absorbance}_{\text{blank}}) \times \text{Volume (mL)} \times \text{Dilution factor}}{\text{Weight sample (g)}}$$



**Figure 20** Flame Furnace Atomic Absorption Spectroscopy at the Department of Mineral Resources.

#### **Titration** for anion: Cl<sup>-</sup>

For Titration analysis, the samples were analysed at the Department of Mineral Resources. The powdered samples of evaporitic rocks about  $1.000 \pm 0.001$  g were dissolved 60 mL of deionized water then put them on hotplates (150°C) until these samples completely

dissolved. Each sample was added 1 mL of  $K_2Cr_2O_4$ , as indicator. Then the chosen sample were titrated with  $AgNO_3$  as the standard solution until colour of samples changed from light yellow to dark yellow (Figure 22). Finally, Cl concentrations were calculated by this equation:

$$\text{Concentration of Cl (wt\%)} = \frac{(\text{Volume } AgNO_3 \text{ of sample (mL)} - \text{Volume } AgNO_3 \text{ of blank (mL)}) \times 35,450 \times \text{Volume of dilution (mL)}}{\text{Volume of sample (mL)} \times \text{Weight of sample (g)} \times 10,000}$$



**Figure 21** Titration analysis at the Department of Mineral Resources.

#### **UV-Visible spectroscopy** for anion: $SO_4^{2-}$

For UV-Visible spectroscopy analysis, the samples were analysed at the Department of Mineral Resources. Fifty-four samples of evaporitic rocks were grinded into powder. For buffer solution A is mixture solution consisted of  $MgCl_2$  in 30 g,  $CH_3COONa$  in 5 g and  $KNO_3$  in 1 g next added  $CH_3COOH$  in 20 mL with deionized water in 500 mL and diluted again with deionized water in 1,000 mL. Mixing the solutions between standard solution of  $SO_4$  in 25 mL and Buffer Solution A in 10 mL by magnetic stirring, next adding  $BaCl_2$  in 0.2 mL. These solutions are determined by a HITACHI U-2900 spectrophotometer (Figure 23) to measure the ratio optical density with 410 nm of wavelength in 1 minutes. Finally,  $SO_4$  concentrations were calculated by this equation:

$$\text{Concentration of SO}_4 \text{ (ppm)} = \frac{\text{Optical density of sample} \times \text{Volume of dilution (mL)}}{\text{Optical density of standard} \times \text{Weight of sample (g)}}$$



**Figure 22** A HITACHI U-2900 spectrophotometer at the Department of Mineral Resources.

### 3.3.2 Inductively coupled plasma mass spectrometry (ICP-MS)

For trace element and REE were divided into two section according to the materials and objective in this study consisted of rock salt and claystone. The sixteen samples of rock salts (anhydrite, halite and carnallite) were analyzed for trace elements and the forty-five samples of claystone analyzed for REE consisted of La, Ce, Pr, Nd, Sm, Eu, Gd, Tb, Dy, Ho, Er, Tm, Yb, Lu, and Y.

For ICP-MS analysis at SGS Canada Inc. - Minerals – Lakefield. Each powder of claystone of five borehole and evaporitic rocks of borehole K-203 were fused with sodium peroxide. These samples are determined by Perkin Elmer Elan 6100 ICP-MS with several calibration standards (SY-4, RTS-3A and OREAS-602) and internal standard solution (50 ppb Re and 10 ppb Rh). At SGS Canada Inc. - Minerals – Lakefield has not analyzed boron element, so we must analyze that an element at Xi'an, China.

For ICP-MS analysis at the State Key Laboratory of Loess and Quaternary Geology, Institute of Earth Environment, Chinese Academy of Sciences (IEECAS) Xi'an, China. Firstly, the twenty-three samples of rock salts (halite and carnallite) were cleaned with ethanol and heated at  $>40^{\circ}\text{C}$  in an air-dry oven around 10-12 hours. After that, the samples were crushed with an agate mortar to 200 mesh size. Samples with weight of about  $2.000 \pm 0.001$  grams were dissolved in pure

water 15 ml and these solution uses 0.2  $\mu\text{m}$  Whatman nylon filters. Then, the dissolved solution was diluted in pure water 30 times and diluted again in 2%  $\text{HNO}_3$  30 times, respectively (Figure 24). However, some samples with low boron concentrations were dissolved again in pure water and then diluted with 2%  $\text{HNO}_3$  only 10 times. The boron concentrations were analyzed by a Perkin Elmer Nexion 300D ICP-MS (Figure 25).



**Figure 23** Diluted solution for analyzed boron concentrations in laboratory of boron at IEECAS.



**Figure 24** A Perkin Elmer Nexion 300D ICP-MS at IEECAS.

### 3.3.3 Boron concentrations and Boron Isotope ( $\delta^{11}\text{B}$ )

Boron isotopes was analysis at the State Key Laboratory of Loess and Quaternary Geology, Institute of Earth Environment, Chinese Academy of Sciences (IEECAS) in Xi'an. He et al. (2015 and 2019) mentioned the processing of B chromatography by the Amberlite IRA 743 resin (80–100 mesh sizes). Firstly, the twenty-three samples of halite and carnallite are make the solutions about 300 ng by dissolved in pure water. Secondly, these solutions were used the Amberlite IRA 743 resin (80–100 mesh sizes) with 6.5 ml of pure water and 5 ml of 0.5 mole/L  $\text{HNO}_3$  (Figure 26). These steps are productive for remove the cations from solution and this solution has boron content about 100 ppb. Finally, the boron isotopes were analyzed using a NEPTUNE Plus MC-ICP-MS (Thermo Fisher Scientific, Germany) (Figure 27; He et al., 2019).



**Figure 25** Diluted solution for analyzed boron isotope in laboratory of boron at IEECAS.



**Figure 26** A NEPTUNE Plus MC-ICP-MS (Thermo Fisher Scientific, Germany) at IEECAS.

The two stable boron isotopes were mainly consisted of  $^{10}\text{B}$  and  $^{11}\text{B}$  that showing significant isotope fractionation.  $^{10}\text{B}$  such as  $\text{B}(\text{OH})_4^-$  is occurred in the tetragonal form, whereas  $^{11}\text{B}$  such as  $\text{B}(\text{OH})_3$  is occurred in the trigonal form. The values of boron isotopic composition are distinguished the evaporite settings between marine and non-marine (Palmer and Swihart, 1996; Vengosh et al., 1992; Warren, 2005 and Xiao et al., 2013). The values of marine source are between  $+18.2\text{‰}$  to  $31.7\text{‰}$  and non-marine source between  $-30.1\text{‰}$  to  $+7.0\text{‰}$  (Figure 28).

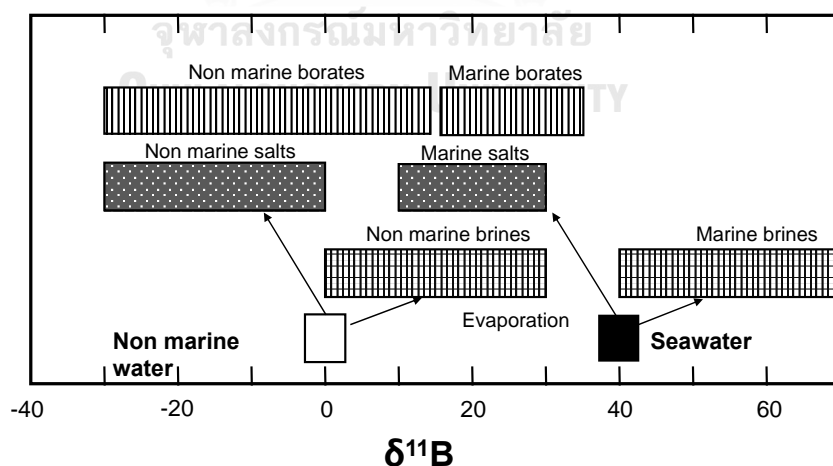


**Figure 27** The range boron isotopic composition for form of evaporitic rocks to relate the provenance distinguished between marine and non-marine (modified from Palmer and Swihart, 1996).

## Chapter 4

### Results

#### 4.1 Stratigraphy of boreholes K-201 K-202 K-203 K-204 and K-205

##### 4.1.1 Borehole K-201

Located: Wat Nong I–Lo, Tambon Ban Tan, Amphoe Bamnet Narong, Changwat Chaiyaphum

Latitude: 15°30'48.8" N, Longitude: 101°44'1.1" E

Elevation: 212 meters (MSL)

Date of drilling: 23 March 2018 – 26 April 2018

Depth: 0-200 meters

##### Unit S1

The unit S1 was cored from 110.5-200.0 meters. They are composed of thick bed of halite with anhydrite stringers and carnallite and upper unit including several color bands salt, respectively from lower to upper.

The interval between 110.5-200.0 meters is halite. Almost halite is clear, transparent, white, and smoky dark bands, milky white medium to coarse grained associated with anhydrite stringers along these unit. Both intervals between 161.0-164.3 meters and 152.2-155.0 meters founded orange and honey halite associate with reddish brown clay (Figure 29). The interval between 164.3-200.0 meters is piece of halite, milky white medium to coarse grained (Figure 30). It contains the anhydrite stringers associated with smoky dark bands of halite.



**Figure 28** a section of lower portion of unit S1 of K-201. Clear, transparent, white, and smoky dark bands halite close to the contact of orange and honey halite associate with reddish brown clay at 152.2 meters T = top; B = bottom.



**Figure 29** Core photograph showing piece of halite of unit S1 from K-201. T = top; B = bottom.

The interval between 110.5-119.0 meters is potash zone including several color bands salt interbedded with carnallite (Figure 31). The carnallite associate with halite are present at both interval between 115.0-119.0 meters and 112.0-114.0 meters. Carnallite is brown, deep red, red, orange, pink and colorless, medium to coarse grained (Figure 32) which some zone of carnallite is composed of milky white, clear, and smoky dark of massive halite. The several color bands salt is orange, red, gray, smoky dark, milky white and colorless that salts are thin beds at both interval between 114.0-115.0 meters and 110.5-112.0 meters.



**Figure 30** Core photographs showing several color bands salt interbedded with carnallite of unit S1 from K-201. T = top; B = bottom.



**Figure 31** Close up of carnallite showing granular and medium to coarse grained at 117.8 meters from K-201.

#### Unit C1

The unit C1 is claystone at 100.3-110.5 meters. Claystone is mostly weak red to reddish brown and greenish gray in some portion (Figure 33), semi-consolidated, mud grained and well sorted. At the intervals between 107.0-108.0 meters showing reddish brown clay interbedded with greenish gray, which are about 1 meter thick.



**Figure 32** Core photograph showing mudstone of unit C1 from K-201. T = top; B = bottom.

#### Unit S2

The unit S2 was cored from 72.4-100.3 meters. They are composed of anhydrite in upper unit and thick bed of halite associated with anhydrite stringers in the lower unit, respectively from lower to upper.

Halite is milky white, colorless, smoky dark and honey associated with anhydrite stringers at 73.5-100.3 meters. There are two halite sequences, the lower unit at interval

between 88.7-100.3 meters is halite. Halite is pale yellowish brown namely honey and orange halite associated with inclined smoky dark bands, decreased until absent of anhydrite stringers from upper to lower (Figure 34). The upper unit at interval between 88.7-100.3 meters consists of milky white, colorless, and smoky dark associated with anhydrite stringers that gray, white and dark smoky anhydrite bands overlying inclined halite beds (Figure 35) about 2-5 centimeters thick. The interval between 72.4-73.5 meters is anhydrite and gypsum. Anhydrite associated with gypsum are white and light gray, and hard to brittle.



**Figure 33** Core photograph showing honey halite associated with inclined smoky dark bands halite of unit S2 from K-201. T = top; B = bottom.



**Figure 34** Core photograph showing halite associated with anhydrite stringers that gray, white and dark smoky anhydrite bands overlying inclined halite beds of unit S2 from K-201.

## Unit C2

The unit C2 are two sequences consist of siltstone and claystone at 31.0-72.4 meters. Lower unit is very dark gray claystone associated with greenish gray spot, semi-consolidated, mud grained and well sorted at the intervals between 68.1-72.4 meters. At the intervals between 62.7-68.1 meters is dark reddish-brown claystone associated with light greenish gray spot, semi-consolidated, mud grained and well sorted. Upper unit is reddish brown siltstone associated with light greenish gray spot, very fine to silt grained, well sorted, sub-rounded to rounded, low sphericity at the intervals between 31.0-62.7 meters.



**Figure 35** Core photograph showing siltstone of unit C2 from K-201. T = top; B = bottom.

## Unit Q

The unit Q was cored from 0.0-31.0 meters. They are composed of clayey sand interbedded with sand and upper part of unit is sandy clay.

The interval between 13.4-31.0 meters is clayey sand. The clayey sand is semi-consolidated pale yellow (fresh surface) and strong brown (weathering surface), contains mainly fine to very fine grained, well sorted, rounded to sub-rounded, high sphericity.

The interval between 8.0-13.4 meters is sand. The sand is unconsolidated brown to pale brown and several colors of grain consist of black, gray, orange, brown, yellow, white and colorless, very coarse to very fine grained, sub-angular to sub-rounded, moderated sorted, high to low sphericity.

The interval between 7.0-8.0 meters is clayey sand. The clayey sand is semi-consolidated pale brown, contains mainly fine to very fine grained but some interval has nodule of limestone, poorly sorted, rounded to sub-rounded, high to low sphericity.

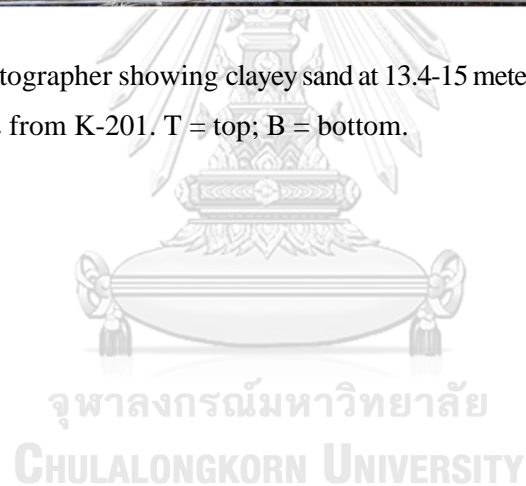
The interval 7.0-5.0 meters is sand. The sand is unconsolidated reddish yellow, and several colors of grain consist of black, gray, orange, brown, yellow, white, and colorless, very

coarse to very fine grained, sub-angular to sub-rounded, moderated sorted, high to low sphericity.

The interval 0.0-5.0 meters is sandy clay. The sandy clay is unconsolidated very pale brown and several colors of grain consist of black, gray, orange, brown and colorless, contains mainly fine to very fine grained, sub-angular to sub-rounded, moderated sorted, high to low sphericity.



**Figure 36** Core photograph showing clayey sand at 13.4-15 meters and sand at 10-13.4 meters of unit C2 from K-201. T = top; B = bottom.



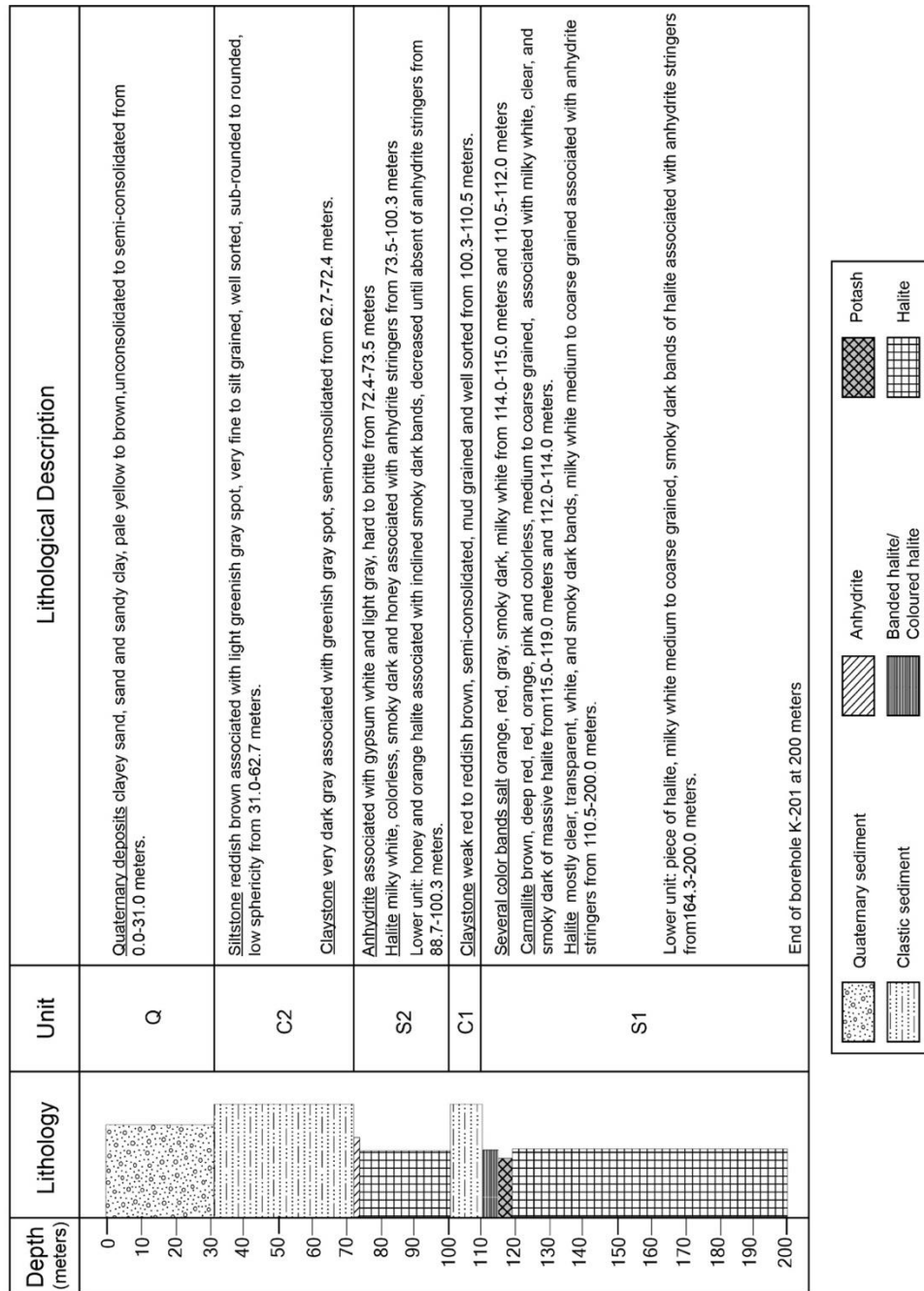


Figure 37 Lithological description of borehole K-201 of Maha Sarakham Formation in Changwat Chaiyaphum, northeastern Thailand.

#### 4.1.2 Borehole K-202

Located: Ban Mai Na Di, Tambon Ban Kham, Amphoe Chaturat, Changwat Chaiyaphum

Latitude: 15°31'32.1" N, Longitude: 101°44'43.8" E

Elevation: 210 meters (MSL)

Date of drilling: 4 May 2018 – 10 May 2018

Depth: 0-150 meters

##### Unit S1

The unit S1 was cored from 83.2-200.0 meters. They are three sequences consist of halite with anhydrite stringers, sylvinite several color bands salt, respectively from lower to upper.

First, lower unit is halite at 113-200.0 meters. Almost halite is clear, milky white, and quite horizontal smoky dark bands associated with anhydrite stringers along these unit (Figure 39). The thickness of anhydrite bed is about 0.5-2.0 centimeters. Carnallite spots are founded at interval between 105.3-106.0 meters and 112.7-113.0 meters.

Second, middle unit is mixing between halite with sylvite namely sylvinite at 87.2-113.0 meters. The interval between 103.0-113.0 meters is sylvinite (Figure 40). Halite is colorless, white, greenish gray and smoky dark bands, large crystals illustrated about 0.2 and over 1.0 centimeters, massive, invisible anhydrite stringers. Sylvite is colorless and cloudy white, sylvite large crystals illustrated about 0.2-1.5 centimeters and cube (Figure 42A). The interval between 87.2-103.0 meters is blue sylvinite (Figure 41). Sylvite is almost bluish and colorless, little cloudy white, massive, crystals illustrated about over 1.0 centimeters. Halite is blue sapphire (Figure 42B), colorless and little cloudy white, that blue halite occurs with sylvite, 87.2-113.0 meters.

Finally, upper unit is several color bands salt at 83.2-87.2 meters. Several color bands salt is orange, red, brown, and grey, grain of crystals illustrated about 1.0-3.0 centimeters, invisible anhydrite stringers.



**Figure 38** Core photograph showing halite of unit S1 from K-202. T = top; B = bottom.



**Figure 39** Core photograph showing sylvinitic and halite of unit S1 from K-202. T = top; B = bottom.



**Figure 40** Core photograph showing bluish sylvite and halite of unit S1 from K-202. T = top; B = bottom.



**Figure 41** A) Transparent sylvite crystals showing cube of unit S1 from K-202.

B) Close up of blue halite of unit S1 from K-202.

### Unit C1

The unit C1 was cored from 60.5-83.2 meters. Claystone is reddish brown and dark reddish brown associated with light greenish gray spot (Figure 43), semi-consolidated, mud grained and well sorted. At the intervals between 78.1-83.2 meters showing dark gray claystone mixing fragments of halite at 77.6, 80.4 and 80.9 meters.



**Figure 42** Core photograph showing mudstone of unit C1 from K-202. T = top; B = bottom.

### Middle anhydrite unit

The middle anhydrite unit was cored from 56.7-60.5 meters. Anhydrite is white and dark gray associated with black carbonaceous matter layers, massive, laminated with locally nodular cloudy white grains, inclined laminated showing 40°-50° dipping, micro folded, drag fold and faulting (Figure 44).



**Figure 43** Close up of Anhydrite showing micro folded, drag fold and faulting of middle anhydrite unit from K-202.

#### Unit C2

The unit C2 was cored from 38.0-56.7 meters. Claystone is reddish brown associated with light greenish gray spot (Figure 45), semi-consolidated, mud grained and well sorted. At the intervals between 45.0-45.4 meters is discovered calcareous rock and very dark greenish gray claystone with tasting of salty near contact anhydrite at 52.9-56.7 meters.



**Figure 44** Core photograph showing reddish brown mudstone until then very dark greenish gray claystone at 52.9 meters of unit C2 from K-202. T = top; B = bottom.

#### Unit Q

The unit Q was cored from 0.0-38.0 meters. They are 3 sequences including sand, clayey sand and sand mixing granule grained. Firstly, lower unit is sands at 32.0-38.0 meters. Sands are yellowish brown, unconsolidated, fine to very fine grained, well sorted,

subrounded to rounded, low sphericity and colors of grain including black, red, brown, yellow, and colorless.

Second, middle unit is clayey sand at 5.0-32.0 meters. Clayey sand is strong brown, yellowish brown, and reddish brown, semi-consolidated, fine to very fine grained, well sorted, subrounded to rounded, low to high sphericity, organic matter in some portion. At the intervals between 21.0-23.0 meters is sands. Sands are reddish brown, unconsolidated, fine to very fine grained, well sorted, subrounded, low sphericity and colors of grain including black, red, brown, yellow, and colorless.

Last, upper unit is sands mixing granule grained at 0.0-5.0 meters. sands mixing granule grained are silt to granule grained, unconsolidated, poorly sorted, subangular to subrounded, high to low sphericity and colors of grain including black, red, brown, yellow, gray, and colorless.



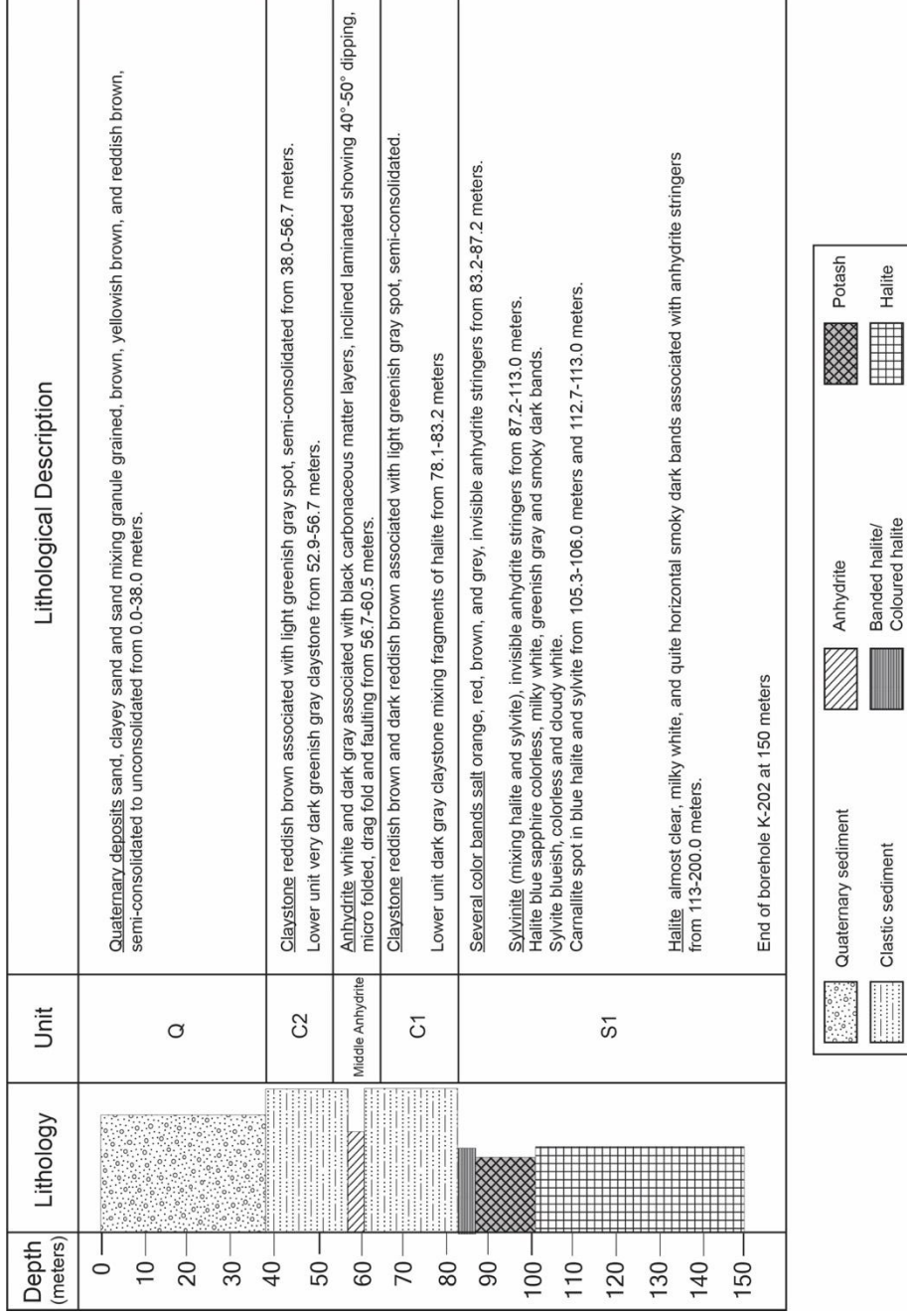


Figure 45 Lithological description of borehole K-202 of Maha Sarakham Formation in Changwat Chaiyaphum, northeastern Thailand.

### 4.1.3 Borehole K-203

Located: Ban Non Khro Tai, Tambon Ban Kham, Amphoe Chaturat, Changwat Chaiyaphum

Latitude: 15°31'36.5" N, Longitude: 101°45'26.7" E

Elevation: 206 meters (MSL)

Date of drilling: 4 May 2018 – 4 June 2018

Depth: 314 meters

#### Unit S1

The unit S1 was cored from 173.3-314.0 meters. They are three sequences consist of halite with anhydrite stringers, carnallite mixing halite, and several color bands salt, respectively from lower to upper.

First, lower unit is halite at 225.2-314.0 meters. Almost halite is clear, milky white, and quite horizontal smoky dark bands associated with anhydrite stringers (Figure 47). The thickness of anhydrite bed is about 1.0 centimeters. Size of scattered milky white are about 1-3 centimeters.

Second, middle unit is carnallite mixing halite (Figure 48) at 176.2-225.2 meters. Carnallite is deep red to light red, orange, pink that carnallite occur with transparent, colorless, milky white and, little smoky dark bands, invisible anhydrite stringers. Almost grains milky white of grains size are about 0.2-0.7 centimeters.

Finally, upper unit is several color bands salt (Figure 49) at 173.3-176.2 meters. Several color bands salt is orange, red, brown, grey, and smoky dark bands, quite horizontal color band, length of color bands about 1-10 centimeters, invisible anhydrite stringers.



**Figure 46** Core photograph showing halite associated with anhydrite stringers at lower part of unit S1 from K-203. T = top; B = bottom.



**Figure 47** Core photograph showing carnallite mixing halite of medium unit S1 from K-203.

T = top; B = bottom.



**Figure 48** Core photograph showing several color bands salt of upper unit S1 from K-203.

T = top; B = bottom.

### Unit C1

The unit C1 was cored from 150.7-173.3 meters that unit has two sequences consist of lower unit (claystone) and upper unit (claystone mixing fragments of halite and carnallite).

Lower unit is claystone at 160.0-173.3 meters. Claystone is dark brown, dark gray and reddish gray associated with light greenish gray spot, semi-consolidated, mud grained and well sorted. Upper unit is claystone mixing fragments of halite and carnallite at 150.7-160.0 meters. Claystone is reddish brown to dark reddish brown, semi-consolidated, mud grained, well sorted. Carnallite is red, pink, and orange with form veins associated with fragments of smoky dark halite (Figure 50).



**Figure 49** Core photograph showing claystone of unit C1 from K-203. White circle = fragments of carnallite; T = top; B = bottom.

### Unit S2

The unit s2 was cored from 59.4-150.7 meters. They are three sequences consist of halite associated with anhydrite stringers, anhydrite marker, and halite, respectively from lower to upper unit.

First, lower unit is halite (Figure 51) at 131.4-150.7 meters. Almost halite is dark honey and honey with some colorless and quite horizontal smoky dark bands and decreased and absent anhydrite stringers from top to bottom of lower unit S2.

Second, middle unit is anhydrite marker (Figure 52) at 130.0-131.4 meters. Anhydrite is white and dark gray associated with black carbonaceous matter layers, massive, laminated with locally nodular cloudy white grains.

Finally, upper unit is halite associated with anhydrite stringers (Figure 53) at 59.4.3-130.0 meters. Almost halite is honey with some colorless and quite horizontal smoky dark bands associated with quite horizontal and inclined layers of anhydrite stringers. Four composition of halite in upper unit S2 including darker honey color of halite, smoky dark bands, milky white grains, and anhydrite stringers are increasing from top to bottom of upper unit S2. Anhydrite stringers are dark gray associated with black carbonaceous matter layers. The thickness of anhydrite stringers for each bed

are 1-30 centimeters. At the intervals between 59.4-59.6 meters is anhydrite that top portion of upper unit S2. Anhydrite is white and gray associated with black carbonaceous matter layers, laminated.



**Figure 50** Core photograph showing halite of lower unit S2 from K-203. T = top; B = bottom.



**Figure 51** Core photograph showing anhydrite marker at 130.0-131.4 meters of middle unit S2 from K-203. T = top; B = bottom.



**Figure 52** Core photograph showing halite associated with anhydrite stringers of upper unit S2 from K-203. T = top; B = bottom

### Unit C2

The unit C2 was cored from 13.7-59.4 meters. Claystone is reddish brown associated with light greenish gray spot (Figure 54), semi-consolidated, mud grained and well sorted. At the middle portion of unit C2 from 28.1-50.0 meters is discovered colorless gypsum fragments and veins about less than 1 centimeters and near contact anhydrite at 55.3-59.4 meters founded almost very dark gray claystone with gray claystone in some portion and tasting of salty.



**Figure 53** Core photographs showing claystone of unit C2 from K-203. T = top; B = bottom.

### Unit Q

The unit Q was cored from 0.0-13.7 meters. They are three sequences including clayey sand, sand, and clayey sand. Firstly, lower unit is clayey sand at 9.7-13.7 meters. Clayey sand is white, very pale brown, and yellowish brown, semi-consolidated, fine to very fine grained, well sorted, subrounded to rounded, low sphericity.

Second, middle unit is sand at 8.0-9.7 meters. Sands are light yellowish brown to yellowish brown, unconsolidated, medium to very fine grained, well sorted, subrounded to rounded, low sphericity, and colors of grain including black, red, brown, yellow, gray, and colorless.

Last, upper unit is clayey sand at 0.0-8.0 meters. Clayey sand is yellow and light yellowish brown, coarse to very fine grained, unconsolidated, poorly sorted, subangular to subrounded, high to low sphericity and colors of grain including black, red, brown, yellow, gray, and colorless at 0.0-7.3 meters. At the intervals between 7.3-8.0 meters is clayey sand. Clayey sand is white and very pale brown, semi-consolidated, medium to very fine grained, well sorted, surrounded to rounded, low sphericity and colors of grain including black, red, brown, yellow, and colorless.

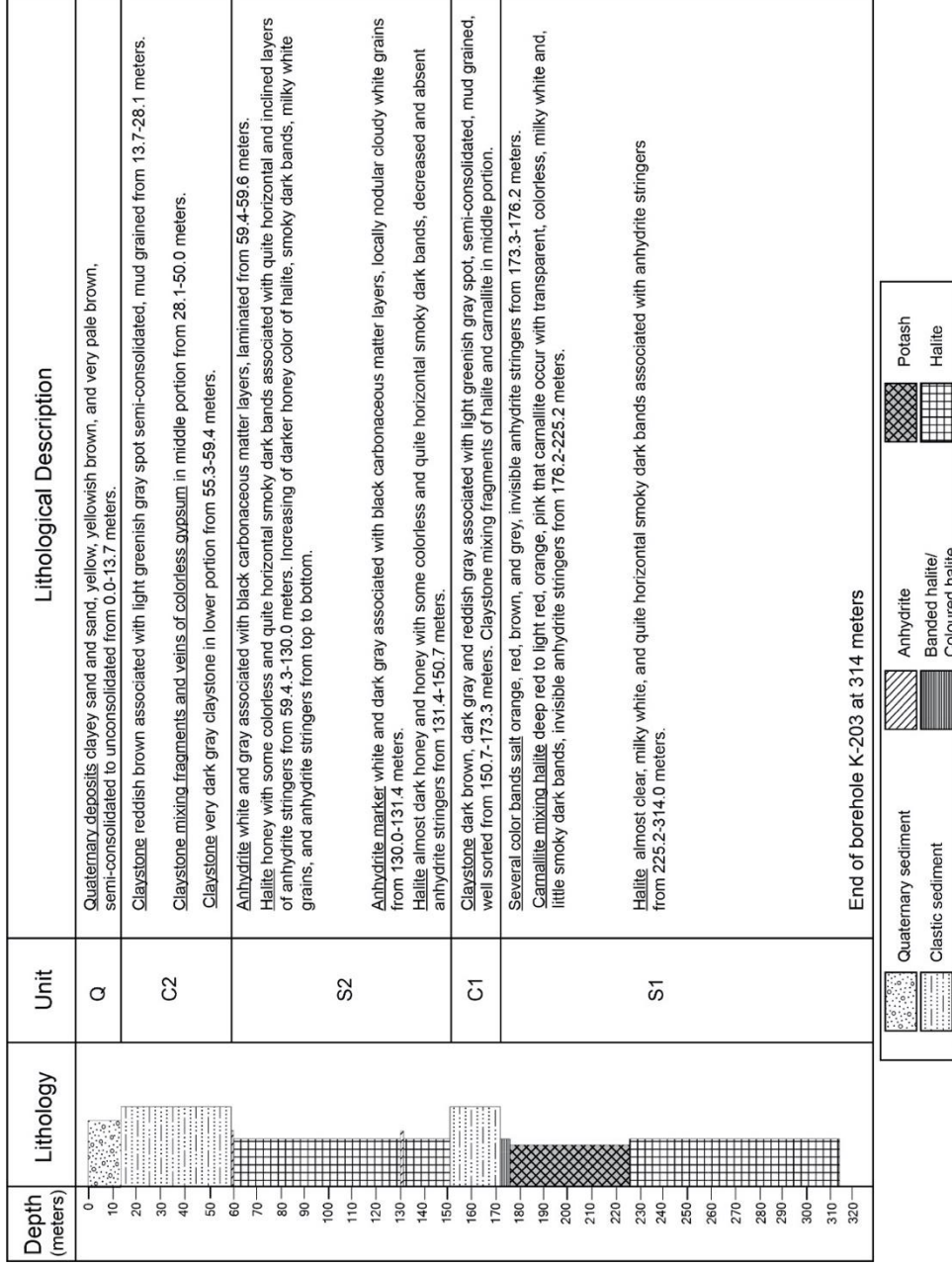


Figure 54 Lithological description of borehole K-203 of Maha Sarakham Formation in Changwat Chaiyaphum, northeastern Thailand.

#### 4.1.4 Borehole K-204

Located: Ban Mai Na Di, Tambon Ban Kham, Amphoe Chaturat, Changwat Chaiyaphum

Latitude: 15°31'11.8" N, Longitude: 101°44'50.3" E

Elevation: 203 meters (MSL)

Date of drilling: 10 June 2018 – 25 June 2018

Depth: 150 meters

#### Unit S1

The unit s1 was cored from 60.0-150.0 meters. They are two sequences consist of halite associated with anhydrite stringers and anhydrite, respectively from lower to upper unit.

Lower unit is halite associated with anhydrite stringers at 62.4-150.0 meters (Figure 56). Almost halite is clear, transparent, white, and smoky dark bands, milky white, piece of halite, medium to coarse grained associated with anhydrite stringers along these unit. Anhydrite stringers are increasing from top to bottom of lower unit S1 and thickness of anhydrite about 5.0-20.0 centimeters.

Upper unit is anhydrite at 62.0-62.4 meters (Figure 57). Anhydrite is white and dark gray associated with black carbonaceous matter layers that thickness of layers about 0.1-10 centimeters, massive, inclined laminated with locally nodular cloudy white grains that grains size of anhydrite about 2.0 centimeters.



**Figure 55** Core photograph showing halite associated with anhydrite stringers of unit S1 from K-204. T = top; B = bottom.



**Figure 56** Core photograph showing anhydrite at 62.0-62.4 meters of unit S1 from K-204.

T = top; B = bottom.

#### Unit C1

The unit C1 was cored from 29.0-60.0 meters. Claystone is almost reddish brown with some dark reddish gray (claystone mixing with breccias of anhydrite and gypsum) associated with light greenish gray spot (Figure 58), semi-consolidated, mud grained and well sorted. At the lower portion of unit C1 near contact anhydrite from 54.0-60.0 meters is dark gray claystone and tasting of salty. At the upper portion of unit C1 from 31.0-33.5 meters is claystone mixing with breccias of anhydrite and gypsum that breccias size about over 2.0 centimeters.



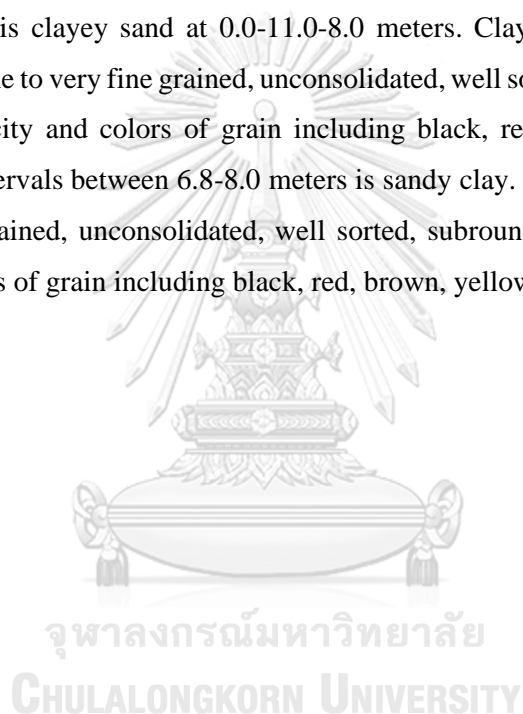
**Figure 57** Core photograph showing reddish brown claystone and dark reddish gray claystone mixing with breccias of anhydrite and gypsum at 31.0-33.5 meters of unit C1 from K-204. T = top; B = bottom.

#### Unit Q

The unit Q was cored from 0.0-29.0 meters. They are two sequences including clayey sand at 0.0-13.0 meters and sand at 13.0-29.0 meters.

Lower unit is sand interbedded with thin beds of clay. At the intervals 26.0-28.8, 23.0-25.0 and 13.0-19.5 meters are very pale brown and brownish yellow sand, medium to fine grained, well sorted, subrounded to subangular, low to high sphericity and colors of grain including black, red, brown, yellow, and colorless. At the intervals 25.0-26.7, 20.0-22.6 and 17.0-19.5 are very pale brown and brownish yellow sand coarse to fine grained, moderately sorted, subrounded to subangular, low to high sphericity and colors of grain including black, red, brown, yellow, and colorless. At the intervals 28.8-29.0, 25.7-26.0, 22.6-23.0 and 19.5-20.0 meters are very pale brown and dark clay (near contact unit C1 at 19.5-20.0 meters), semi-consolidated and well sorted.

Upper unit is clayey sand at 0.0-11.0-8.0 meters. Clayey sand is yellow and light yellowish brown, fine to very fine grained, unconsolidated, well sorted, subrounded to rounded, high to low sphericity and colors of grain including black, red, brown, yellow, gray, and colorless. At the intervals between 6.8-8.0 meters is sandy clay. Sandy clay yellowish brown, fine to very fine grained, unconsolidated, well sorted, subrounded to rounded, high to low sphericity and colors of grain including black, red, brown, yellow, gray, and colorless.



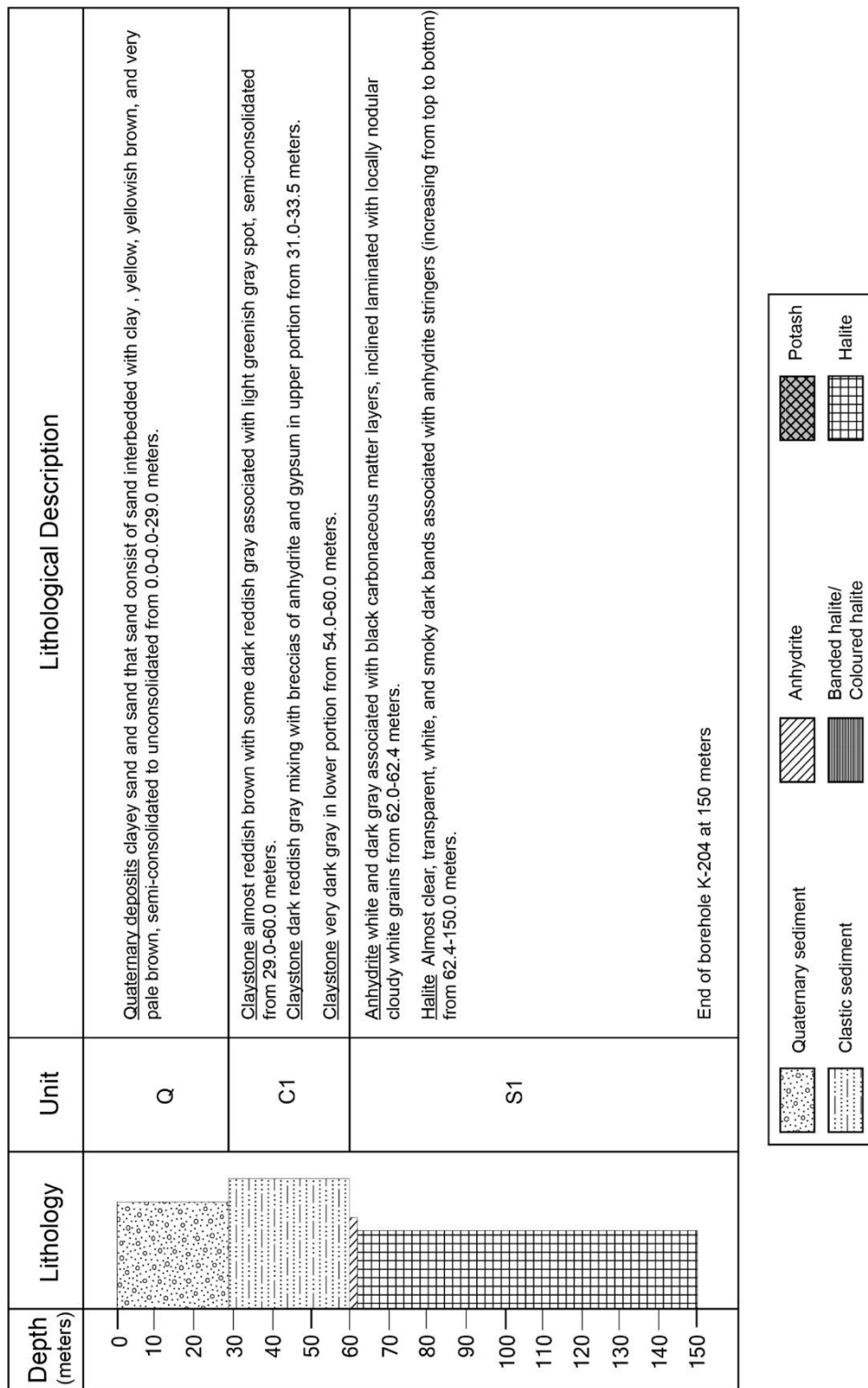


**Figure 58** Lithological description of borehole K-204 of Maha Sarakham Formation in Chaiyaphum province, northeastern Thailand.

#### 4.1.5 Borehole K-205

Located: Ban Kut Khaen Samakkhi School, Tambon Ban Tan, Amphoe Bamnet Narong, Changwat Chaiyaphum

Latitude: 15°32'08.0" N, Longitude: 101°43'35.3" E

Elevation: 216 meters (MSL)

Date of drilling: 1 July 2018 – 13 July 2018

Depth: 137 meters

#### Unit S1

The unit S1 was cored from 96.6-137.0 meters. They are two sequences consist of sylvite and halite associated with anhydrite stringers, respectively from lower to upper unit.

Lower unit is sylvite at 134.2-137.0 meters (Figure 60) that sylvite intergrown with halite and carnallite. Sylvite is almost colorless with little cloudy white, large crystal about 2.0-4.0 centimeter. Halite is colorless and smoky dark bands associated with orange and red of carnallite.

Upper unit is halite associated with inclined anhydrite stringers at 96.6-134.2 meters (Figure 61). Halite is dark honey to lighter honey color until then milky white but increasing smoky dark bands and anhydrite stringers from top of the bottom of upper unit S2. Thickness of anhydrite stringers are about 0.5-2.0 centimeters.



**Figure 59** Core photograph showing sylvite intergrown with halite and carnallite at 135.0-137.0 meters of unit S1 from K-205. T = top; B = bottom.



**Figure 60** Core photograph showing halite associated with inclined anhydrite stringers of unit S1 from K-205. T = top; B = bottom.

#### Unit C1

The unit C1 was cored from 70.6-96.6 meters. Claystone is reddish brown associated with light greenish gray spot (Figure 62), semi-consolidated, mud grained and well sorted. At the intervals between 91.0-96.6 meters is dark gray to dark gray very claystone mixing fragments of colorless halite and tasting of salty.



**Figure 61** Core photograph showing reddish brown claystone of unit C1 from K-205. T = top; B = bottom.

#### Middle anhydrite unit

The middle anhydrite unit was cored from 66.6-70.6 meters. Anhydrite is white and dark gray associated with black carbonaceous matter layers, massive, laminated with locally nodular cloudy white grains that large cloudy white grains size about 4.0-6.0 centimeter (Figure 63)



**Figure 62** Core photograph showing anhydrite 66.6-70.0 meters of middle anhydrite unit from K-205. T = top; B = bottom.

#### Unit C2

The unit C2 was cored from 18.5-66.6 meters. Claystone is reddish brown and black in weathering surface associated with light greenish gray spot (Figure 64), semi-consolidated, mud grained and well sorted.



**Figure 63** Core photograph showing reddish brown claystone of unit C2 from K-205. T = top; B = bottom.

#### Unit Q

The unit Q was cored from 0.0-18.5 meters. They are two sequences including clayey sand and sand. Lower unit is sand at 11.0-18.5 meters. Sand is very pale brown, very coarse to very fine grained, moderately sorted, subrounded to subangular, low to high sphericity and colors of grain including black, red, brown, yellow, and colorless.

Upper unit is clayey sand at 0.0-11.0-8.0 meters. Clayey sand is yellow and light yellowish brown, fine to very fine grained, semi-consolidated to unconsolidated, well sorted,

subrounded to rounded, high to low sphericity and colors of grain including black, red, brown, yellow, gray, and colorless. At the intervals between 5.0-9.0 meters is sand. Sand is reddish yellow, unconsolidated, medium to very fine grained, moderately sorted, subrounded to rounded, high to low sphericity.



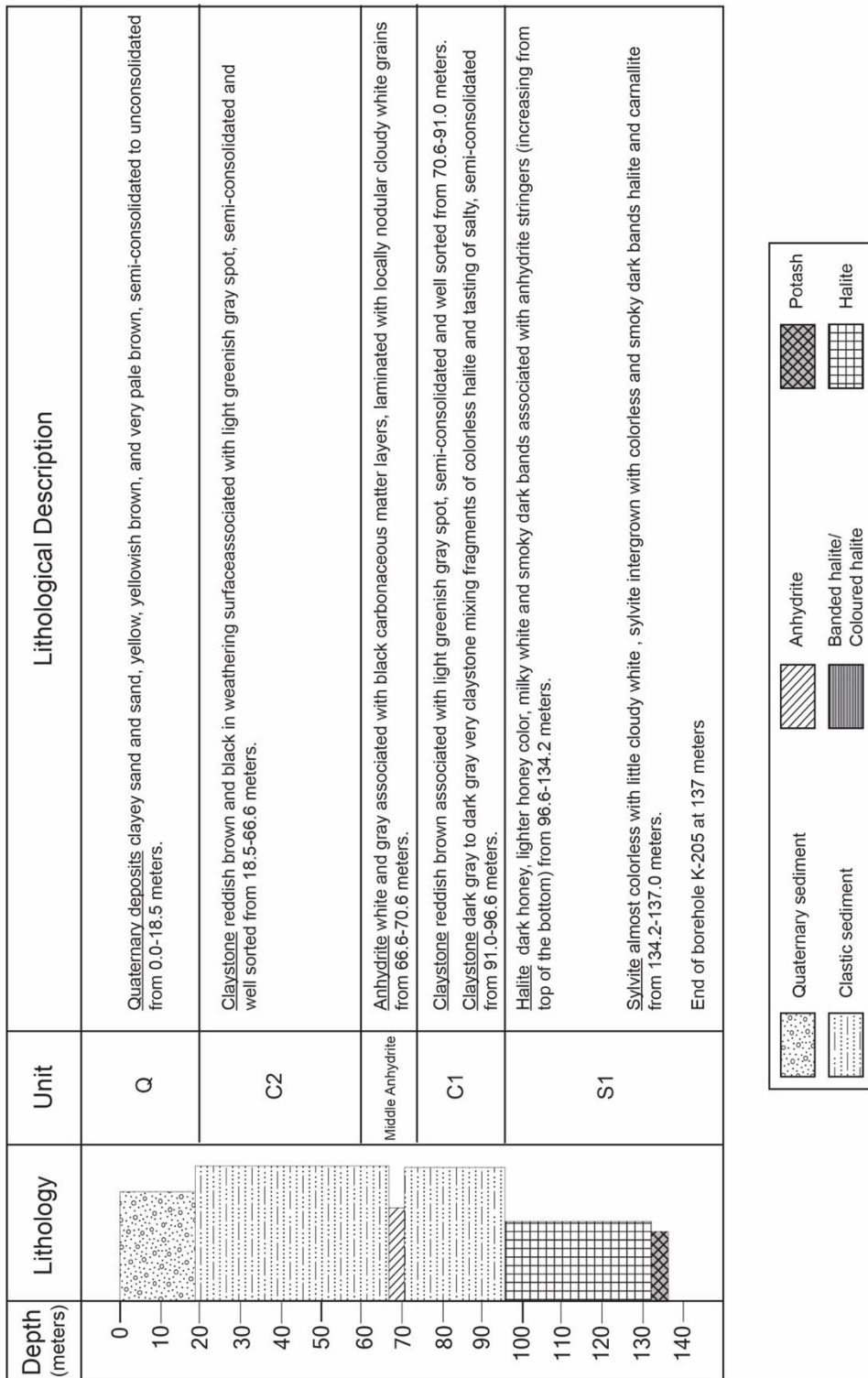


**Figure 64** Lithological description of borehole K-205 of Maha Sarakham Formation in Changwat Chaiyaphum, northeastern Thailand.

## 4.2 Geochemistry of rock salt in borehole K-203.

### 4.2.1 Elemental compositions of evaporitic rocks

Elemental compositions of anhydrite, halite and carnallite in borehole K-203 are shown in Table 3.

For Unit S1 of halite and carnallite in borehole K-203, the elemental compositions are divided into three group including the major elements, minor elements and trace elements. The major elements of halite are comprising of sodium (Na) values vary from 35.51–31.24 wt% and chlorine (Cl) values vary from 60.28–53.47 wt%. The minor and trace elements of halite are consisting of sulfate (SO<sub>4</sub>) values vary from 2.98–0.11wt%, calcium (Ca) values vary from 0.35–0.01 wt%, Potassium (K) values vary from 0.35–0.02 wt%, magnesium (Mg) values vary from 0.38–0.01 wt%, and boron (B) values vary from 100.80–7.15 ppb.

The major elemental compositions of carnallite are Na values vary from 26.57–1.2wt%, K values vary from 9.26–1.49 wt%, Mg values vary from 9.87–1.22 wt%, Fe values vary from 0.38–0.01 wt% and Cl values vary from 55.79–7.05 wt%. The minor and trace elemental compositions of carnallite are Ca values vary from 0.37–0.01 wt%, SO<sub>4</sub> values vary from 0.30–0.01 wt%, strontium (Sr) values vary from 1362–17 ppm, rubidium (Rb) values vary from 50.90–7.00 ppm, zirconium (Zr) values vary from 12.10–0.60 ppm and B values vary from 281.40–10.00 ppb.

For Unit S2 of anhydrite and halite in borehole K-203, the major elemental compositions of halite are including Na values vary from 36.46–30.72 wt% and Cl values vary from 60.25– 20.27 wt%. The minor and trace elements of halite are consisting of K values vary from 1.25–0.02wt%,Mg values vary from 0.64–0.01wt%, Fe values vary from 0.11–0.02wt%, and B values vary from 18.21–4.46 ppb. In some depths have founded anhydrite stringers associated with halite that anhydrite layers presented high values of some elemental composition are Ca values vary from 1.40– 24.84 wt% and SO<sub>4</sub> values vary from 3.27– 32.98 wt%.







| Name    | Description | Unit | Depths (m)      | Na (%) | K (%)  | Ca (%) | Mg (%) | Fe (%) | Cl (%) | SO <sub>4</sub> <sup>2-</sup> (%) | Mn (ppm) | Cu (ppm) | Zn (ppm) | Ba (ppm) | Pb (ppm) | Sr (ppm) | Rb (ppm) | Zr (ppm) | B (ppb) |       |
|---------|-------------|------|-----------------|--------|--------|--------|--------|--------|--------|-----------------------------------|----------|----------|----------|----------|----------|----------|----------|----------|---------|-------|
| K203_42 | Halite      | S1   | 250.00 - 255.00 | 34.45  | 0.03   | 0.03   | 0.05   | -      | 59.92  | 0.04                              | -        | -        | -        | -        | -        | -        | -        | -        | -       | 12.84 |
| K203_43 | Halite      | S1   | 255.00 - 260.00 | 34.46  | 0.04   | 0.17   | 0.06   | -      | 57.64  | 2.45                              | -        | -        | -        | -        | -        | -        | -        | -        | -       | -     |
| K203_44 | Halite      | S1   | 260.00 - 265.00 | 32.43  | 0.05   | 0.28   | 0.05   | -      | 56.43  | 2.69                              | -        | -        | -        | -        | -        | -        | -        | -        | -       | 54.47 |
| K203_45 | Halite      | S1   | 265.00 - 270.00 | 34.44  | 0.02   | 0.09   | 0.02   | -      | 59.67  | 1.05                              | -        | -        | -        | -        | -        | -        | -        | -        | -       | -     |
| K203_46 | Halite      | S1   | 270.00 - 275.00 | 34.66  | 0.06   | 0.11   | 0.05   | -      | 60.23  | 0.80                              | -        | -        | -        | -        | -        | -        | -        | -        | -       | 100.8 |
| K203_47 | Halite      | S1   | 275.00 - 280.00 | 33.23  | 0.10   | 0.22   | 0.05   | -      | 59.76  | 2.93                              | -        | -        | -        | -        | -        | -        | -        | -        | -       | -     |
| K203_48 | Halite      | S1   | 280.00 - 285.00 | 34.77  | 0.02   | 0.04   | 0.03   | -      | 59.60  | 0.13                              | -        | -        | -        | -        | -        | -        | -        | -        | -       | 14.98 |
| K203_49 | Halite      | S1   | 285.00 - 290.00 | 35.51  | 0.0040 | 0.01   | 0.01   | -      | 59.99  | 0.11                              | -        | -        | -        | -        | -        | -        | -        | -        | -       | -     |
| K203_50 | Halite      | S1   | 290.00 - 295.00 | 32.99  | 0.02   | 0.04   | 0.01   | -      | 60.28  | 0.14                              | -        | -        | -        | -        | -        | -        | -        | -        | -       | 12.75 |
| K203_51 | Halite      | S1   | 295.00 - 300.00 | 35.17  | 0.05   | 0.15   | 0.02   | -      | 59.43  | 2.41                              | -        | -        | -        | -        | -        | -        | -        | -        | -       | -     |
| K203_52 | Halite      | S1   | 300.00 - 305.00 | 34.16  | 0.07   | 0.12   | 0.17   | -      | 59.26  | 1.79                              | -        | -        | -        | -        | -        | -        | -        | -        | -       | 9.85  |
| K203_53 | Halite      | S1   | 305.00 - 310.00 | 34.42  | 0.03   | 0.07   | 0.05   | -      | 60.09  | 0.94                              | -        | -        | -        | -        | -        | -        | -        | -        | -       | 7.15  |
| K203_54 | Halite      | S1   | 310.00 - 314.00 | 34.56  | 0.03   | 0.04   | 0.01   | -      | 59.56  | 0.25                              | -        | -        | -        | -        | -        | -        | -        | -        | -       | -     |

**Note:** " n.d. " = non-detected; " - " = no data

#### 4.2.2 Boron isotope of evaporitic rocks

Boron isotopic composition of halite and carnallite in borehole K-203 are shown in Table 4. For Unit S1 of halite and carnallite in borehole K-203,  $\delta^{11}\text{B}$  values of halite range from 22.21‰ to 28.19‰ (average 25.31‰, n=10) and  $\delta^{11}\text{B}$  values of carnallite are covered a wide range from 12.26‰ to 32.62‰ (average of 26.13‰, n=4). For Unit S2 of halite in borehole K-203, the  $\delta^{11}\text{B}$  values of halite range from 21.46‰ to 28.80‰ (average of 24.42‰, n=9)

The ranges of evaporitic rocks in this study are noticeably range of marine origin (Figure 66). The values of boron isotopic composition marine origin show range from +18.2‰ to 31.7‰ and non-marine origin range from -30.1‰ to +7.0‰ for the distinguished of the evaporite origins are described by Palmer and Swihart (1996); Swihart et al. (1986); Vengosh et al. (1992).

**Table 4** Boron isotope composition of borehole K-203.

| Name    | Description | Unit | Depths<br>(m)   | $\delta^{11}\text{B}$<br>(‰) | Error<br>( $\pm 2\sigma$ ) |
|---------|-------------|------|-----------------|------------------------------|----------------------------|
| K203_01 | Halite      | S2   | 59.60 - 65.00   | 23.84                        | 0.27                       |
| K203_03 | Halite      | S2   | 70.00 - 75.00   | 23.86                        | 0.02                       |
| K203_05 | Halite      | S2   | 80.00 - 85.00   | 24.79                        | 0.19                       |
| K203_07 | Halite      | S2   | 90.00 - 95.00   | 23.60                        | 0.37                       |
| K203_10 | Halite      | S2   | 100.00 - 105.00 | 25.51                        | 0.21                       |
| K203_12 | Halite      | S2   | 110.00 - 115.00 | 28.80                        | 0.15                       |
| K203_14 | Halite      | S2   | 120.00 - 125.00 | 26.40                        | 0.21                       |
| K203_17 | Halite      | S2   | 130.00 - 135.00 | 21.46                        | 0.08                       |
| K203_19 | Halite      | S2   | 140.00 - 145.00 | 21.55                        | 0.04                       |
| K203_23 | Halite      | S1   | 173.00 - 175.00 | 28.19                        | 0.24                       |
| K203_25 | Carnallite  | S1   | 193.00 - 200.00 | 32.62                        | 0.10                       |
| K203_27 | Carnallite  | S1   | 200.00 - 205.00 | 12.26                        | 0.06                       |
| K203_30 | Carnallite  | S1   | 210.00 - 215.00 | 31.08                        | 0.29                       |
| K203_36 | Carnallite  | S1   | 220.00 - 225.00 | 28.54                        | 0.17                       |
| K203_38 | Halite      | S1   | 230.00 - 235.00 | 26.17                        | 0.11                       |
| K203_41 | Halite      | S1   | 240.00 - 245.00 | 26.45                        | 0.32                       |
| K203_42 | Halite      | S1   | 250.00 - 255.00 | 26.78                        | 0.06                       |
| K203_44 | Halite      | S1   | 260.00 - 265.00 | 27.90                        | 0.05                       |
| K203_46 | Halite      | S1   | 270.00 - 275.00 | 25.12                        | 0.14                       |
| K203_48 | Halite      | S1   | 280.00 - 285.00 | 24.64                        | 0.28                       |
| K203_50 | Halite      | S1   | 290.00 - 295.00 | 22.98                        | 0.11                       |
| K203_52 | Halite      | S1   | 300.00 - 305.00 | 22.21                        | 0.12                       |
| K203_53 | Halite      | S1   | 305.00 - 310.00 | 22.68                        | 0.15                       |

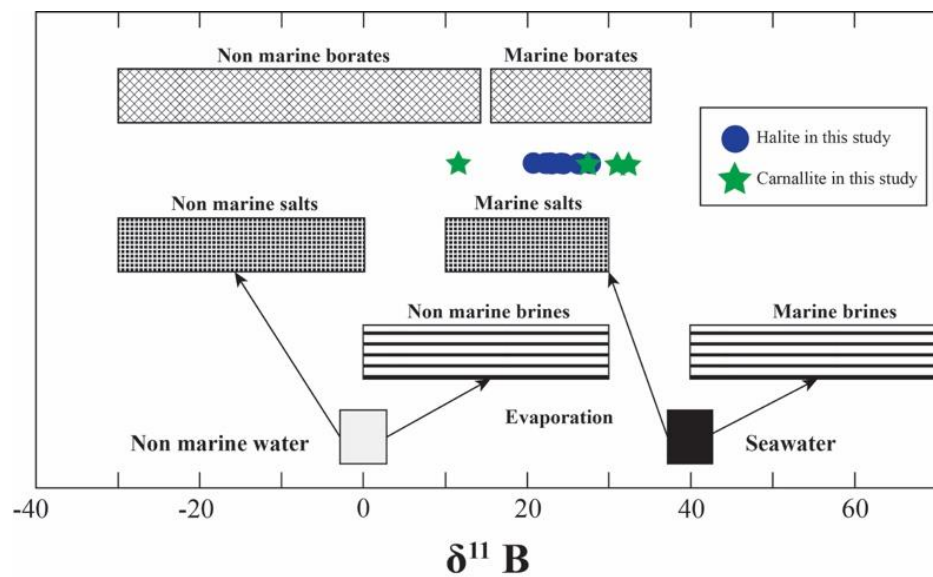


**Figure 65** Range of  $\delta^{11}\text{B}$  within borehole K-203 (modified from Palmer & Swihart, 1996; Swihart et al., 1986; Vengosh et al., 1992)

#### 4.3 Rare earth elements (REE) compositions of clastic rocks.

The results of REE and values of REE that calculated based on chondrite normalized values by Taylor and McLennan (1985) in claystone of five boreholes (K-201-205) are showed in Table 5 and Table 6, respectively.

For chondrite normalized of REE pattern of unit C1 and C2 in claystone are enriched of LREE relative to slightly flatted HREE (Figure 67) with negative anomalies of Eu ( $\text{Eu}/\text{Eu}^*$  of 0.47–0.75, averaging 0.69) and Ce ( $\text{Ce}/\text{Ce}^*$  of 0.92–1.02, averaging 0.96).

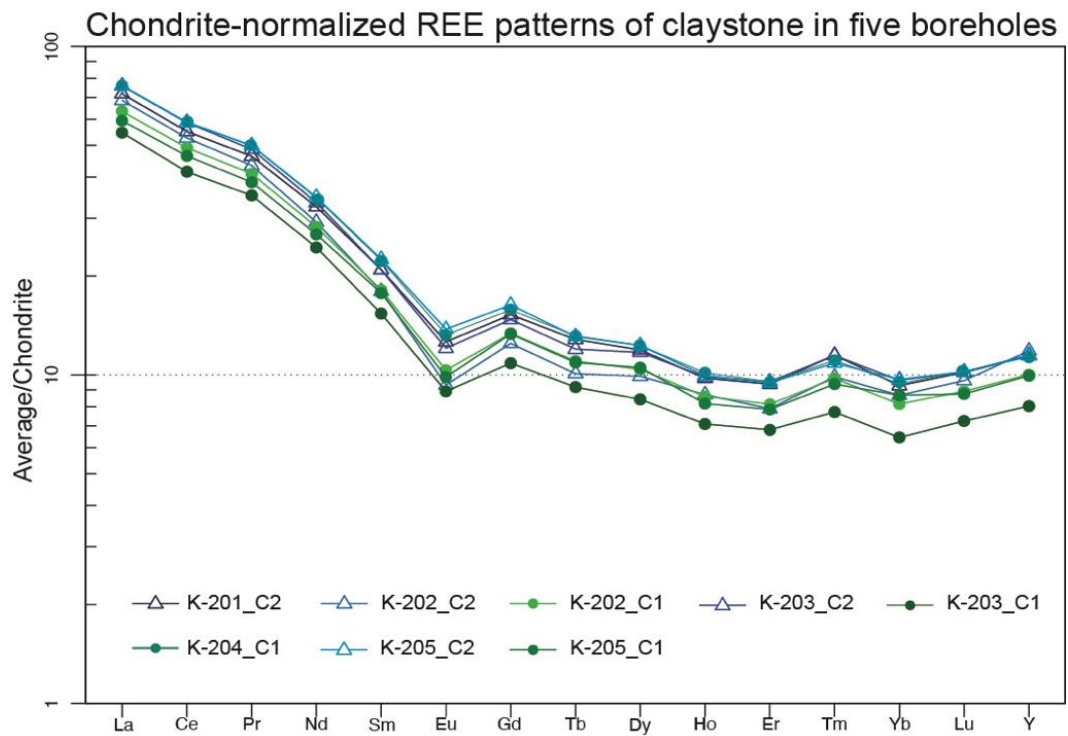


**Figure 66** Chondrite-normalized REE patterns representative the average of unit C1 and C2 plotted using chondrite normalizing values of Taylor and McLennan (1985).

**Table 5** REE compositions (in ppm) determined by ICP-MS analysis of clay and sand in five boreholes (K-201–205).

| No. | Name    | Materials | Unit | Depth (m.)    | La    | Ce    | Pr   | Nd    | Sm   | Eu   | Gd   | Tb   | Dy   | Ho   | Er   | Tm   | Yb   | Lu   | Y     |     |
|-----|---------|-----------|------|---------------|-------|-------|------|-------|------|------|------|------|------|------|------|------|------|------|-------|-----|
|     |         |           |      |               | ppm   | ppm   | ppm  | ppm   | ppm  | ppm  | ppm  | ppm  | ppm  | ppm  | ppm  | ppm  | ppm  | ppm  | ppm   | ppm |
| 1   | K201_C1 | Clay      | C2   | 30.90 - 44.00 | 26.00 | 51.80 | 6.33 | 23.10 | 5.10 | 1.16 | 4.81 | 0.78 | 4.65 | 0.87 | 2.47 | 0.42 | 2.40 | 0.41 | 26.20 |     |
| 2   | K201_C2 | Clay      | C2   | 47.44 - 62.70 | 26.20 | 52.60 | 6.38 | 22.80 | 4.80 | 1.09 | 4.80 | 0.76 | 4.59 | 0.82 | 2.26 | 0.43 | 2.30 | 0.38 | 23.80 |     |
| 3   | K201_C3 | Clay      | C2   | 70.00 - 72.45 | 26.80 | 53.80 | 6.33 | 23.40 | 4.60 | 1.04 | 4.39 | 0.69 | 4.38 | 0.80 | 2.27 | 0.39 | 2.20 | 0.37 | 22.10 |     |
| 4   | K202_C1 | Clay      | C2   | 51.00 - 53.00 | 29.00 | 55.80 | 6.65 | 23.00 | 4.30 | 0.80 | 3.92 | 0.61 | 3.99 | 0.80 | 2.15 | 0.40 | 2.40 | 0.42 | 27.00 |     |
| 5   | K202_C2 | Clay      | C2   | 53.00 - 59.00 | 21.30 | 45.00 | 5.24 | 18.50 | 4.00 | 0.82 | 3.71 | 0.56 | 3.55 | 0.68 | 1.78 | 0.31 | 1.90 | 0.31 | 22.70 |     |
| 6   | K202_C3 | Clay      | C1   | 59.60 - 65.00 | 34.80 | 69.10 | 7.92 | 26.50 | 5.30 | 1.05 | 4.69 | 0.72 | 4.49 | 0.83 | 2.28 | 0.39 | 2.30 | 0.37 | 23.50 |     |
| 7   | K202_C4 | Clay      | C1   | 65.00 - 70.00 | 9.40  | 22.20 | 2.75 | 10.80 | 2.60 | 0.39 | 2.50 | 0.37 | 2.13 | 0.36 | 0.93 | 0.18 | 1.00 | 0.17 | 11.40 |     |
| 8   | K202_C5 | Clay      | C1   | 70.00 - 75.00 | 27.80 | 55.80 | 6.66 | 24.20 | 4.70 | 1.01 | 4.48 | 0.70 | 4.07 | 0.75 | 2.29 | 0.38 | 2.10 | 0.40 | 22.70 |     |
| 9   | K202_C6 | Clay      | C1   | 80.00 - 83.00 | 26.20 | 54.50 | 6.50 | 23.30 | 5.10 | 1.06 | 4.69 | 0.64 | 4.20 | 0.79 | 2.10 | 0.38 | 2.20 | 0.35 | 21.80 |     |
| 10  | K202_C7 | Clay      | C1   | 85.00 - 90.00 | 25.70 | 49.80 | 6.05 | 21.70 | 4.30 | 0.96 | 3.92 | 0.59 | 3.78 | 0.72 | 1.99 | 0.33 | 2.00 | 0.33 | 20.60 |     |
| 11  | K202_C8 | Clay      | C1   | 90.00 - 95.00 | 26.60 | 51.90 | 6.28 | 22.10 | 4.50 | 0.98 | 4.49 | 0.70 | 4.35 | 0.80 | 2.16 | 0.38 | 2.20 | 0.39 | 22.50 |     |

| No. | Name     | Materials | Unit | Depth (m.)      | La    | Ce    | Pr   | Nd    | Sm   | Eu   | Gd   | Tb   | Dy   | Ho   | Er   | Tm   | Yb   | Lu   | Y     |     |
|-----|----------|-----------|------|-----------------|-------|-------|------|-------|------|------|------|------|------|------|------|------|------|------|-------|-----|
|     |          |           |      |                 | ppm   | ppm   | ppm  | ppm   | ppm  | ppm  | ppm  | ppm  | ppm  | ppm  | ppm  | ppm  | ppm  | ppm  | ppm   | ppm |
| 12  | K202_C9  | Clay      | C1   | 92.85 - 93.00   | 25.90 | 51.60 | 6.25 | 22.60 | 5.00 | 1.05 | 4.45 | 0.67 | 4.16 | 0.76 | 2.14 | 0.37 | 2.20 | 0.35 | 22.30 |     |
| 13  | K202_C10 | Clay      | C1   | 95.00 - 100.00  | 15.80 | 32.70 | 3.91 | 14.50 | 3.20 | 0.89 | 4.69 | 0.90 | 5.69 | 1.07 | 2.89 | 0.51 | 2.80 | 0.45 | 28.70 |     |
| 14  | K202_C11 | Clay      | C1   | 100.00 - 105.00 | 17.30 | 35.60 | 4.21 | 14.90 | 3.00 | 0.70 | 2.92 | 0.46 | 2.79 | 0.50 | 1.47 | 0.24 | 1.40 | 0.24 | 15.90 |     |
| 15  | K203_C1  | Clay      | C2   | 13.50 - 23.50   | 28.60 | 58.90 | 6.91 | 25.00 | 5.00 | 1.13 | 4.86 | 0.73 | 4.79 | 0.86 | 2.43 | 0.44 | 2.50 | 0.39 | 25.90 |     |
| 16  | K203_C2  | Clay      | C2   | 23.50 - 28.00   | 26.20 | 52.90 | 6.42 | 22.90 | 4.80 | 1.10 | 4.60 | 0.71 | 4.54 | 0.84 | 2.31 | 0.40 | 2.30 | 0.38 | 25.00 |     |
| 17  | K203_C3  | Clay      | C2   | 28.00 - 35.00   | 28.90 | 57.90 | 6.81 | 24.40 | 5.00 | 1.06 | 4.82 | 0.65 | 4.34 | 0.77 | 2.13 | 0.39 | 2.30 | 0.35 | 22.50 |     |
| 18  | K203_C4  | Clay      | C2   | 35.00 - 40.00   | 28.10 | 56.30 | 6.71 | 24.00 | 5.00 | 0.99 | 4.33 | 0.66 | 4.34 | 0.77 | 2.31 | 0.40 | 2.20 | 0.36 | 23.10 |     |
| 19  | K203_C5  | Clay      | C2   | 40.00 - 45.00   | 28.90 | 58.00 | 6.86 | 24.20 | 4.80 | 1.05 | 4.24 | 0.65 | 4.61 | 0.83 | 2.31 | 0.42 | 2.30 | 0.35 | 23.70 |     |
| 20  | K203_C6  | Clay      | C2   | 45.00 - 50.00   | 30.10 | 58.70 | 6.67 | 23.00 | 4.50 | 0.88 | 3.95 | 0.64 | 3.81 | 0.76 | 2.13 | 0.39 | 2.30 | 0.39 | 20.90 |     |
| 21  | K203_C7  | Clay      | C2   | 51.00 - 53.00   | 26.70 | 54.70 | 6.59 | 23.80 | 4.70 | 1.10 | 4.54 | 0.74 | 4.50 | 0.86 | 2.45 | 0.40 | 2.30 | 0.40 | 23.80 |     |
| 22  | K203_C8  | Clay      | C2   | 53.00 - 59.00   | 25.20 | 51.40 | 6.35 | 23.10 | 4.80 | 1.08 | 4.73 | 0.78 | 4.77 | 1.02 | 2.92 | 0.46 | 2.90 | 0.48 | 28.00 |     |
| 23  | K203_C9  | Clay      | C1   | 150.80 - 155.00 | 17.90 | 34.40 | 4.24 | 15.30 | 3.10 | 0.67 | 2.80 | 0.43 | 2.68 | 0.52 | 1.46 | 0.23 | 1.40 | 0.22 | 14.90 |     |
| 24  | K203_C10 | Clay      | C1   | 155.00 - 160.00 | 22.20 | 43.30 | 5.27 | 18.70 | 3.70 | 0.82 | 3.44 | 0.56 | 3.25 | 0.61 | 1.79 | 0.29 | 1.60 | 0.29 | 17.20 |     |

| No. | Name     | Materials | Unit | Depth (m.)      | La    | Ce    | Pr   | Nd    | Sm   | Eu   | Gd   | Tb   | Dy   | Ho   | Er   | Tm   | Yb   | Lu   | Y    |       |
|-----|----------|-----------|------|-----------------|-------|-------|------|-------|------|------|------|------|------|------|------|------|------|------|------|-------|
|     |          |           |      |                 | ppm   | ppm   | ppm  | ppm   | ppm  | ppm  | ppm  | ppm  | ppm  | ppm  | ppm  | ppm  | ppm  | ppm  | ppm  | ppm   |
| 25  | K203_C11 | Clay      | C1   | 160.00 - 165.00 | 21.90 | 43.80 | 5.28 | 19.30 | 4.00 | 0.88 | 4.05 | 0.64 | 3.78 | 0.70 | 1.91 | 0.32 | 1.80 | 0.32 | 0.32 | 19.30 |
| 26  | K203_C12 | Clay      | C1   | 165.00 - 170.00 | 18.20 | 37.50 | 4.50 | 16.20 | 3.40 | 0.73 | 3.00 | 0.50 | 3.13 | 0.58 | 1.62 | 0.27 | 1.60 | 0.27 | 0.27 | 16.10 |
| 27  | K204_C1  | Sand      | C1   | 29.00 - 33.60   | 27.90 | 59.40 | 7.01 | 26.30 | 5.50 | 1.27 | 5.31 | 0.80 | 5.06 | 0.91 | 2.48 | 0.41 | 2.40 | 0.40 | 0.40 | 25.70 |
| 28  | K204_C2  | Clay      | C1   | 29.00 - 35.00   | 26.30 | 53.80 | 6.58 | 23.30 | 4.80 | 1.01 | 4.69 | 0.75 | 4.37 | 0.83 | 2.21 | 0.39 | 2.30 | 0.38 | 0.38 | 23.50 |
| 29  | K204_C3  | Clay      | C1   | 35.00 - 40.00   | 30.10 | 59.40 | 7.10 | 25.70 | 5.30 | 1.19 | 4.94 | 0.79 | 4.83 | 0.87 | 2.48 | 0.40 | 2.40 | 0.42 | 0.42 | 24.30 |
| 30  | K204_C4  | Clay      | C1   | 40.00 - 45.00   | 28.30 | 55.70 | 6.81 | 23.90 | 5.00 | 1.13 | 4.55 | 0.72 | 4.64 | 0.89 | 2.35 | 0.40 | 2.40 | 0.39 | 0.39 | 23.60 |
| 31  | K204_C5  | Clay      | C1   | 45.00 - 50.00   | 29.40 | 56.20 | 6.98 | 25.00 | 5.00 | 1.16 | 4.83 | 0.76 | 4.68 | 0.87 | 2.36 | 0.37 | 2.20 | 0.37 | 0.37 | 23.70 |
| 32  | K204_C6  | Clay      | C1   | 50.00 - 55.00   | 27.80 | 56.90 | 6.94 | 24.50 | 5.20 | 1.14 | 4.67 | 0.77 | 4.70 | 0.85 | 2.38 | 0.41 | 2.30 | 0.39 | 0.39 | 23.50 |
| 33  | K204_C7  | Clay      | C1   | 55.00 - 59.95   | 25.50 | 52.10 | 6.35 | 23.40 | 5.30 | 1.17 | 4.79 | 0.75 | 4.49 | 0.82 | 2.32 | 0.41 | 2.30 | 0.38 | 0.38 | 22.40 |
| 34  | K205_C1  | Clay      | C2   | 20.00 - 30.00   | 28.10 | 53.50 | 6.60 | 23.60 | 4.80 | 1.12 | 4.62 | 0.71 | 4.46 | 0.84 | 2.25 | 0.38 | 2.40 | 0.37 | 0.37 | 22.90 |
| 35  | K205_C2  | Clay      | C2   | 30.00 - 35.00   | 29.70 | 56.20 | 6.43 | 22.90 | 5.00 | 1.12 | 4.76 | 0.73 | 4.70 | 0.85 | 2.45 | 0.42 | 2.40 | 0.40 | 0.40 | 24.90 |
| 36  | K205_C3  | Clay      | C2   | 35.00 - 40.00   | 28.80 | 54.20 | 6.48 | 23.80 | 5.00 | 1.16 | 4.67 | 0.74 | 4.59 | 0.84 | 2.33 | 0.38 | 2.40 | 0.40 | 0.40 | 23.60 |
| 37  | K205_C4  | Clay      | C2   | 40.00 - 45.00   | 30.30 | 69.00 | 8.95 | 31.70 | 6.40 | 1.42 | 5.96 | 0.88 | 5.22 | 0.91 | 2.53 | 0.39 | 2.40 | 0.39 | 0.39 | 25.20 |

| No. | Name     | Materials | Unit | Depth (m.)    | La    | Ce    | Pr   | Nd    | Sm   | Eu   | Gd   | Tb   | Dy   | Ho   | Er   | Tm   | Yb   | Lu   | Y     |     |
|-----|----------|-----------|------|---------------|-------|-------|------|-------|------|------|------|------|------|------|------|------|------|------|-------|-----|
|     |          |           |      |               | ppm   | ppm   | ppm  | ppm   | ppm  | ppm  | ppm  | ppm  | ppm  | ppm  | ppm  | ppm  | ppm  | ppm  | ppm   | ppm |
| 38  | K205_C5  | Clay      | C2   | 45.00 - 50.00 | 28.60 | 57.40 | 6.86 | 24.50 | 5.20 | 1.22 | 5.01 | 0.76 | 4.66 | 0.84 | 2.35 | 0.40 | 2.40 | 0.41 | 24.10 |     |
| 39  | K205_C6  | Clay      | C2   | 50.00 - 55.00 | 25.50 | 49.80 | 6.06 | 22.30 | 4.70 | 1.15 | 4.71 | 0.69 | 4.41 | 0.76 | 2.19 | 0.35 | 2.30 | 0.36 | 22.60 |     |
| 40  | K205_C7  | Clay      | C2   | 55.00 - 60.00 | 26.30 | 53.10 | 6.39 | 23.30 | 5.00 | 1.18 | 5.05 | 0.76 | 4.60 | 0.84 | 2.28 | 0.39 | 2.40 | 0.39 | 24.00 |     |
| 41  | K205_C8  | Clay      | C2   | 60.00 - 66.60 | 25.30 | 57.00 | 6.97 | 25.60 | 5.50 | 1.22 | 5.18 | 0.80 | 4.83 | 0.88 | 2.47 | 0.42 | 2.50 | 0.39 | 24.80 |     |
| 42  | K205_C9  | Clay      | C1   | 75.00 - 80.00 | 24.40 | 48.20 | 5.75 | 20.30 | 4.20 | 0.87 | 3.83 | 0.60 | 3.73 | 0.64 | 1.76 | 0.30 | 1.90 | 0.31 | 19.20 |     |
| 43  | K205_C10 | Clay      | C1   | 80.00 - 85.00 | 23.80 | 47.40 | 5.57 | 19.80 | 3.90 | 0.83 | 3.42 | 0.56 | 3.52 | 0.61 | 1.72 | 0.30 | 1.80 | 0.29 | 18.20 |     |
| 44  | K205_C11 | Clay      | C1   | 85.00 - 90.00 | 15.30 | 33.60 | 4.01 | 14.60 | 3.80 | 0.80 | 4.63 | 0.70 | 4.52 | 0.79 | 2.21 | 0.40 | 2.60 | 0.40 | 24.00 |     |
| 45  | K205_C12 | Clay      | C1   | 90.00 - 97.60 | 23.70 | 48.50 | 5.83 | 21.50 | 4.50 | 0.93 | 4.43 | 0.67 | 4.28 | 0.74 | 2.13 | 0.35 | 2.30 | 0.33 | 22.10 |     |

**Table 6** The chondrite normalizing value of REE values following Taylor and McLennan (1985) in claystone of five boreholes (K-201-205).

| Name    | Unit | Depth (m.)    | La    | Ce    | Pr    | Nd    | Sm    | Eu    | Gd    | Tb    | Dy    | Ho    | Er   | Tm    | Yb   | Lu    | Y     | Eu/Er* | Ce/Ce* |
|---------|------|---------------|-------|-------|-------|-------|-------|-------|-------|-------|-------|-------|------|-------|------|-------|-------|--------|--------|
| K201_C1 | C2   | 30.90 - 44.00 | 70.84 | 54.13 | 46.20 | 32.49 | 22.08 | 13.33 | 15.72 | 13.45 | 12.20 | 10.24 | 9.92 | 11.67 | 9.68 | 10.79 | 12.48 | 0.72   | 0.95   |
| K201_C2 | C2   | 47.44 - 62.70 | 71.39 | 54.96 | 46.57 | 32.07 | 20.78 | 12.53 | 15.69 | 13.10 | 12.05 | 9.65  | 9.08 | 11.94 | 9.27 | 10.00 | 11.33 | 0.69   | 0.95   |
| K201_C3 | C2   | 70.00 - 72.45 | 73.02 | 56.22 | 46.20 | 32.91 | 19.91 | 11.95 | 14.35 | 11.90 | 11.50 | 9.41  | 9.12 | 10.83 | 8.87 | 9.74  | 10.52 | 0.71   | 0.97   |
| K202_C1 | C2   | 51.00 - 53.00 | 79.02 | 58.31 | 48.54 | 32.35 | 18.61 | 9.20  | 12.81 | 10.52 | 10.47 | 9.41  | 8.63 | 11.11 | 9.68 | 11.05 | 12.86 | 0.60   | 0.94   |
| K202_C2 | C2   | 53.00 - 59.00 | 58.04 | 47.02 | 38.25 | 26.02 | 17.32 | 9.43  | 12.12 | 9.66  | 9.32  | 8.00  | 7.15 | 8.61  | 7.66 | 8.16  | 10.81 | 0.65   | 1.00   |
| K202_C3 | C1   | 59.60 - 65.00 | 94.82 | 72.20 | 57.81 | 37.27 | 22.94 | 12.07 | 15.33 | 12.41 | 11.78 | 9.76  | 9.16 | 10.83 | 9.27 | 9.74  | 11.19 | 0.64   | 0.98   |
| K202_C4 | C1   | 65.00 - 70.00 | 25.61 | 23.20 | 20.07 | 15.19 | 11.26 | 4.48  | 8.17  | 6.38  | 5.59  | 4.24  | 3.73 | 5.00  | 4.03 | 4.47  | 5.43  | 0.47   | 1.02   |
| K202_C5 | C1   | 70.00 - 75.00 | 75.75 | 58.31 | 48.61 | 34.04 | 20.35 | 11.61 | 14.64 | 12.07 | 10.68 | 8.82  | 9.20 | 10.56 | 8.47 | 10.53 | 10.81 | 0.67   | 0.96   |
| K202_C6 | C1   | 80.00 - 83.00 | 71.39 | 56.95 | 47.45 | 32.77 | 22.08 | 12.18 | 15.33 | 11.03 | 11.02 | 9.29  | 8.43 | 10.56 | 8.87 | 9.21  | 10.38 | 0.66   | 0.98   |
| K202_C7 | C1   | 85.00 - 90.00 | 70.03 | 52.04 | 44.16 | 30.52 | 18.61 | 11.03 | 12.81 | 10.17 | 9.92  | 8.47  | 7.99 | 9.17  | 8.06 | 8.68  | 9.81  | 0.71   | 0.94   |
| K202_C8 | C1   | 90.00 - 95.00 | 72.48 | 54.23 | 45.84 | 31.08 | 19.48 | 11.26 | 14.67 | 12.07 | 11.42 | 9.41  | 8.67 | 10.56 | 8.87 | 10.26 | 10.71 | 0.67   | 0.94   |
| K202_C9 | C1   | 92.85 - 93.00 | 70.57 | 53.92 | 45.62 | 31.79 | 21.65 | 12.07 | 14.54 | 11.55 | 10.92 | 8.94  | 8.59 | 10.28 | 8.87 | 9.21  | 10.62 | 0.68   | 0.95   |

| Name     | Unit | Depth (m.)      | La    | Ce    | Pr    | Nd    | Sm    | Eu    | Gd    | Tb    | Dy    | Ho    | Er    | Tm    | Yb    | Lu    | Y     | Eu/Er* | Ce/Ce* |
|----------|------|-----------------|-------|-------|-------|-------|-------|-------|-------|-------|-------|-------|-------|-------|-------|-------|-------|--------|--------|
| K202_C10 | C1   | 95.00 - 100.00  | 43.05 | 34.17 | 28.54 | 20.39 | 13.85 | 10.23 | 15.33 | 15.52 | 14.93 | 12.59 | 11.61 | 14.17 | 11.29 | 11.84 | 13.67 | 0.70   | 0.97   |
| K202_C11 | C1   | 100.00 - 105.00 | 47.14 | 37.20 | 30.73 | 20.96 | 12.99 | 8.05  | 9.54  | 7.93  | 7.32  | 5.88  | 5.90  | 6.67  | 5.65  | 6.32  | 7.57  | 0.72   | 0.98   |
| K203_C1  | C2   | 13.50 - 23.50   | 77.93 | 61.55 | 50.44 | 35.16 | 21.65 | 12.99 | 15.88 | 12.59 | 12.57 | 10.12 | 9.76  | 12.22 | 10.08 | 10.26 | 12.33 | 0.70   | 0.98   |
| K203_C2  | C2   | 23.50 - 28.00   | 71.39 | 55.28 | 46.86 | 32.21 | 20.78 | 12.64 | 15.03 | 12.24 | 11.92 | 9.88  | 9.28  | 11.11 | 9.27  | 10.00 | 11.90 | 0.72   | 0.96   |
| K203_C3  | C2   | 28.00 - 35.00   | 78.75 | 60.50 | 49.71 | 34.32 | 21.65 | 12.18 | 15.75 | 11.21 | 11.39 | 9.06  | 8.55  | 10.83 | 9.27  | 9.21  | 10.71 | 0.66   | 0.97   |
| K203_C4  | C2   | 35.00 - 40.00   | 76.57 | 58.83 | 48.98 | 33.76 | 21.65 | 11.38 | 14.15 | 11.38 | 11.39 | 9.06  | 9.28  | 11.11 | 8.87  | 9.47  | 11.00 | 0.65   | 0.96   |
| K203_C5  | C2   | 40.00 - 45.00   | 78.75 | 60.61 | 50.07 | 34.04 | 20.78 | 12.07 | 13.86 | 11.21 | 12.10 | 9.76  | 9.28  | 11.67 | 9.27  | 9.21  | 11.29 | 0.71   | 0.97   |
| K203_C6  | C2   | 45.00 - 50.00   | 82.02 | 61.34 | 48.69 | 32.35 | 19.48 | 10.11 | 12.91 | 11.03 | 10.00 | 8.94  | 8.55  | 10.83 | 9.27  | 10.26 | 9.95  | 0.64   | 0.97   |
| K203_C7  | C2   | 51.00 - 53.00   | 72.75 | 57.16 | 48.10 | 33.47 | 20.35 | 12.64 | 14.84 | 12.76 | 11.81 | 10.12 | 9.84  | 11.11 | 9.27  | 10.53 | 11.33 | 0.73   | 0.97   |
| K203_C8  | C2   | 53.00 - 59.00   | 68.66 | 53.71 | 46.35 | 32.49 | 20.78 | 12.41 | 15.46 | 13.45 | 12.52 | 12.00 | 11.73 | 12.78 | 11.69 | 12.63 | 13.33 | 0.69   | 0.95   |
| K203_C9  | C1   | 150.80 - 155.00 | 48.77 | 35.95 | 30.95 | 21.52 | 13.42 | 7.70  | 9.15  | 7.41  | 7.03  | 6.12  | 5.86  | 6.39  | 5.65  | 5.79  | 7.10  | 0.69   | 0.93   |
| K203_C10 | C1   | 155.00 - 160.00 | 60.49 | 45.25 | 38.47 | 26.30 | 16.02 | 9.43  | 11.24 | 9.66  | 8.53  | 7.18  | 7.19  | 8.06  | 6.45  | 7.63  | 8.19  | 0.70   | 0.94   |
| K203_C11 | C1   | 160.00 - 165.00 | 59.67 | 45.77 | 38.54 | 27.14 | 17.32 | 10.11 | 13.24 | 11.03 | 9.92  | 8.24  | 7.67  | 8.89  | 7.26  | 8.42  | 9.19  | 0.67   | 0.95   |

| Name     | Unit | Depth (m.)      | La    | Ce    | Pr    | Nd    | Sm    | Eu    | Gd    | Tb    | Dy    | Ho    | Er    | Tm    | Yb   | Lu    | Y     | Eu/Er* | Ce/Ce* |
|----------|------|-----------------|-------|-------|-------|-------|-------|-------|-------|-------|-------|-------|-------|-------|------|-------|-------|--------|--------|
| K203_C12 | C1   | 165.00 - 170.00 | 49.59 | 39.18 | 32.85 | 22.78 | 14.72 | 8.39  | 9.80  | 8.62  | 8.22  | 6.82  | 6.51  | 7.50  | 6.45 | 7.11  | 7.67  | 0.70   | 0.97   |
| K204_C1  | C1   | 29.00 - 33.60   | 76.02 | 62.07 | 51.17 | 36.99 | 23.81 | 14.60 | 17.35 | 13.79 | 13.28 | 10.71 | 9.96  | 11.39 | 9.68 | 10.53 | 12.24 | 0.72   | 1.00   |
| K204_C2  | C1   | 29.00 - 35.00   | 71.66 | 56.22 | 48.03 | 32.77 | 20.78 | 11.61 | 15.33 | 12.93 | 11.47 | 9.76  | 8.88  | 10.83 | 9.27 | 10.00 | 11.19 | 0.65   | 0.96   |
| K204_C3  | C1   | 35.00 - 40.00   | 82.02 | 62.07 | 51.82 | 36.15 | 22.94 | 13.68 | 16.14 | 13.62 | 12.68 | 10.24 | 9.96  | 11.11 | 9.68 | 11.05 | 11.57 | 0.71   | 0.95   |
| K204_C4  | C1   | 40.00 - 45.00   | 77.11 | 58.20 | 49.71 | 33.61 | 21.65 | 12.99 | 14.87 | 12.41 | 12.18 | 10.47 | 9.44  | 11.11 | 9.68 | 10.26 | 11.24 | 0.72   | 0.94   |
| K204_C5  | C1   | 45.00 - 50.00   | 80.11 | 58.73 | 50.95 | 35.16 | 21.65 | 13.33 | 15.78 | 13.10 | 12.28 | 10.24 | 9.48  | 10.28 | 8.87 | 9.74  | 11.29 | 0.72   | 0.92   |
| K204_C6  | C1   | 50.00 - 55.00   | 75.75 | 59.46 | 50.66 | 34.46 | 22.51 | 13.10 | 15.26 | 13.28 | 12.34 | 10.00 | 9.56  | 11.39 | 9.27 | 10.26 | 11.19 | 0.71   | 0.96   |
| K204_C7  | C1   | 55.00 - 59.95   | 69.48 | 54.44 | 46.35 | 32.91 | 22.94 | 13.45 | 15.65 | 12.93 | 11.78 | 9.65  | 9.32  | 11.39 | 9.27 | 10.00 | 10.67 | 0.71   | 0.96   |
| K205_C1  | C2   | 20.00 - 30.00   | 76.57 | 55.90 | 48.18 | 33.19 | 20.78 | 12.87 | 15.10 | 12.24 | 11.71 | 9.88  | 9.04  | 10.56 | 9.68 | 9.74  | 10.90 | 0.73   | 0.92   |
| K205_C2  | C2   | 30.00 - 35.00   | 80.93 | 58.73 | 46.93 | 32.21 | 21.65 | 12.87 | 15.56 | 12.59 | 12.34 | 10.00 | 9.84  | 11.67 | 9.68 | 10.53 | 11.86 | 0.70   | 0.95   |
| K205_C3  | C2   | 35.00 - 40.00   | 78.47 | 56.64 | 47.30 | 33.47 | 21.65 | 13.33 | 15.26 | 12.76 | 12.05 | 9.88  | 9.36  | 10.56 | 9.68 | 10.53 | 11.24 | 0.73   | 0.93   |
| K205_C4  | C2   | 40.00 - 45.00   | 82.56 | 72.10 | 65.33 | 44.59 | 27.71 | 16.32 | 19.48 | 15.17 | 13.70 | 10.71 | 10.16 | 10.83 | 9.68 | 10.26 | 12.00 | 0.70   | 0.98   |
| K205_C5  | C2   | 45.00 - 50.00   | 77.93 | 59.98 | 50.07 | 34.46 | 22.51 | 14.02 | 16.37 | 13.10 | 12.23 | 9.88  | 9.44  | 11.11 | 9.68 | 10.79 | 11.48 | 0.73   | 0.96   |

| Name     | Unit | Depth (m.)    | La    | Ce    | Pr    | Nd    | Sm    | Eu    | Gd    | Tb    | Dy    | Ho    | Er   | Tm    | Yb    | Lu    | Y     | Eu/Er* | Ce/Ce* |
|----------|------|---------------|-------|-------|-------|-------|-------|-------|-------|-------|-------|-------|------|-------|-------|-------|-------|--------|--------|
| K205_C6  | C2   | 50.00 - 55.00 | 69.48 | 52.04 | 44.23 | 31.36 | 20.35 | 13.22 | 15.39 | 11.90 | 11.57 | 8.94  | 8.80 | 9.72  | 9.27  | 9.47  | 10.76 | 0.75   | 0.94   |
| K205_C7  | C2   | 55.00 - 60.00 | 71.66 | 55.49 | 46.64 | 32.77 | 21.65 | 13.56 | 16.50 | 13.10 | 12.07 | 9.88  | 9.16 | 10.83 | 9.68  | 10.26 | 11.43 | 0.72   | 0.96   |
| K205_C8  | C2   | 60.00 - 66.60 | 68.94 | 59.56 | 50.88 | 36.01 | 23.81 | 14.02 | 16.93 | 13.79 | 12.68 | 10.35 | 9.92 | 11.67 | 10.08 | 10.26 | 11.81 | 0.70   | 1.01   |
| K205_C9  | C1   | 75.00 - 80.00 | 66.49 | 50.37 | 41.97 | 28.55 | 18.18 | 10.00 | 12.52 | 10.34 | 9.79  | 7.53  | 7.07 | 8.33  | 7.66  | 8.16  | 9.14  | 0.66   | 0.95   |
| K205_C10 | C1   | 80.00 - 85.00 | 64.85 | 49.53 | 40.66 | 27.85 | 16.88 | 9.54  | 11.18 | 9.66  | 9.24  | 7.18  | 6.91 | 8.33  | 7.26  | 7.63  | 8.67  | 0.69   | 0.96   |
| K205_C11 | C1   | 85.00 - 90.00 | 41.69 | 35.11 | 29.27 | 20.53 | 16.45 | 9.20  | 15.13 | 12.07 | 11.86 | 9.29  | 8.88 | 11.11 | 10.48 | 10.53 | 11.43 | 0.58   | 1.01   |
| K205_C12 | C1   | 90.00 - 97.60 | 64.58 | 50.68 | 42.55 | 30.24 | 19.48 | 10.69 | 14.48 | 11.55 | 11.23 | 8.71  | 8.55 | 9.72  | 9.27  | 8.68  | 10.52 | 0.64   | 0.97   |

**Note:**  $Eu/Eu^* = Eu_N / ((Sm_N \times Gd_N)^{0.5})$ ;  $Ce/Ce^* = Ce_N / ((La_N \times Pr_N)^{0.5})$

## Chapter 5

### Discussion

#### 5.1 Stratigraphic correlation

lithostratigraphic columns in this study are described by Hite (1971); Hite and Japakasetr (1979); Japakasetr and Workman (1981); Suwanich (1986); Utha-Aroon (1993) El Tabakh et al. (1999). These columns composed of massive evaporitic rock separated by red clastic sedimentary rock that lithology members are classified 5 units including Units S1, C1, S2, C2 and Q, respectively from bottom to top. The stratigraphic correlation of five boreholes illustrated by a cross-section A-A' that position of cross-section is shown in Figure 68. The position of boreholes is reorganized in K-201, K-205, K-204, K-202, and K-203 by direction of cross-section A-A' from southwest (SW) to northeast (NE). The lithostratigraphic sequences is described below.

##### **Unit S1: Lower Salt Unit**

Unit S1 is the lowest member in this study that range in depth of this member found from 110.5-200.0, 96.0-137.0, 62.0-150.0, 83.2-150.0 and 173.3-314.0 meters, in K-201, K-205, K-204, K-202, and K-203, respectively (pink shade in Figure 69). This evaporitic member is consisting of massive halite, carnallite, sylvite and banded halite. The bottom of this unit is possibly the contact with the basal anhydrite layer (El Tabakh et al., 1999; El Tabakh et al., 2003; Swihart et al., 1986).

Lithostratigraphic description of Unit S1, halite has a greater thickness than another salt unit (33.2-140.7 meters in thickness), is clear, transparent, white, milky white with medium to coarse grained, smoky dark bands associated with anhydrite stringers. Especially, Unit S1 are founded potash zone (carnallite and sylvite) and banded halite overlie a thick bed of halite that carnallite has brown, deep red, red, orange, pink and colourless and medium to coarse grained. Banded halite is observed several thin layers of colour in orange, red, grey, smoky dark, milky and colourless. Blue sapphire sylvinite (halite associated with sylvite), Bluish sylvinite intergrown with carnallite are appeared in borehole K-202. In addition, borehole K-205 is founded cloudy white sylvinite intergrown with carnallite. However, Unit S1 of borehole K-204 has disappear the potash zone that overlie of massive halite is illustrated a thick bed of anhydrite.

##### **Unit C1: Lower Clastic Unit**

Unit C1 overlies unit S1 and the adjacent of upper part Unit C1 is divided into two unit. Borehole K-201, K-202, K-203 and K-205 has underlies unit S2 but K-204 is underlined unit

Q. The thickness of Unit C1 is about 10.2-31.0 meter and depth interval has found at 100.3-110.5, 70.6-96.6, 29.0-60.0, 60.5-83.2, and 150.7-173.3 meters in K-201, K-205, K-204, K-202, and K-203, respectively (brown shade in Figure 69).

Lithostratigraphic description of Unit C1 consists of reddish brown and dark gray claystone associated with many spots of light greenish gray, semi-consolidated, mud-sized, well sorted. In addition, dark grey claystone mixing fragments of halite and carnallite is founded at the contact Lower Clastic Unit and Lower Salt Unit.

#### **Unit S2: Middle/Upper Salt Unit**

Unit S2 has found in boreholes K-201, K-205, K-202, and K-203 with range in depth 72.4-100.3, 66.6-70.6, 56.7-60.5 and 59.4-150.7 meters, respectively but this unit are disappeared in boreholes K-204 (blue shade in Figure 69). Unit S2 has 2 groups including halite and a thick anhydrite bed that Unit S2 overlies Lower Clastic Unit and underlies Middle/Upper Clastic Unit.

Lithostratigraphic description of Unit C1 in boreholes K-201 and K-203 consist of light to dark yellow honey color of halite and anhydrite stringers are observed in smoky dark bands of halite. For boreholes K-202 and K-205 have only an anhydrite bed that bed is exhibited colors; white to dark gray associated with carbonaceous layers (black)

#### **Unit C2: Middle/Upper Clastic Unit**

Unit C2 has found in boreholes K-201, K-205, K-202, and K-203 with range in depth 31.0-72.4, 18.5-66.6, 52.9-56.7 and 13.7-59.4 meters, respectively but this unit are disappeared in boreholes K-204 (light brown shade in Figure 69). The thickness of Unit C2 is about 3.8-42.7 meter that Unit C2 overlies Middle/Upper Salt Unit and underlies Quaternary Deposits Unit.

Lithostratigraphic description of Middle/Upper Clastic Unit consists of reddish brown to dark gray siltstone and claystone and well sorted and some depth has found fragments of gypsum.

#### **Unit Q: Quaternary Deposits Unit**

Unit S1 is the uppermost member in this study that range in depth of this member found from 31.0-0.0, 18.5-0.0, 29.0-0.0, 38.0-0.0 and 13.7-0.0 meters, in K-201, K-205, K-204, K-202, and K-203, respectively (yellow shade in Figure 69). The thickness of Unit Q is about 13.7-38.0 meter that Unit Q overlies Middle/Upper Clastic Unit.

Lithostratigraphic description of Quaternary Deposits Unit consists of clayey sand, sand and sandy clay that unit is unconsolidated to semi-consolidated within yellow to brown.

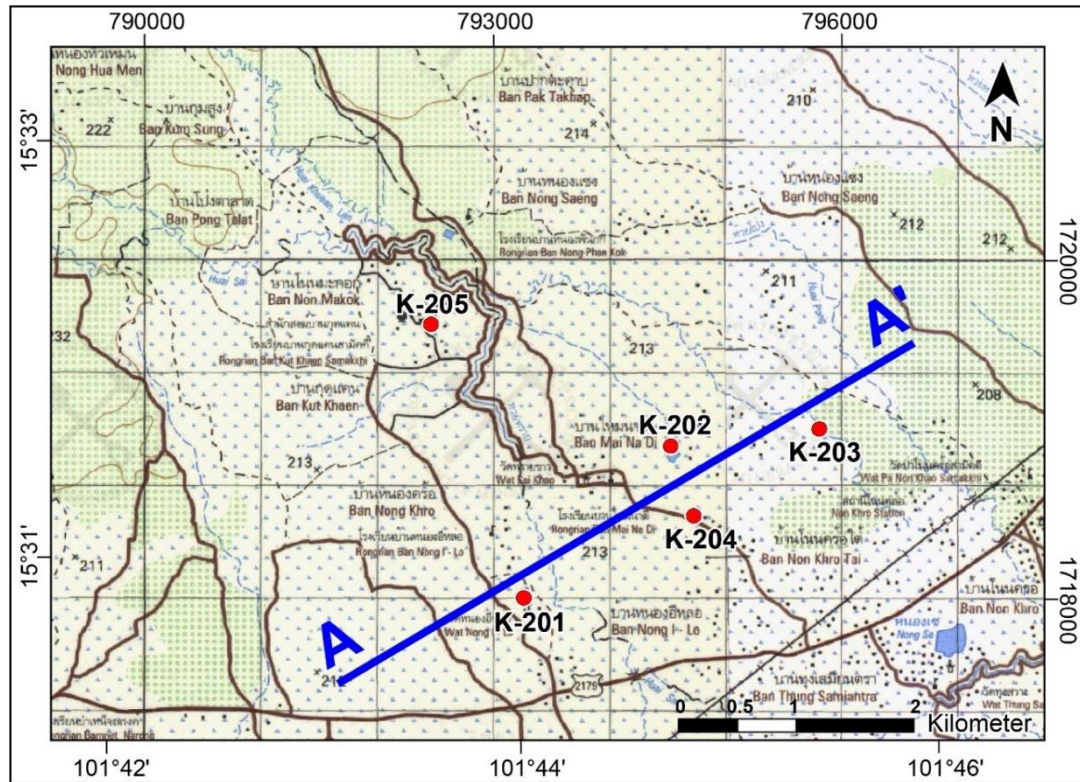


**Figure 67** A direction of cross-section A-A' (SW and NE) references from Map L7018 (1997) by Royal Thai Survey Department.

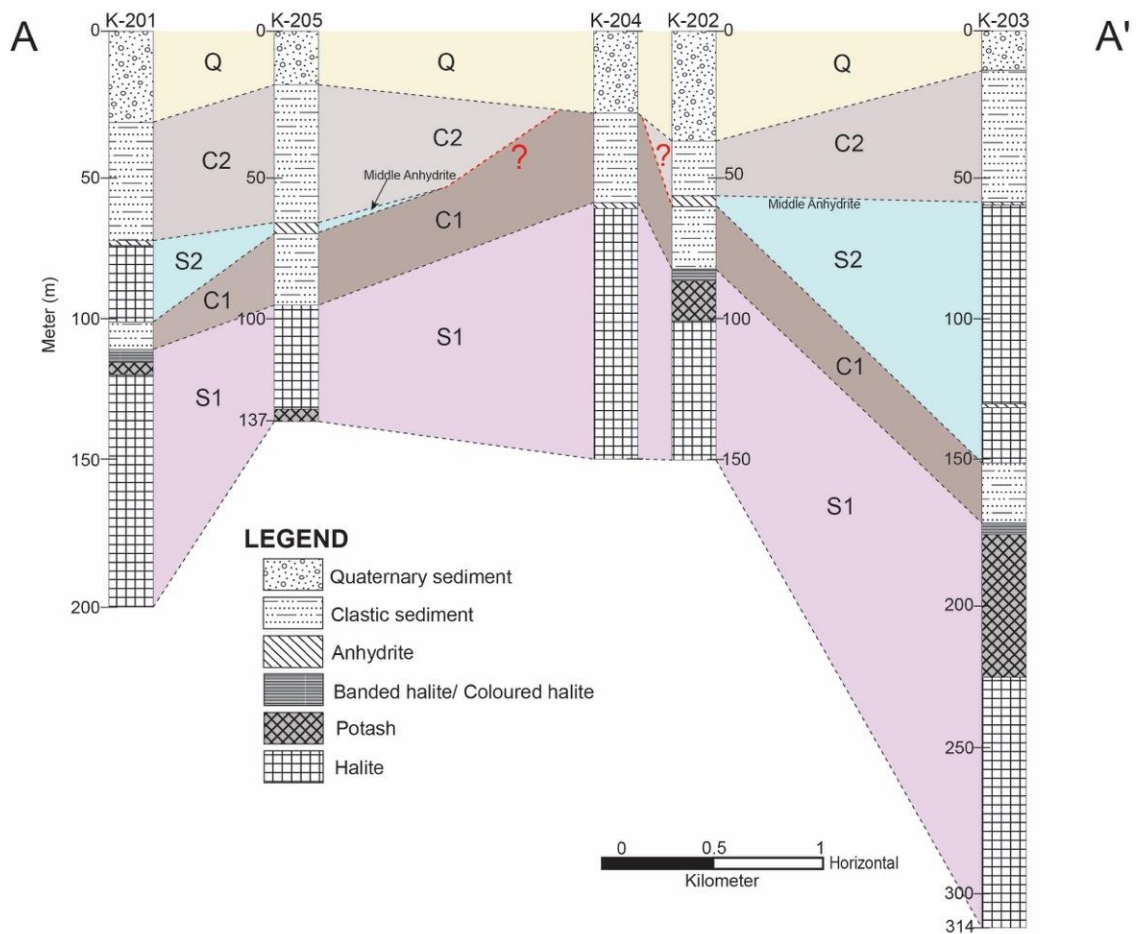


**Figure 68** A cross-section A-A' (boreholes; K-201–205) show lithostratigraphic correlation. Black dash line = the correlation of rock members; Red dash line = a forecast of correlation of rock members (after Rattana et al., in press).

The characteristic of lithostratigraphic columns in this study have two cycles of evaporitic rocks and separated by claystone. However, only borehole K-204 has found a member of evaporitic rocks as Lower Salt Unit (S1) that all boreholes are an incomplete of Maha Sarakham Formation (Yumuang et al., 1986). The lowest unit founded a whole borehole in this study consist of a thick bed of halite, carnallite, sylvite and banded halite but borehole K-204 is a thick bed of anhydrite overlies massive halite. The geophysical analysis base on gravity exploration infers the Bouguer anomaly map (Figure 70) that position of borehole K-204 is define a dome structure by high positive anomaly (Shen & Siritongkham, 2020). This interpretation is compared by lithostratigraphic columns that borehole K-204 has halite and an anhydrite bed without

potash minerals (Figure 71). The result of borehole K-204 is cooperation agreement by (Suwanich, 1986) and Yumuang et al. (1986).

For middle anhydrite, of Middle/Upper Salt Unit in boreholes K-202 and K-205, is chemical deformation by groundwater. Halite interbedded with a great thickness of anhydrite was dissolute until without massive halite that result mentioned by Utha-Aroon (1993). Yumuang et al. (1986) has reported another cause by physical deformation that evident is originate a dome structure by regional tectonic or different loading overlying evaporitic rock. A dome structure has two identity portions that portions are including crest of dome in borehole K-204 and limbs of dome in borehole K-201, K-205, K-202 and K-203, respectively (Figure 71). The limbs of dome have shown potash mineral (carnallite and sylvite) that zone of potash is chemical deformed by groundwater (Warren, 2016). Combined the study of Suwanich (1986) comparative with the data of columns in this study (Figure 71) are improved the credibility of stratigraphic cross-section A-A' (Figure 72). Thus, stratigraphic correlation in this study is presented dome structure of rock salt.

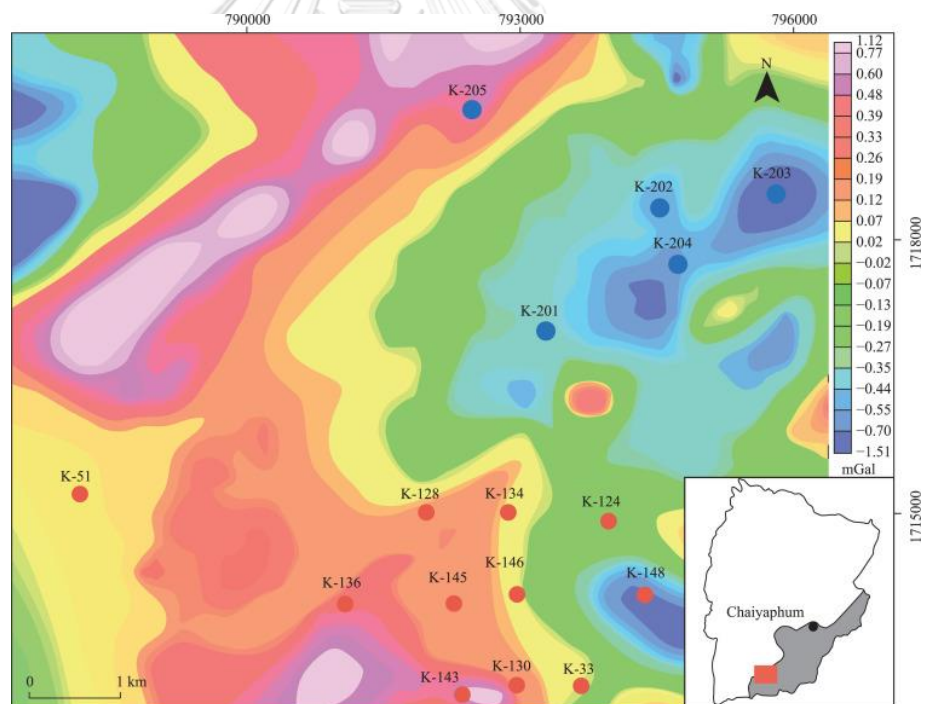


**Figure 69** The Bouguer anomaly map of this study area in five boreholes; K-201-205 (blue circle) (after Shen & Siritongkham, 2020)

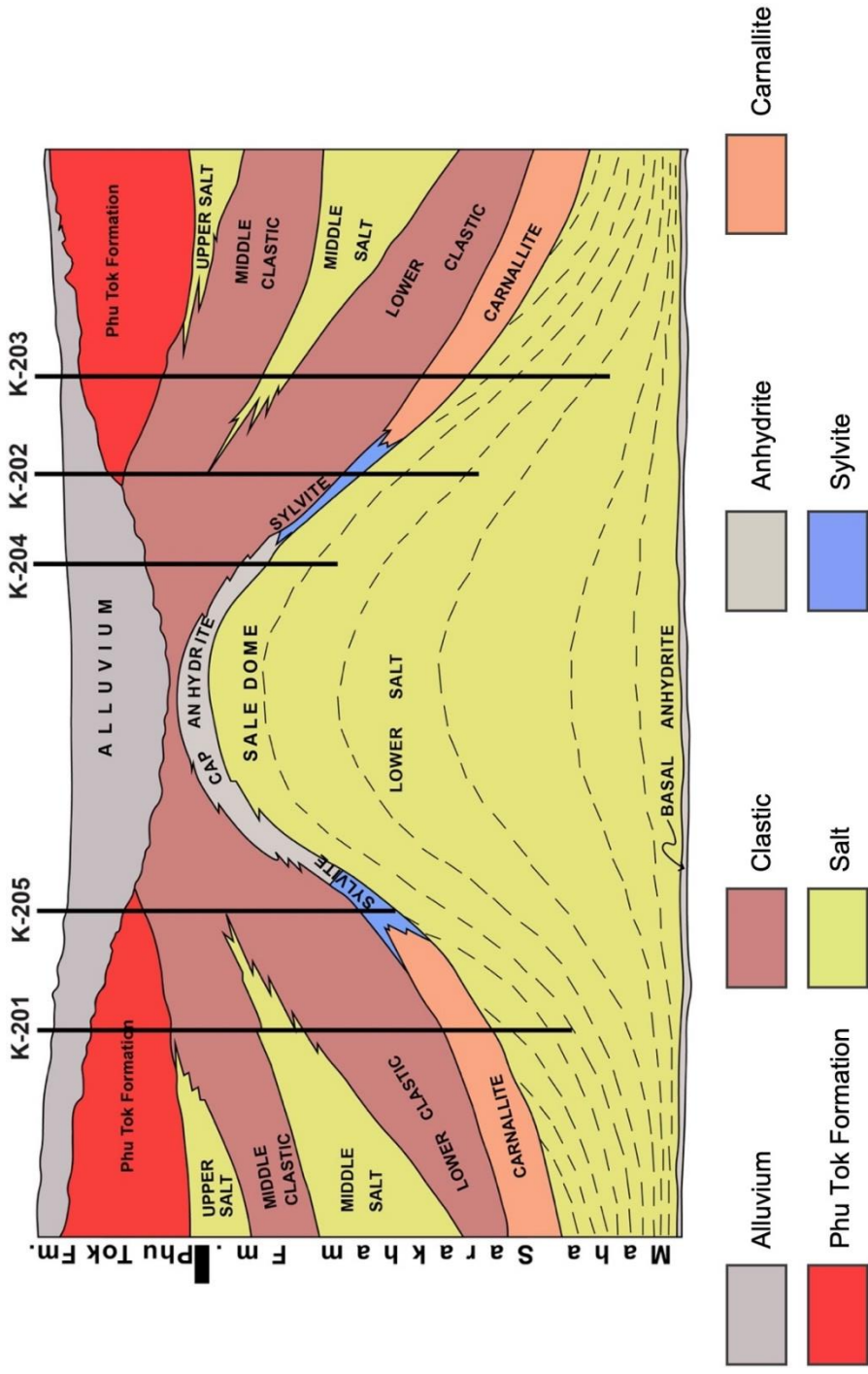


**Figure 70** Model of the Maha Sarakham Formation compared lithostratigraphic columns in this study (modified from Suwanich, 1983). Solid line showing the locations and depth of five boreholes.

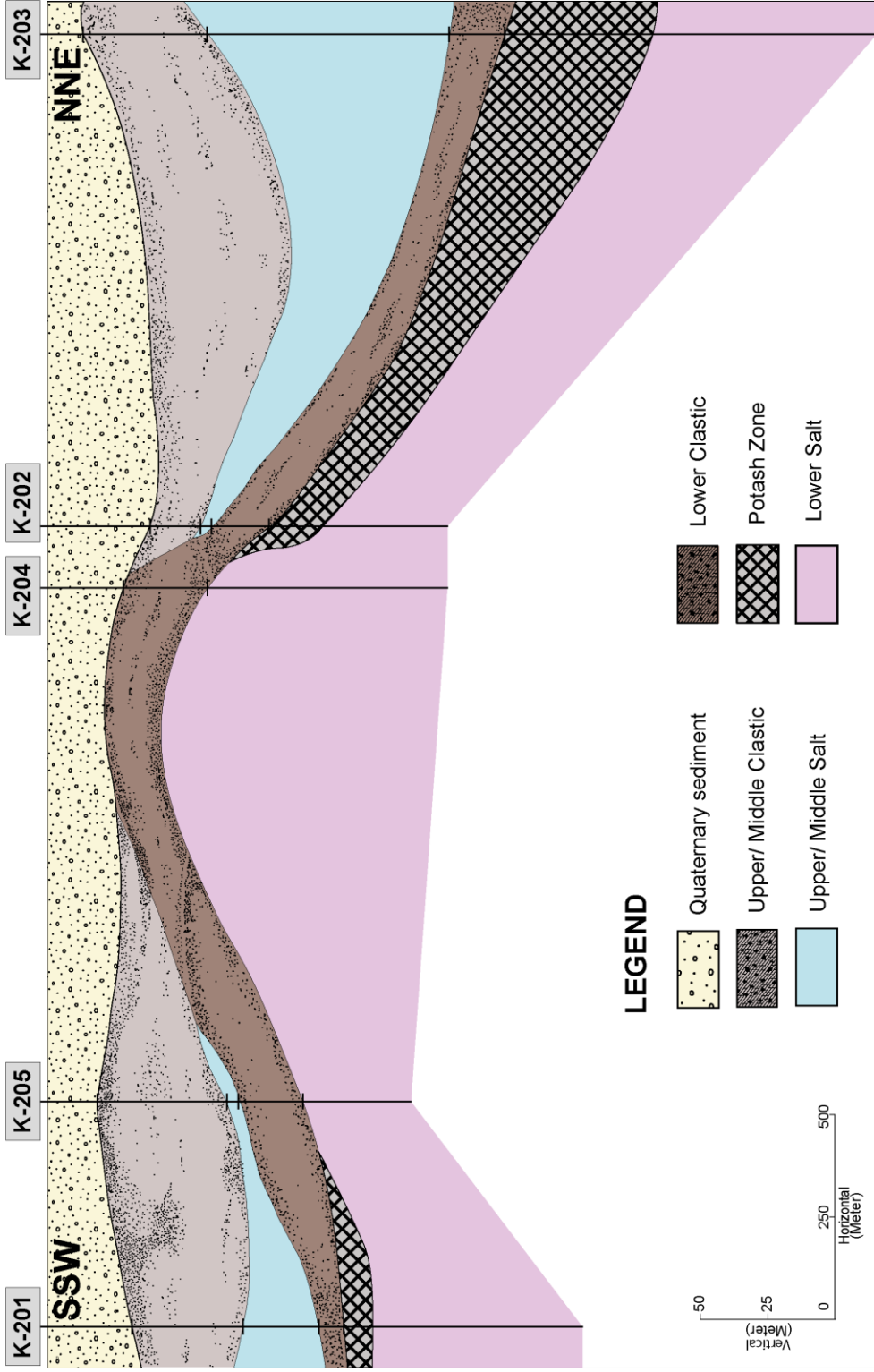


**Figure 71** A cross-section A-A' show a dome structure and lithostratigraphic correlation with located of five boreholes (K-201–205).

## 5.2 The origins of evaporitic rock base on geochemical characteristics in borehole K-203.

In this study, the Geochemical characteristics of Maha Sarakham Formation (anhydrite, halite and carnallite) consisted of major, minor and trace element cooperated with values of boron isotopic composition, all results are useful inferred the paleo-environment and source of rock salt of borehole K-203.

The correlation of elemental compositions and depth of K-203 are shown in Figure 73. Lower Salt Unit is divided into three components that consists of massive halite, carnallite and banded halite, respectively from bottom to top. In the first stage of evaporation, the Na and Cl plots are high concentrations and stable. These results infer halite precipitation that deposition is corresponding with the pattern variation of Na and Cl. In some depth of halite show narrow variation of Ca and SO<sub>4</sub> contents that illustrated a small amount of anhydrite interbedded with massive halite.  $\delta^{11}\text{B}$  of Unit S1 in massive halite exhibit 22.21‰ and 28.19‰ (average of 24.99‰ (n=9)) that values are interpreted marine deposits in halite for first major evaporation.

The middle part of Unit S1 in potash layer (carnallite) has enriched of K and Mg and depleted of Na and Cl that results are interpreted the increasing hypersaline paleo-seawater to bittern salt precipitation. Some variations of trace element are observed in carnallite. The wide variation of Sr and B concentrations are founded at depth interval 192.0 - 194.0 and 210.0 - 215.0 meters, about 1,362 ppm and 10 ppb, respectively. There variation of trace elements is still unclear to interpretation of evaporites origin. The uppermost of Unit S1 is banded halite that consisted of thin beds (carnallite and halite). Banded halite shows the variation trends of elemental compositions according to the dominant composition of host rocks that halite and carnallite at depth interval 172.3 - 176.25 and 165.0 - 170.0 meters, respectively.  $\delta^{11}\text{B}$  of Unit S1 in carnallite show 12.26‰ and 32.62‰ (average of 26.13‰ (n=4)) that values are interpreted marine deposits. At depth 200.0 - 205.0 meters, a sample of carnallite is show minimum value of boron isotope. The uppermost part of Unit S1 in banded halite shows the fluctuated variation according to dominant composition of host rocks that are thin beds (halite and carnallite).

Middle/Upper Salt Unit S2 is divided into two components that consists of massive halite interbedded or associate with great thickness of anhydrites or anhydrite stringers at depth interval 115.0 - 120.0 and 92.85 - 93.0 meter from bottom to top. For the elemental contents of Unit S2, the variation of major elements including Na, Cl, Ca and SO<sub>4</sub> which are occurred according to component of parent rocks. These spots are indicated the type of evaporitic rocks and other spots do not have significant to interpret the salts formed from evaporation.  $\delta^{11}\text{B}$  of

Unit S2 in massive halite exhibit vary from 21.46‰ to 28.80‰, with an average of 24.42‰ (n=9) that values are interpreted marine deposits in halite of Unit S2.

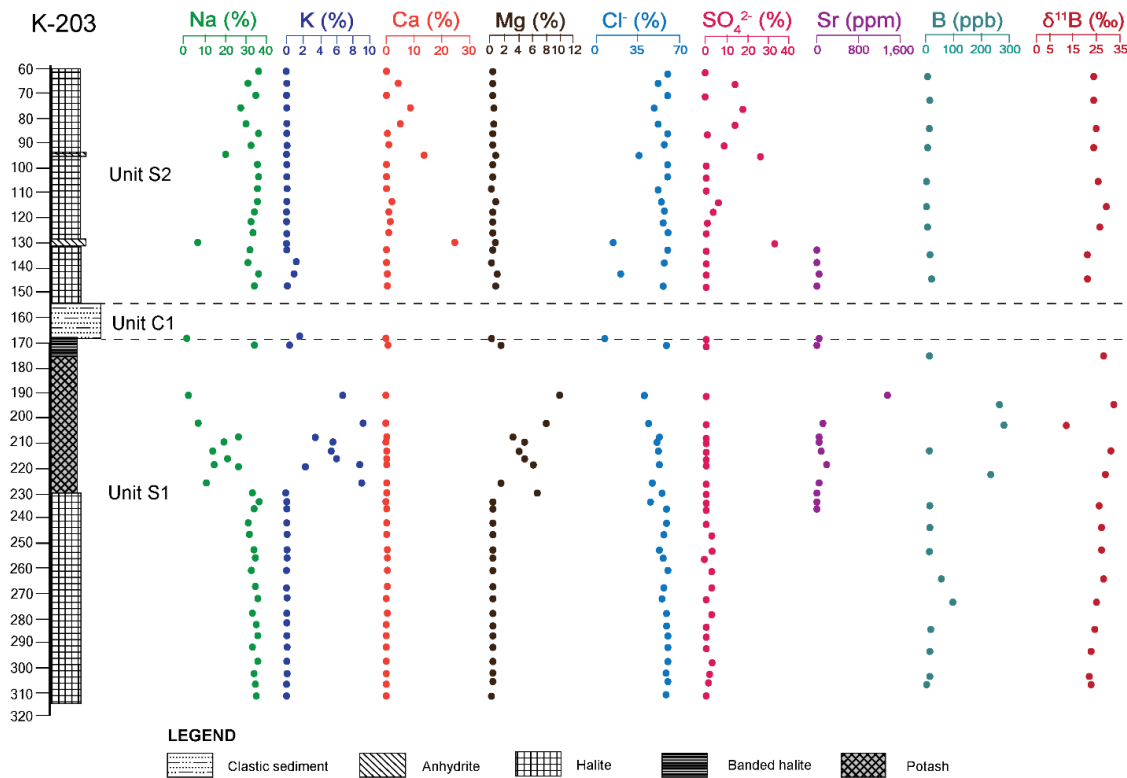


**Figure 72** Profile of elemental compositions and boron isotopic composition compared sampling depths in borehole K-203. (after Rattana et al., in press)

The origin and depositional environment interpreted from elemental compositions and values of boron isotope that all results are shown in model stages depositional environment of Maha Sarakham Formation (Figure 74). These results have revealed that the formation of borehole K-203 can be divided into four stages (after Rattana et al., in press).

Initial stage to formed evaporitic rock from seawater (Figure 74A, B), the variations in the concentrations (Na, Cl, K, Mg) of Unit S1 are correlated with changes in halite and carnallite. These minerals formed seawater evaporation that presented by  $\delta^{11}\text{B}$  values (22.21‰ and 28.19‰). Many studies (e.g. El Tabakh et al., 1999; Qin et al., 2020; Ren et al., 2018; Tan et al., 2010; Yumuang et al., 1986; Zhang et al., 2013) have been indicated the marine evaporitic setting of the Khorat Plateau. Yumuang et al. (1986) presents model influx of open marine to restricted marine that formed the evaporitic rocks namely bar-basin theory and his study is corresponding the high sea-level of the world (Wright et al., 2020) during Middle Cretaceous (Cenomanian) (2016; Hansen et al., 2002). Cretaceous seawater has enriched in Ca and depleted

in  $\text{SO}_4$  that studied by Hardie (1990); Timofeeff et al. (2006); Wang and Lowenstein (2017). At depth interval 165.0 - 170.0 meters, has increasing small amount of Ca concentration about 0.37 ppm that cooperated with identity Cretaceous seawater.

2) Seawater re-input stage (Figure 74C), the relationship of chemical compositions (Na, Cl, Ca,  $\text{SO}_4$ ) in halite and anhydrite that minerals are the dominant of Unit S2. This unit is created seawater evaporation that presented by  $\delta^{11}\text{B}$  values (21.46‰ to 28.80‰). Morley (2012) and Zhenhan et al. (2016) mentioned re-input of marine into the Khorat Plateau that evidence is occurred During the Late Cretaceous by the movement of the Indochina plate. Next, the paleoenvironment of the Khorat Plateau is changed to fluvial and aeolian (Hasegawa et al., 2010) when the second and third evaporitic cycles have been formed already. This environment has formed the Phu Tok Formation by clastic sediment overlying the Maha Sarakham Formation (evaporitic rocks).

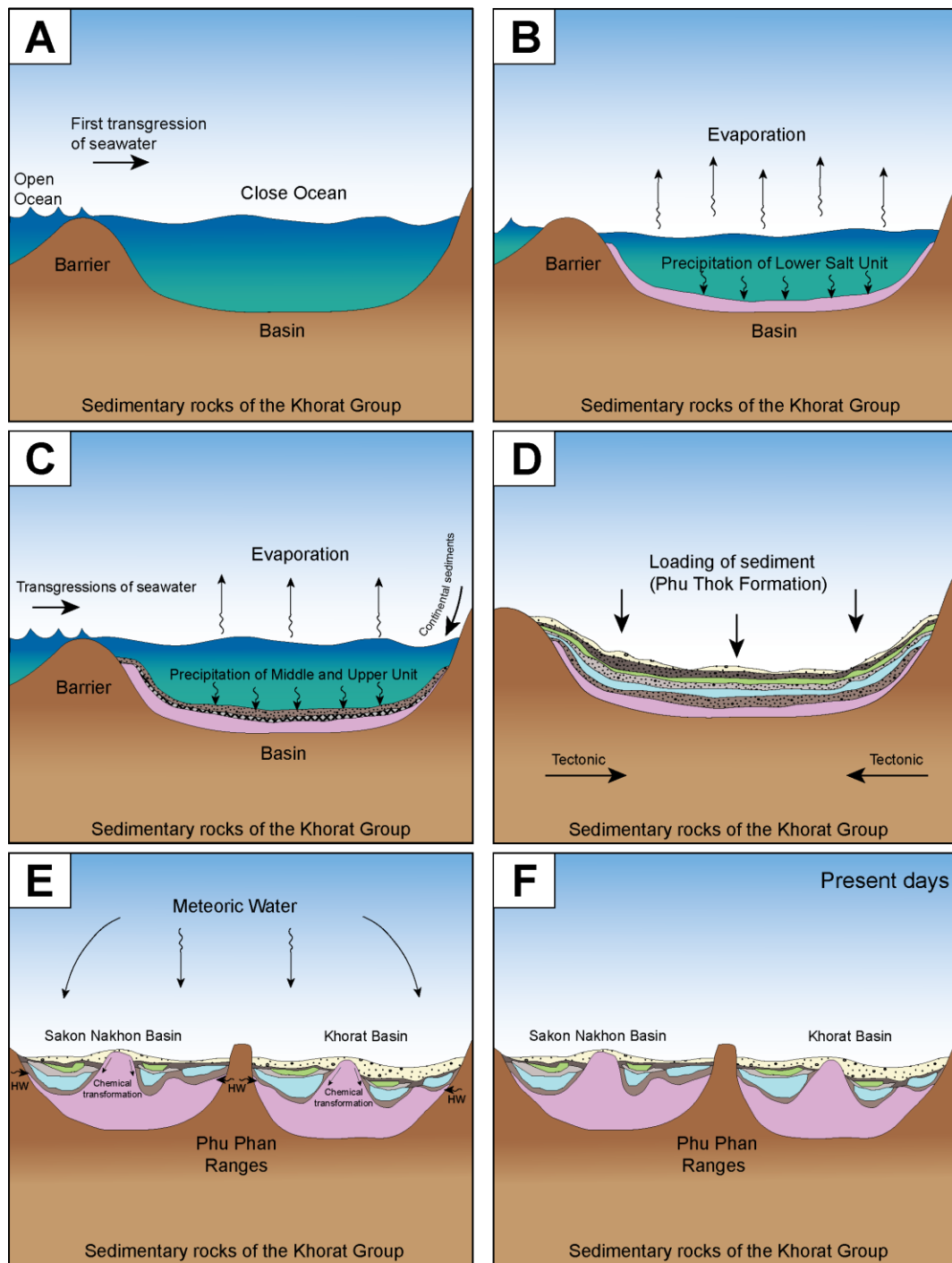
3) Deformation stage (Figure 74D), the horizontal beds of the Maha Sarakham Formation have deformed to dome structure by loading of overburden or regional tectonic (Yumuang et al., 1986). This tectonic has collision of the Eurasia and India plates as Himalayan orogeny that cause is made rotate clockwise of Indochina plate and separation within the Khorat Plateau into Sakon Nakhon basin in the north and Khorat basin in the south by the Phu Phan ranges lies in the NW-SE direction (El Tabakh et al., 1999; Meesook, 2000; Songtham et al., 2011; Veeravinantanakul et al., 2018).

4) Hydrothermal input stage (Figure 74E and F), the possible events of hydrothermal input the Maha Sarakham Formation that evident was recorded by the chemical concentration of carnallite. The pattern of  $\delta^{11}\text{B}$  values in this study and previous studies from the Sakon Nakhon Basin (Ren et al., 2018; Tan et al., 2010; Zhang et al., 2013) and the Khorat Basin (Qin et al., 2020) that comparative data is illustrate the similarity pattern (Figure 76). Zhang et al. (2013) and Ren et al. (2018) presented the lower  $\delta^{11}\text{B}$  value of evaporitic rocks that results are indicated the input of freshwater. The previous works are cooperated the  $\delta^{11}\text{B}$  value in this study that a minimum  $\delta^{11}\text{B}$  value of carnallite at depth 200.0 - 205.0 meters presented 12.26‰.

However, the anomalies data of carnallite (Unit S1) are including B and Sr concentrations and  $\delta^{11}\text{B}$  value at depth interval 172.3 - 176.25, 165.0 - 170.0 and 200- 205 meters, respectively which these results have been indicated extending event of mainly marine origin of Lower Salt Unit. Boron concentration is mainly enriched in  $\text{K-MgSO}_4$  minerals than halite (Vengosh et al., 1992) which at depth 210.00 - 214.00 meters was presented the decreasing boron concentration in 10 ppb that significance inferred the terrestrial water influx

to basin (Ren et al., 2018). The anomaly data of Sr concentration was detected about 1,362 ppm at depth interval 165.0 - 170.0 meters. Kushnir (1982) described the events for high concentration of Sr that events are explained by the initial stage of evaporation with suited temperature to formed anhydrite. At depth interval 165.0 - 170.0 meters, has increasing small amount of Ca concentration about 0.37 ppm. Both of elements of carnallite (Unit S1) between Ca and Sr are positive correlation and depleted in SO<sub>4</sub>. Many studies (e.g. Hardie, 1990; Timofeeff et al., 2006; Wang & Lowenstein, 2017) have been presented the characteristic of cretaceous seawater that inferred the enriched in Ca and depleted in SO<sub>4</sub>. The characteristic of cretaceous seawater has inferred the deposits of potash minerals associated with hydrothermal water. Hardie (1990) represented trachyhydrite precipitation that is the influence of hydrothermal water input potash minerals. In addition, Hardie (1990) presented the high concentrations including Fe, Mn, Pb, Zn, Cu and Ba that are the significant of hydrothermal origin. The results of their element are shown in Table 3. Carnallite (Unit S1) at depth interval 165.0 - 170.0 meters is founded trace concentration e.g. Fe (0.38 % wt); Mn 50 ppm; Zn (5 ppm) and Ba (23 ppm) that nearly values was described by Hardie (1990). This event of hydrothermal water input during or after extension of tectonic stress (Figure 74E and F) that formed tachyhydrites and saddle dolomites with high temperatures (Bo et al., 2015). This relationship of geothermal activity has shared from the Yanjing–Lanping–Simao–northern Laos (north to the south direction). Wang and Lowenstein (2017) disappeared the hydrothermal event, faulting and volcanism but El Tabakh et al. (1999) has granite intrusions during upper Cretaceous on the Khorat Plateau that granite is the source of hydrothermal fluid.

Hence, this allows for the assumption of the influence of hydrothermal/ freshwater input potash mineral by the anomalies of trace element concentrations and  $\delta^{11}\text{B}$  value of carnallite.



Hydrothermal Water (HW)

**LEGEND**

- |   |                    |   |                |   |             |
|---|--------------------|---|----------------|---|-------------|
|  | Phu Thok Formation |  | Middle Clastic |  | Potash Zone |
|  | Upper Clastic      |  | Middle Salt    |  | Lower Salt  |
|  | Upper Salt         |  | Lower Clastic  |   |             |

**Figure 73** model stage of origins of Maha Sarakham Formation (after Rattana et al., in press).

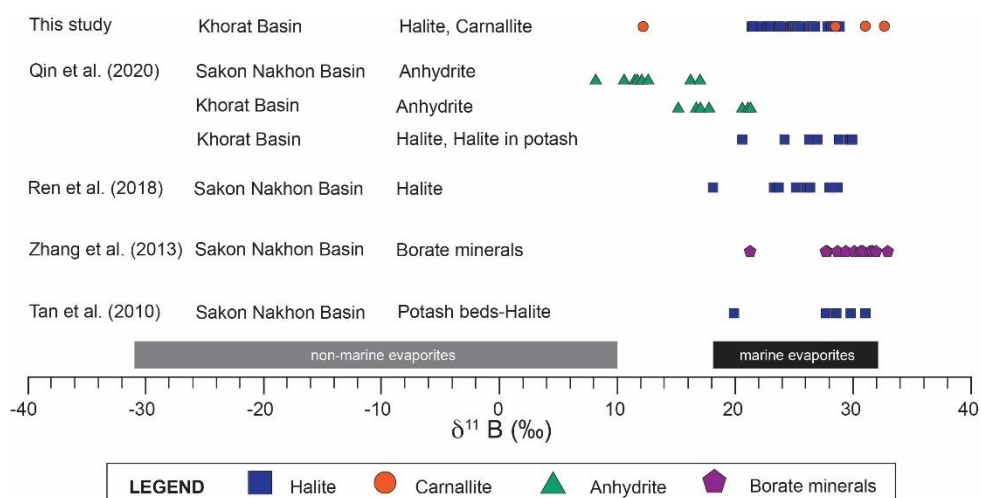


**Figure 74**  $\delta^{11}\text{B}$  values of halite and carnallite of Borehole K-203 in this study using  $\delta^{11}\text{B}$  values to distinguish non-marine and marine origins based on Palmer and Swihart (1996); Swihart et al. (1986); Vengosh et al. (1992). the  $\delta^{11}\text{B}$  ranges of marine evaporitic rocks compares with previous studies from the Sakon Nakhon Basin (Ren et al., 2018; Tan et al., 2010; Zhang et al., 2013) and the Khorat Basin (Qin et al., 2020) (after Rattana et al., in press).

### 5.3 The provenance of clastic unit in five boreholes (Borehole K-201-205)

The Cretaceous Mengyejing Formation is located on Simao basin in China which is a part of Indochina block (Figure 75). This formation is consisted of continental sedimentary rocks (sandstone, siltstone and mudstone) and evaporitic rocks (gypsum, halite and potash) (Lou et al., 2021; Wang et al., 2015; 2014) that age of Mengyejing Formation from the SHRIMP U-Pb dating is Cretaceous (Albian to Cenomanian) (Wang et al., 2015). Both basins, Simao basin in China and Khorat basin in Thailand, are Cretaceous (Albian to Cenomanian) which is the same time of the origin evaporation. Hence, we aim to make the relation of the provenance of clastic unit from REE pattern of both basins.

The characteristic of REE pattern can use to inferred regarding the source of sedimentary rocks that REE pattern is illustrated in spider diagram of chondrite normalizing values by Taylor and McLennan (1985). The chondrite normalized REE patterns of claystone (Unit C1 and C2) in this study are represent enriched of LREE relative to slightly flattened HREE with the negative anomalies of Eu and rather be anomaly of Ce (Figure 76). Moreover, Wang et al. (2014) inferred the chondrite normalized REE patterns of sandstone the Simao basin that studied is compared with chondrite normalized REE patterns in this study.

For REE patterns of Wang et al. (2014), enriched of LREE relative to slightly flattened HRE with the negative anomalies of Eu ( $\text{Eu}/\text{Eu}^*$  of 0.55–0.84, average 0.66) and Ce ( $\text{Ce}/\text{Ce}^*$  of 0.64–1.04, average 0.86). These results are presented similarity of both REE patterns with negative anomalies (Eu and Ce) that REE pattern can usefully interpret the source rock of both clastic sedimentary rocks.

Thus, the similarity of both chondrites normalized REE patterns that results corresponded with hypothesizes infers the same original terrigenous sedimentary rocks (Figure 78; Carter & Bristow, 2003; Wang et al., 2014). The original of continental sedimentary rocks are recycled sedimentary rocks from felsic rocks that rocks transported from the Simao basin into the Khorat basin when high sea level of the Cretaceous ocean (Wang et al., 2014). This transportation is temporally connection of both basin from the ocean rise and input to the continental crust. Lithostatic correlation during Jurassic to Cretaceous, of both blocks (Sibumasu and Indochina), this result made the model of recharge paleo-seawater that data studied by Qin et al. (2020). A model mentioned the process of transported from Shan Boundary ocean into the Lanping-Simao basin and the Khorat Plateau (Sakon Nakhon and Khorat Basins) respectively. The inlet way of paleo-seawater into both basins in Thailand and a part of Laos that location show southwestern corner of the Khorat Plateau (El Tabakh et al., 1999).

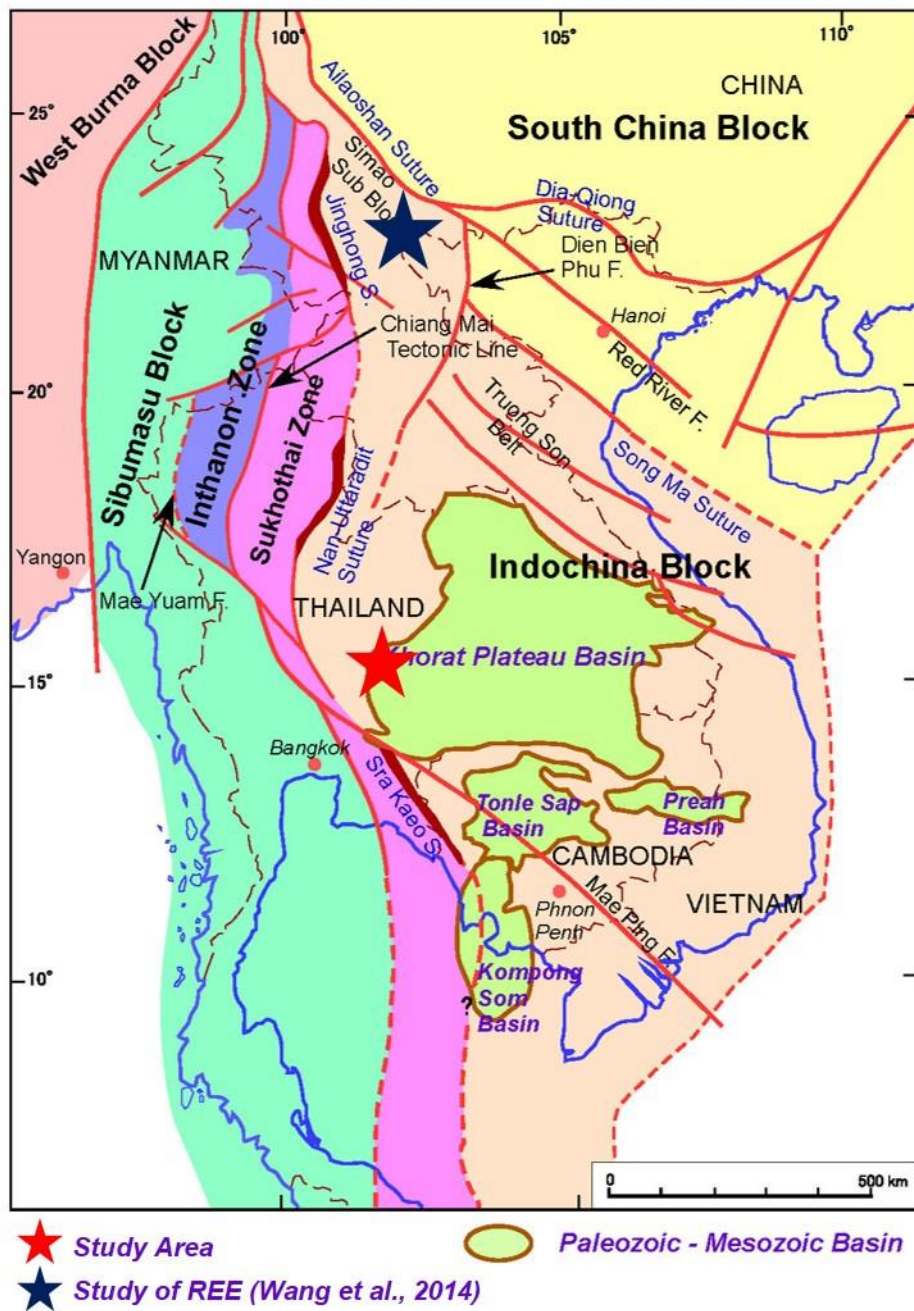


**Figure 75** Major tectonic units in the mainland Southeast Asia showing the location of the study area of REE in Simao basin (blue star) and location of this study area (modified from Minezaki et al., 2019).

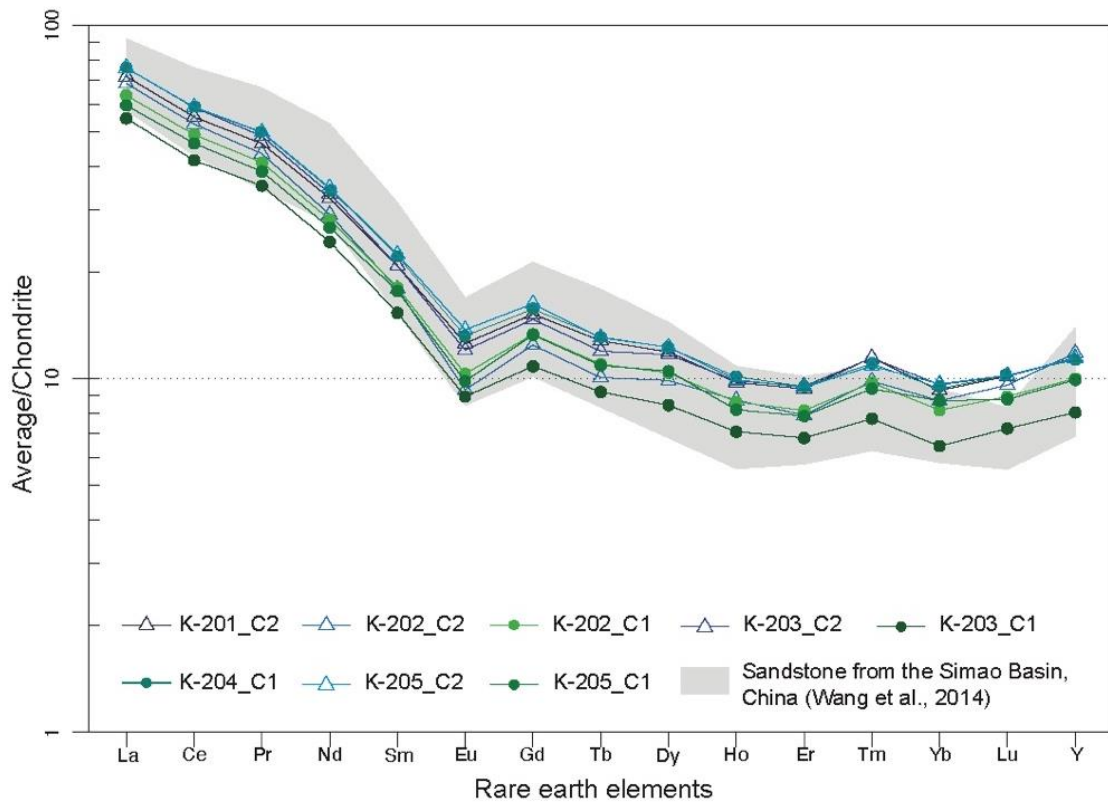


**Figure 76** Chondrite normalized REE patterns representative each clastic unit in five boreholes plotted. The gray shade showing previous work of chondrite normalized REE patterns in Simao basin consist of Zhenyuan, Jinggu, Simao, Mengia and Jiangcheng area (Wang et ai., 2014). Normalizing values of chondrite are Taylor and McLennan (1985) (after Rattana et al., in press).

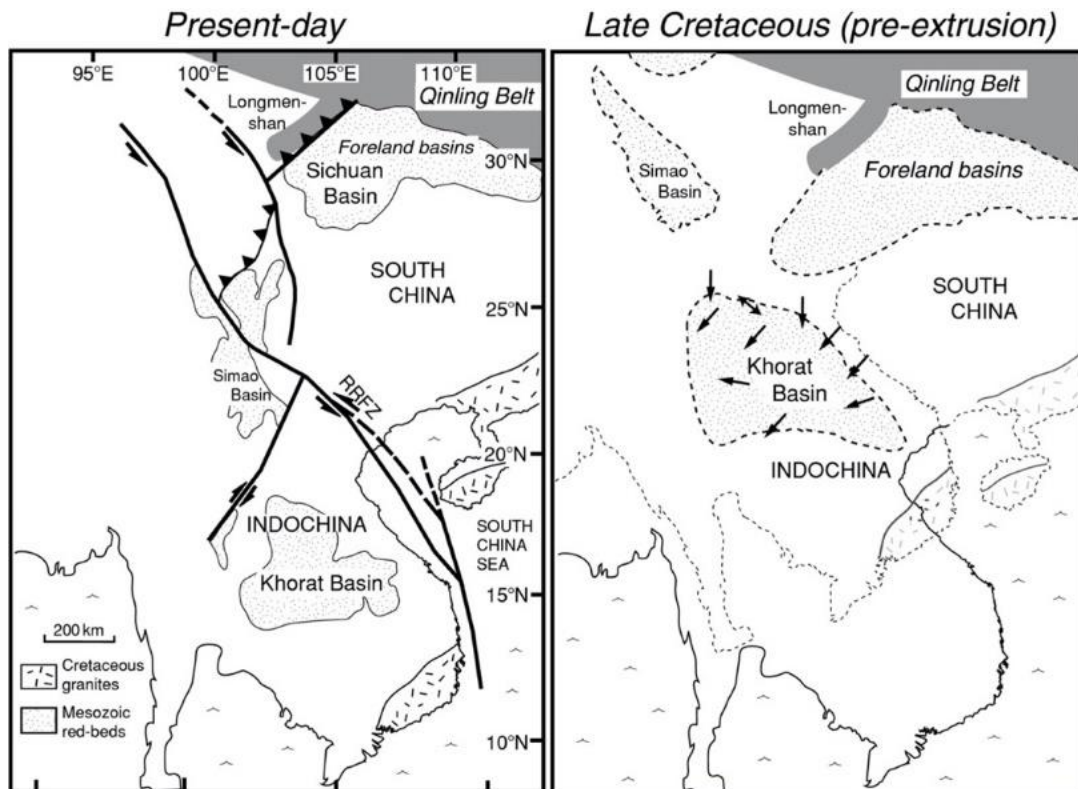


**Figure 77** the direction of paleocurrent sediment from Qinling foreland into Khorat Basin of paleogeography before the rotation basin from extrusion and the located of Khorat basin in the present-day (Carter and Bristow, 2003).

## Chapter 6

### Conclusion

#### 6.1 Conclusion

1) Lithostratigraphy of five boreholes; K-201–205 including Units S1 (Lower Salt Unit), C1 (Lower Clastic Unit), S2 (Middle/Upper Salt Unit), C2 (Middle/Upper Clastic Unit) and Q (Quaternary Deposits Unit), respectively from bottom to top

2) A stratigraphic correlation of the Maha Sarakham Formation in this study area represented the salt dome structure in.

3) The major origin of the Maha Sarakham Formation is marine origin that result is interpreted by  $\delta^{11}\text{B}$  values of halite (21.46‰–32.62‰). However, the possible event of influx of hydrothermal fluids maybe occurred in the Khorat Basin that records (anomalies of  $\delta^{11}\text{B}$  values and trace elements (B, Sr, Fe, Mn, Pb, Zn, Cu and Ba) preserved in carnallite of Unit S1.

4) The similar provenance of sedimentary rock has analyses by the similar patterns of chondrite normalized REE in both the Khorat Basin of Thailand and the Simao Basin of China.

#### 6.2 Recommendation

1) For the further study, they should be choosing the complete stratigraphy of Maha Sarakham Formation as three sequences of rock salt that indicated all evidence of Maha Sarakham Formation.

2) For sampling analysis, they should be sampling in the same depth that position of chemical analysis between trace elements and isotope analyses. These methods are confirmed all result that most importantly to authentic in this study.

3) For elemental composition analysis for the further study, they should be analysing every rock type in the column because some depth maybe detects some elemental composition to confirm interpretation in this study.

4) For the results of trace elements should be repeat analyses to confirm fluctuation values of trace elements in carnallite.

5) Geochemistry analysis for the further study, they should be focus on trace elements and other isotopes such as bromine concentration, strontium isotope, chlorine isotope, and sulphur isotopes that cooperated with boron isotope for more detail to confirm the origin of Maha Sarakham Formation.



จุฬาลงกรณ์มหาวิทยาลัย  
**CHULALONGKORN UNIVERSITY**



จุฬาลงกรณ์มหาวิทยาลัย  
**CHULALONGKORN UNIVERSITY**

## REFERENCES

- Babel, M., & Schreiber, B. C. (2014). 9.17 - Geochemistry of Evaporites and Evolution of Seawater. In H. D. Holland & K. K. Turekian (Eds.), *Treatise on Geochemistry (Second Edition)* (pp. 483-560). Elsevier. <https://doi.org/10.1016/B978-0-08-095975-7.00718-X>
- Bo, Y., Liu, C., Zhao, Y., & Wang, L. (2015). Chemical and isotopic characteristics and origin of spring waters in the Lanping–Simao Basin, Yunnan, Southwestern China. *Geochemistry*, 75(3), 287-300.
- Bunopas, S., Vella, P., Fontaine, H., Hada, S., Burrett, C., Haines, P., Pottisat, S., Wongwanich, T., Chaodamrong, P., Howard, K. T., & Khositantont, S. (2001). Growth of Asia in the Late Triassic Continent–Continent Collision of Shan–Thai and Indochina Against South China. *Gondwana Research*, 4(4), 584-585. [https://doi.org/10.1016/S1342-937X\(05\)70388-9](https://doi.org/10.1016/S1342-937X(05)70388-9)
- Carter, A., & Bristow, C. (2003). Linking hinterland evolution and continental basin sedimentation by using detrital zircon thermochronology: A study of the Khorat Plateau Basin, eastern Thailand. *Basin Research*, 15, 271-285. <https://doi.org/10.1046/j.1365-2117.2003.00201.x>
- DMR. (2010). *Geologic map of Thailand*. Geological Survey Division, Department of Mineral Resources, Thailand.
- DMR. (2014). *Geology of Thailand*. Department of Mineral Resources, Ministry of Natural Resources and Environment, Bangkok, Thailand.
- El Tabakh, M., Utha-Aroon, C., & Schreiber, B. C. (1999). Sedimentology of the Cretaceous Maha Sarakham evaporites in the Khorat Plateau of northeastern Thailand. *Sedimentary Geology*, 123(1), 31-62. [https://doi.org/10.1016/S0037-0738\(98\)00083-9](https://doi.org/10.1016/S0037-0738(98)00083-9)
- El Tabakh, M., Utha-Aroon, C., Warren, J. K., & Schreiber, B. C. (2003). Origin of dolomites in the Cretaceous Maha Sarakham evaporites of the Khorat Plateau, northeast Thailand. *Sedimentary Geology*, 157(3), 235-252. [https://doi.org/10.1016/S0037-0738\(02\)00235-X](https://doi.org/10.1016/S0037-0738(02)00235-X)
- Fan, Q., Ma, Y., Cheng, H., Wei, H., Yuan, Q., Qin, Z., & Shan, F. (2015). Boron occurrence in halite and boron isotope geochemistry of halite in the Qarhan Salt Lake, western China. *Sedimentary Geology*, 322, 34-42.
- Hansen, B., Wemmer, K., Eckhardt, M., Putthapiban, P., & Assavapatchara, S. (2016). Isotope Dating of the Potash and Rock Salt Deposit at Bamnet Narong, NE-Thailand. *Open Journal of Geology*, 06, 875-894. <https://doi.org/10.4236/ojg.2016.68067>
- Hansen, B., Wemmer, K., Pawlig, S., Ruprecht, J., Assavapatchara, S., Nontaso, M., Chairangsee, C., & Putthapiban, P. (2002). Isotopic evidence for a Late Cretaceous age of the potash and rock salt deposit at Bamnet Narong, NE Thailand. *Symposium on the Geology of Thailand, Bangkok, August 2002*, 26-31.
- Hardie, L. A. (1990). The roles of rifting and hydrothermal CaCl<sub>2</sub> brines in the origin of potash evaporites; an hypothesis. *American Journal of Science*, 290(1), 43. <https://doi.org/10.2475/ajs.290.1.43>
- Hasegawa, H., Imsamut, S., Charusiri, P., Tada, R., Horiuchi, Y., & Hisada, K.-I. (2010). 'Thailand was a desert' during the mid-Cretaceous: Equatorward shift of the subtropical

- high-pressure belt indicated by eolian deposits (Phu Thok Formation) in the Khorat Basin, northeastern Thailand. *Island Arc*, 19(4), 605-621. <https://doi.org/https://doi.org/10.1111/j.1440-1738.2010.00728.x>
- He, M., Jin, Z., Lu, H., & Ren, T. (2015). Efficient separation of boron using solid-phase extraction for boron isotope analysis by MC-ICP-MS [10.1039/C5AY01743B]. *Analytical Methods*, 7(24), 10322-10327. <https://doi.org/10.1039/C5AY01743B>
- He, M.-Y., Deng, L., Lu, H., & Jin, Z.-D. (2019). Elimination of the boron memory effect for rapid and accurate boron isotope analysis by MC-ICP-MS using NaF [10.1039/C9JA00007K]. *Journal of Analytical Atomic Spectrometry*, 34(5), 1026-1032. <https://doi.org/10.1039/C9JA00007K>
- Hite, R. (1971). Potential for potash and related mineral resources, Khorat Plateau, northeast Thailand and central Laos. Unpub. *US Geol. Survey Project Report*.
- Hite, R. J., & Japakasetr, T. (1979). Potash deposits of the Khorat plateau, Thailand and Laos. *Economic Geology*, 74(2), 448-458.
- Japakasetr, T., & Workman, D. R. (1981). Evaporite Deposits of Northeast Thailand. *Energy Resources of the Pacific Region*, 179-187.
- Kushnir, J. (1982). The partitioning of seawater cations during the transformation of gypsum to anhydrite. *Geochimica et Cosmochimica Acta*, 46(3), 433-446. [https://doi.org/https://doi.org/10.1016/0016-7037\(82\)90234-4](https://doi.org/https://doi.org/10.1016/0016-7037(82)90234-4)
- Li, M., Yan, M., Fang, X., Zhang, Z., Wang, Z., Sun, S., Li, J., & Liu, X. (2018). Origins of the Mid-Cretaceous evaporite deposits of the Sakhon Nakhon Basin in Laos: Evidence from the stable isotopes of halite. *Journal of Geochemical Exploration*, 184, 209-222. <https://doi.org/https://doi.org/10.1016/j.gexplo.2017.11.001>
- Li, Q., Zhang, X., Fan, Q., Qin, Z., Wang, J., & Shan, F. (2020). Influence of non-marine fluid inputs on potash deposits in northeastern Thailand: evidence from  $\delta^{37}\text{Cl}$  value and Br/Cl ratio of halite. *Carbonates and Evaporites*, 35. <https://doi.org/10.1007/s13146-019-00534-y>
- Liu, W. G., Xiao, Y. K., Peng, Z. C., An, Z. S., & He, X. X. (2000). Boron concentration and isotopic composition of halite from experiments and salt lakes in the Qaidam Basin. *Geochimica et Cosmochimica Acta*, 64(13), 2177-2183. [https://doi.org/https://doi.org/10.1016/S0016-7037\(00\)00363-X](https://doi.org/https://doi.org/10.1016/S0016-7037(00)00363-X)
- Lou, P., Miao, Z., Zheng, M., Zhang, X., Ruan, Z., & Xu, Q. (2021). Paleogeographic Characteristics of the Mengyejing Formation in the Simao Basin during Its Depositional Period and Its Indication of Potash Mineralization: A Case Study of MZK-3 Well. *Minerals*, 11, 338. <https://doi.org/10.3390/min11040338>
- Meesook, A. (2000). Cretaceous environments of northeastern Thailand. In *Developments in Palaeontology and Stratigraphy* (Vol. 17, pp. 207-223). Elsevier.
- Metcalfe, I. (2017). Tectonic evolution of Sundaland. *Bulletin of the Geological Society of Malaysia*, 63, 27-60. <https://doi.org/10.7186/bgsm63201702>
- Minezaki, T., Hisada, K.-i., Hara, H., & Kamata, Y. (2019). Tectono-stratigraphy of Late Carboniferous to Triassic successions of the Khorat Plateau Basin, Indochina block, northeastern Thailand: Initiation of the Indosinian Orogeny by collision of the Indochina and South China blocks. *Journal of Asian Earth Sciences*, 170, 208-224.
- Morley, C. (2012). Late Cretaceous–Early Paleogene tectonic development of SE Asia. *Earth-Science Reviews*, 115, 37–75. <https://doi.org/10.1016/j.earscirev.2012.08.002>

- Palmer, M. R., & Swihart, G. H. (1996). Chapter 13 Boron isotope geochemistry: an overview. In *Boron: Mineralogy, Petrology and Geochemistry* (pp. 709-744). Mineralogical Society of America.
- Qin, Z., Li, Q., Zhang, X., Fan, Q., Wang, J., Du, Y., Ma, Y., Wei, H., Yuan, Q., & Shan, F. (2020). Origin and recharge model of the Late Cretaceous evaporites in the Khorat Plateau. *Ore Geology Reviews*, *116*, 103226. <https://doi.org/https://doi.org/10.1016/j.oregeorev.2019.103226>
- Racey, A., & Goodall, J. G. (2009). Palynology and stratigraphy of the Mesozoic Khorat Group red bed sequences from Thailand. *Geological Society, London, Special Publications*, *315*(1), 69-83.
- Racey, A., Love, M., Canham, A., Goodall, J., Polachan, S., & Jones, P. (1996). Stratigraphy and reservoir potential of the Mesozoic Khorat Group, NE Thailand: Part 1: stratigraphy and sedimentary evolution. *Journal of Petroleum Geology*, *19*(1), 5-39.
- Rattana, P., Choowong, M., He, M.-Y., Tan, L., Lan, J., Bissen, R., & Chawchai, S. (in press). Geochemistry of evaporitic deposits from the Cenomanian (Upper Cretaceous) Maha Sarakham Formation in the Khorat Basin, northeastern Thailand [Unpublished manuscript]. *Cretaceous Research*.
- Ren, Q., Du, Y., Gao, D., Li, B., Zhang, X., Liu, X., & Yuan, X. (2018). A Multi-fluid Constrain for the Forming of Potash Deposits in the Savannakhet Basin: Geochemical Evidence from Halite. *Acta Geologica Sinica-English Edition*, *92*(2), 755-768.
- Sato, K., Liu, Y., Wang, Y., Yokoyama, M., Yoshioka, S. y., Yang, Z., & Otofujii, Y.-i. (2007). Paleomagnetic study of Cretaceous rocks from Pu'er, western Yunnan, China: Evidence of internal deformation of the Indochina block. *Earth and Planetary Science Letters*, *258*(1), 1-15. <https://doi.org/https://doi.org/10.1016/j.epsl.2007.02.043>
- Sattayarak, N. (1983). Review of the continental Mesozoic stratigraphy of Thailand.
- Sattayarak, N., Polachan, S., & Charusirisawad, R. (1991). Cretaceous rock salt in the northeastern part of Thailand. Proceedings of the 7th Regional Conference Geology and Mineral Resources Southeast Asia (GEOSEA VII),
- Shen, L.-j., & Siritongkham, N. (2020). The characteristics, formation and exploration progress of the potash deposits on the Khorat Plateau, Thailand and Laos, Southeast Asia. *China Geology*, *3*(1), 67-82. <https://doi.org/https://doi.org/10.31035/cg2020009>
- Sone, M., & Metcalfe, I. (2008). Parallel Tethyan sutures in mainland Southeast Asia: New insights for Palaeo-Tethys closure and implications for the Indosinian orogeny. *Comptes Rendus Geoscience*, *340*(2), 166-179. <https://doi.org/https://doi.org/10.1016/j.crte.2007.09.008>
- Sone, M., Metcalfe, I., & Chaodumrong, P. (2012). The Chanthaburi terrane of southeastern Thailand: Stratigraphic confirmation as a disrupted segment of the Sukhothai Arc. *Journal of Asian Earth Sciences*, *61*, 16-32. <https://doi.org/https://doi.org/10.1016/j.jseaes.2012.08.021>
- Songtham, W., Grote, P. J., Rugmai, W., Chitnarin, A., Hanta, R., Duangkrayom, J., & Jenjitpaiboon, K. (2011). *Prior to Khorat, Prehistoric Khorat. Northeastern Research Institute of Petrified Wood and Mineral Resources, Nakhon Ratchasima Rajabhat University*.
- Sun, S., Li, M., Yan, M., Fang, X., Zhang, G., Liu, X., & Zhang, Z. (2019). Bromine content and Br/Cl molar ratio of halite in a core from Laos: implications for origin and environmental

- changes. *Carbonates and Evaporites*, 34. <https://doi.org/10.1007/s13146-019-00508-0>
- Suwanich, P. (1986). Potash and Rock Salt in Thailand: Nonmetallic Minerals Bulletin No. 2. *Economic Geology Division, Department of Mineral Resources, Bangkok, Thailand.*
- Swihart, G. H., Moore, P. B., & Callis, E. L. (1986). Boron isotopic composition of marine and nonmarine evaporite borates. *Geochimica et Cosmochimica Acta*, 50(6), 1297-1301. [https://doi.org/https://doi.org/10.1016/0016-7037\(86\)90413-8](https://doi.org/https://doi.org/10.1016/0016-7037(86)90413-8)
- Tan, H., Ma, H., Binkai, L., Zhang, X., & Xiao, Y. (2010). Strontium and boron isotopic constraint on the marine origin of the Khammuane potash deposits in southeastern Laos. *Chinese Science Bulletin*, 55, 3181-3188. <https://doi.org/10.1007/s11434-010-4010-x>
- Taylor, S. R., & McLennan, S. M. (1985). The continental crust: its composition and evolution.
- Timofeeff, M. N., Lowenstein, T. K., da Silva, M. A. M., & Harris, N. B. (2006). Secular variation in the major-ion chemistry of seawater: Evidence from fluid inclusions in Cretaceous halites. *Geochimica et Cosmochimica Acta*, 70(8), 1977-1994. <https://doi.org/https://doi.org/10.1016/j.gca.2006.01.020>
- Utha-Aroon, C. (1993). Continental origin of the Maha Sarakham evaporites, northeastern Thailand. *Journal of Southeast Asian Earth Sciences*, 8(1), 193-203. [https://doi.org/https://doi.org/10.1016/0743-9547\(93\)90021-G](https://doi.org/https://doi.org/10.1016/0743-9547(93)90021-G)
- Veeravinantanakul, A., Kanjanapayont, P., Sangsompong, A., Hasebe, N., & Charusiri, P. (2018). Structure of Phu Phan Range in the Khorat Plateau: Its Apatite Fission Track Ages and Geological Syntheses.
- Vengosh, A., Starinsky, A., Kolodny, Y., Chivas, A. R., & Raab, M. (1992). Boron isotope variations during fractional evaporation of sea water: New constraints on the marine vs. nonmarine debate. *Geology*, 20(9), 799-802. [https://doi.org/10.1130/0091-7613\(1992\)020<0799:Bivdfe>2.3.Co;2](https://doi.org/10.1130/0091-7613(1992)020<0799:Bivdfe>2.3.Co;2)
- Wang, J., & Lowenstein, T. K. (2017). Anomalously high Cretaceous paleobrine temperatures: hothouse, hydrothermal or solar heating? *Minerals*, 7(12), 245.
- Wang, L., Liu, C., Fei, M., Shen, L., Zhang, H., & Zhao, Y. (2015). First SHRIMP U–Pb zircon ages of the potash-bearing Mengyejing Formation, Simao Basin, southwestern Yunnan, China. *Cretaceous Research*, 52, 238-250. <https://doi.org/https://doi.org/10.1016/j.cretres.2014.09.008>
- Wang, L., Liu, C., Gao, X., & Zhang, H. (2014). Provenance and paleogeography of the Late Cretaceous Mengyejing Formation, Simao Basin, southeastern Tibetan Plateau: Whole-rock geochemistry, U–Pb geochronology, and Hf isotopic constraints. *Sedimentary Geology*, 304, 44-58. <https://doi.org/https://doi.org/10.1016/j.sedgeo.2014.02.003>
- Warren, J. K. (2016). *Evaporites: A geological compendium*. Springer.
- Wright, N. M., Seton, M., Williams, S. E., Whittaker, J. M., & Müller, R. D. (2020). Sea-level fluctuations driven by changes in global ocean basin volume following supercontinent break-up. *Earth-Science Reviews*, 208, 103293. <https://doi.org/https://doi.org/10.1016/j.earscirev.2020.103293>
- Yumuang, S., Khantaprab, C., & Taiyagupt, M. (1986). The evaporite deposits in Bamnet Narong area, northeastern Thailand.

- Zhang, X., Ma, H., Ma, Y., Tang, Q., & Yuan, X. (2013). Origin of the late Cretaceous potash-bearing evaporites in the Vientiane Basin of Laos:  $\delta^{11}\text{B}$  evidence from borates. *Journal of Asian Earth Sciences*, 62, 812-818. <https://doi.org/https://doi.org/10.1016/j.jseaes.2012.11.036>
- Zhenhan, W., Zhen, Z., BAROSH, P. J., & Peisheng, Y. (2016). Early Cretaceous Tectonics and Evolution of the Tibetan Plateau. *Acta Geologica Sinica - English Edition*, 90(3), 847-857. <https://doi.org/https://doi.org/10.1111/1755-6724.12728>





จุฬาลงกรณ์มหาวิทยาลัย  
**CHULALONGKORN UNIVERSITY**

## VITA

**NAME** Pranot Rattana

**DATE OF BIRTH** 17 September 1990

**PLACE OF BIRTH** Bangkok, Thailand

**INSTITUTIONS ATTENDED** Bachelor of Science (Geology) from Chiang Mai University in 11 March 2013

**HOME ADDRESS** 61/589 Moo 2 Tatalad Sub-district Sampran District Nakhon Pathom Province 73110



จุฬาลงกรณ์มหาวิทยาลัย  
CHULALONGKORN UNIVERSITY